



**THE MINISTRY OF NATIONAL INFRASTRUCTURES  
GEOLOGICAL SURVEY OF ISRAEL**

**Geotechnical and Hydrogeological Concerns  
in Developing the Infrastructure  
Around Jerusalem**

**Yaacov Arkin and Amos Ecker**

**Jerusalem July, 2007**

**Report GSI/12/2007**

## List of Content

Page

Preface.....	1
Acknowledgments.....	2
Introduction.....	3
Geographic setting.....	10
Geological setting.....	10
Geotechnical subdivisions.....	16
Unit I.....	17
Unit II.....	20
Unit III.....	20
Unit IV.....	21
Unit V.....	21
Unit VI.....	21
Geotechnical and environmental concerns.....	23
Hazards.....	23
Sinkholes.....	31
Karst.....	34
Seismic hazards.....	37
Quarries.....	44
Case histories.....	48
Tunnels and viaducts.....	48
Gilo Short Tunnel.....	51
Gilo Long Tunnel.....	54
Gilo Viaduct.....	58
Mount Scopus Tunnel.....	64
Water Supply.....	70
General.....	70
Groundwater.....	71
Cisterns and pools.....	78
Aqueducts.....	79
Waste materials.....	82
Sewage.....	82
Western drainage system.....	83
Eastern drainage system.....	84
Solid waste.....	84
Bibliography and References.....	85
Appendices.....	94
Preface (in Hebrew).....	106

## List of Figures

	Page
1. Topographic map of Jerusalem and vicinity.....	5
2. Municipality map of Jerusalem (1999).....	6
3. Moderate Resolution Imaging Spectroradiometer (Modis) image showing regional setting, acquired February 29, 2000.....	8
4. Judea Mountains south of Jerusalem. Exposed formations range from the Soreq Formation in the valley to the Kefar Sha'ul Formation.....	9
5. Judea Desert east of Jerusalem.....	9
6. Schematic diagram of the location of Jerusalem in relation to the geological structure.....	11
7. Schematic East-West composite geological cross section through central Israel.....	12
8. Stratigraphic legend of the geology in the vicinity of Jerusalem.....	13
9. Geological map of Jerusalem and vicinity.....	14
10. Factors affecting the geotechnical properties of the rock mass.....	16
11. Geotechnical map of Jerusalem and vicinity.....	18
12. Differential opening of fractures in layered rocks due to changes in brittleness of rock type seen in the Bina and Soreq formations.....	25
13. Principal modes of rock mass and soil failure occurring in the Jerusalem area.....	26
14. Modes of rock fall occurring in the Jerusalem area.....	26
15. Schematic morphology of a cliff face or open cut wall.....	27
16. Soil creep downslope in the Judea Mountains. Note trees tilted and bent downslope.....	28
17. Soil creep downslope in the Judea Mountains. Note telephone pole and trees tilted downslope.....	28
18. Rock fall in roadcut in the Soreq Formation, Jerusalem - Tel Aviv highway near Abu Ghosh.....	29
19. Rock fall in roadcut in the Moza Formation, Jerusalem - Tel Aviv highway.....	29
20. Dip slope failures in road cut.....	30
21. Circular slide and scar in the Moza marl exposure, Tel Aviv - Jerusalem highway.....	30

22. Mudflow in the Moza Formation marl in a roadcut after rains .....	30
23. Damascus Gate sinkhole in artificial fill- material.....	32
24. Geotechnical survey map of the sinkhole area near the Damascus Gate.....	32
25. Geological cross section connecting boreholes. Damascus Gate.....	33
26. Schematic profile of karst processes.....	35
27. Karstic fractures filled with red-brown soil in the Bina Formation limestone, north portal of tunnels, Begin highway, at the entrance to Jerusalem.....	35
28. Karstic holes in the Amminadav Formation seen as brown patches of red-brown soil filling. Herzog Street.....	36
29. Earthquake epicenter simulated by a drop of water.....	40
30. Seismic waves.....	40
31. Typical seismograms of earthquakes recorded from stations north of Jerusalem.....	41
32. Earthquake accelerations versus intensity for foundation conditions (after Leeds, 1973).....	43
33. Ancient quarries and excavations of limestone and dolomite in and around the Old City of Jerusalem.....	45
34. Abandoned quarries within the Jerusalem municipality.....	46
35. Bina limestone blocks used as “marble”. Note line of drillholes Showing method of quarrying.....	47
37. Gilo Project location map.....	49
38. Tunneling method in various lithologies around Jerusalem according to rock mass quality.....	49
39. Cohesion and friction angle in relation to water content in the chalky marl unit of the Kefar Sha’ul Formation in the Gilo Short Tunnel.....	50
40. Geotechnical cross section of the Gilo Short Tunnel alignment.....	52
41. View of the north portal of the Gilo Short Tunnel in the Kefar Sha’ul Formation during construction.....	53
42. Gilo Short Tunnel south portal in the Amminadav Formation.....	53
43. Gilo Short Tunnel work face in the Lower Unit of the Kefar Sha’ul Formation chalky limestone.....	54
44. Geotechnical cross section along the Gilo Long Tunnel.....	55
45. Karstic fractures at the north entrance to the Gilo Long Tunnel.....	56

46. Gilo Long Tunnel at the start of the north portal.....	56
47. Columnar geological section. showing position of the Transition Zone.....	57
48. Dolomite block in the Transition Zone.....	57
49. Geological cross section along the Gilo Viaduct alignment.....	59
50. Gilo Viaduct during construction.....	60
51. Gilo Viaduct-column Do.....	60
52. Foundation pit Do.....	61
53. Foundation pit Do. Drilling exploratory and grouting holes.....	61
54. Gilo Viaduct Foundation Pit Fo - Borehole Fo1.....	62
55. Gilo Viaduct Foundation Fo. Boreholes F1 F2 F3 core. ....	63
56. Gilo Viaduct foundation pit Do. Map of fractures and karst zones.....	63
57. Location of the Mount Scopus Tunnel and exploratory boreholes.....	65
58. Mount Scopus Tunnel, Borehole Z4. Geotechnical properties, lithology and stratigraphy.....	66
59. Mount Scopus Tunnel, Borehole Z4. Photo of borehole core recovery.....	67
60. Geotechnical cross section along the Mount Scopus Tunnel alignment.....	68
61. Plasticity chart for clay in the Menuha Formation marly chalk at the Mount Scopus Tunnel site.....	69
62. Suggested excavation method according to rock mass classification.....	69
63. Hydrogeological map showing subaquifers, boreholes, springs and cisterns.....	72
64. Jerusalem groundwater contour map of the Lower Judea Group Subaquifer (March 1984).....	74
65. Jerusalem and vicinity, groundwater contour map of the Lower Judea Group Subaquifer (March 1984).....	75
66. Jerusalem and vicinity, isochloride map (Mg/l) of the Lower Judea Group Subaquifer (April-May 1985).....	75
67. Structural contour map (m) and structural cross section on base Moza Formation (kumo).....	77
68. Ancient aqueduct network supplying water to Jerusalem.....	80
69. The lower aqueduct located on the southern side of Mt. Zion, partly broken and showing the installed Ottoman clay pipe.....	81

	Page
70. The lower aqueduct between the Sultan's Pools. and the Temple Mount located on the western side of Mt. Zion. An Ottoman clay pipe is installed in the aqueduct.....	81
71. Drainage basins and sewage treatment plants in the Jerusalem area.....	82

### **List of Tables**

1. Geotechnical parameters of the Amminadav, Kefar Sha'ul and Weradim formations. General values from the vicinity of Jerusalem.....	19
2. Representative geotechnical properties of rocks in the Menuha Formation.....	22
3. Representative geotechnical properties of clayey chalk samples.....	22
4. Representative geotechnical properties of soil and alluvium samples.....	22
5. Earth processes causing instability relevant to areas around Jerusalem.....	24
6. The modified Mercalli Intensity Scale.....	38
7. Important historical events.....	42
8. Tunneling classification and methods used around the world.....	48
9. Groundwater elevations, Cl and NO <sub>3</sub> in the Lower Judea Group Subaquifer.(After Baida and Guttmann 1985, Hydrological Service 2007).....	73
10. Chemical analyses (mg/l) of waters from the Upper and the Lower Judea Group subaquifers.....	76
11. Pools and water reservoirs not in use today.....	78

### **List of Appendices**

I. Landmark events in the history of Jerusalem.....	95
II. Conversion table English-Metric (SI units).....	97
III. Measured rock parameters: Amminadav, Weradim, Kefar Sha'ul, Bina and Weradim, and Menuha formations.....	98
IV. Glossary.....	103
V. Author Dr. Yaacov Arkin.....	104
VI. Author Mr. Amos Ecker .....	105

## PREFACE

In early times Jerusalem only occupied a small area and was built mainly on limestone, which was the main source of building stone. In the past water supply was from springs and cisterns, and via an aqueduct system that included channels, bridges, tunnels and pools. Major infrastructure work included impressive buildings such as the Temple.

The expansion of modern Jerusalem westwards is also mainly over limestone and dolomite rocks. Some suburbs, however, have been built over softer rocks of chalk, marl and clay. The rapid development of the city in recent years, which includes tall buildings, highways, tunnels, bridges, a light railway system, water supply to all parts of the city, sewage treatment and purification as well as remedial works on pollution, have set new challenges for the engineers.

Nowadays, a greater understanding of the geology and the geotechnical characteristics of the rocks concerned is essential in planning and construction of all engineering infrastructure programs because of the variety of rock types that occur around Jerusalem. This also applies to archeological investigation of sites that is often required before construction begins.

The physical and mechanical parameters of the geotechnical rock units are described as well as the case histories of the construction of the Gilo tunnels and viaduct and the Mount Scopus tunnel, which were completed several years ago. Additional geotechnical data kept in the Geotechnical Laboratory of the Geological Survey of Israel have been added.

The book also deals with geological hazards such as slope stability, karst phenomena, sinkholes, seismic hazards and quarries that may be encountered during the planning and design of new projects. Particular attention is given to the water supply to Jerusalem, the hydrogeology, the aquifers, the local groundwater divide and the risk of contamination of the aquifer underlying the city.

Appendices include a table of the history of Jerusalem as a tale of destruction and construction and measured geotechnical parameters of the main geological formations in graphs and lists.

**ACKNOWLEDGEMENTS**

Our appreciation goes to Dr. Amos Salamon, Dr. Oded Katz and Dr. Ze'ev Levi for their detailed and well directed comments on reading the manuscript; to Mr. Amos Israeli for his evaluation of the book and to Mr. Mikha Blum, Head of the Waste Material Department of the Gihon Water Company for providing data and discussing the removal of waste material in Jerusalem. Our thanks go to Mrs. B. Katz for editing the manuscript and to colleagues, both at the Geological Survey and in other institutions who have made useful suggestions and comments. Special thanks goes to Mr. Eli Ram for his assistance, loyalty and companionship in most of the work presented in this book. The authors also thank the Geological Survey of Israel for its support and Bat-sheva Cohen for preparing the publication of this work.



## INTRODUCTION

Man has always exploited his environment, for better or worse. By instinct and observation, he has both improved and destroyed his surroundings in peacetime and in war.

In both cases a basic knowledge, conscious or unconscious, of the geology and the surrounding environment has been a major factor affecting the outcome. Impressive engineering works, constructed on the surface and in the underground around Jerusalem in Biblical times and through the ages, must have involved considerable geologic knowledge. The construction of the First and Second temples, the Shiloah Gallery excavations of the 8<sup>th</sup> century BCE, the 2<sup>nd</sup> century BCE aqueduct system that supplied water to Jerusalem, the later catacombs of the Sanhedrin and the Herodian freshwater galleries and underground halls are only a few examples. Present-day highways, tunnels and viaducts are a modest contribution to reestablishing such engineering feats after several thousand years of relatively little development.

The use of the subsurface in Israel in recent times opened a new phase in the exploitation of ground resources for infrastructure development. The shortage of surface area, mainly in densely populated areas, has encouraged planners and designers of major engineering projects to consider going underground. The difficult topography in areas such as Jerusalem and Haifa, the increase in traffic volume on roads, storage and defense problems, as well as the increasing awareness of the impact on the environment, have given a further impetus to this trend. In many cases this has a significant economic impact. Compensation for appropriation of lands, destruction and relocating existing buildings can be significantly reduced by going underground. In many cases the cost of going underground may be offset by the cost of compensation and may provide better access with minimal damage to the environment.

The old and new cities of Jerusalem are situated mainly on Cretaceous hard limestone and dolomite and in places marl and chalk. The new city spread out over Senonian chalk and flint. These rocks occur in a topography of ridges and valleys, carved out in accordance with the geological structure of the region. The ridge tops are rounded and natural and artificial terraces in most areas form the slopes leading down into the valleys.

The Old City of Jerusalem was founded on a fairly flat ridge surrounded by deep valleys in the west, east and south, providing natural protection to the city. There is no natural morphological boundary on the northern extension of this ridge.

Modern Jerusalem spreads out over this and the adjacent ridges. The tops and slopes of these ridges form the builtup areas and the valleys between them generally form the green belts. Figure 1 shows a topographic map of Jerusalem and the vicinity on a scale of 1: 100,000 and Figure 2 shows the municipality boundaries in 1999, which approximate those of today.

Three fundamental factors favored the establishment and development of a city in this area: water, soil and religion. These factors have retained their importance throughout history and up to the present day. Water as an essential natural resource plays a major role in the political, environmental and social development of the region. Surface water in the Jerusalem area is restricted to springs emanating from limestone and dolomite aquifers at locations where they daylight in the topography above marl and clay units, forming a spring line.

Soil-covered terraces associated with these springs were the basis for early agricultural development. Old and modern olive groves as well as orchards typically cover the slopes near these outflows surrounding Jerusalem.

The ancient aqueduct systems that can be traced over the present-day topography channeled water from major springs south of Jerusalem to the old city of Jerusalem up to the end of the Ottoman's rule (1917). Today, however, these springs supply only a minor amount of the water required. The main supply is piped from the coastal plain. Some additional water was pumped from wells tapping the aquifers in Jerusalem and its vicinity; however, these have been abandoned lately due to pollution.

Other geomorphic and economic factors have contributed to the development of the area. These concern access and availability of raw materials for building purposes. Stone, cut or shaped, and aggregate was and is the major source of building material. Since other materials such as wood were not locally available, they had to be imported from great distances. The cedar wood used in the First and Second temples as well as in other later important buildings and structures, some of which still stand today, was imported from Lebanon.

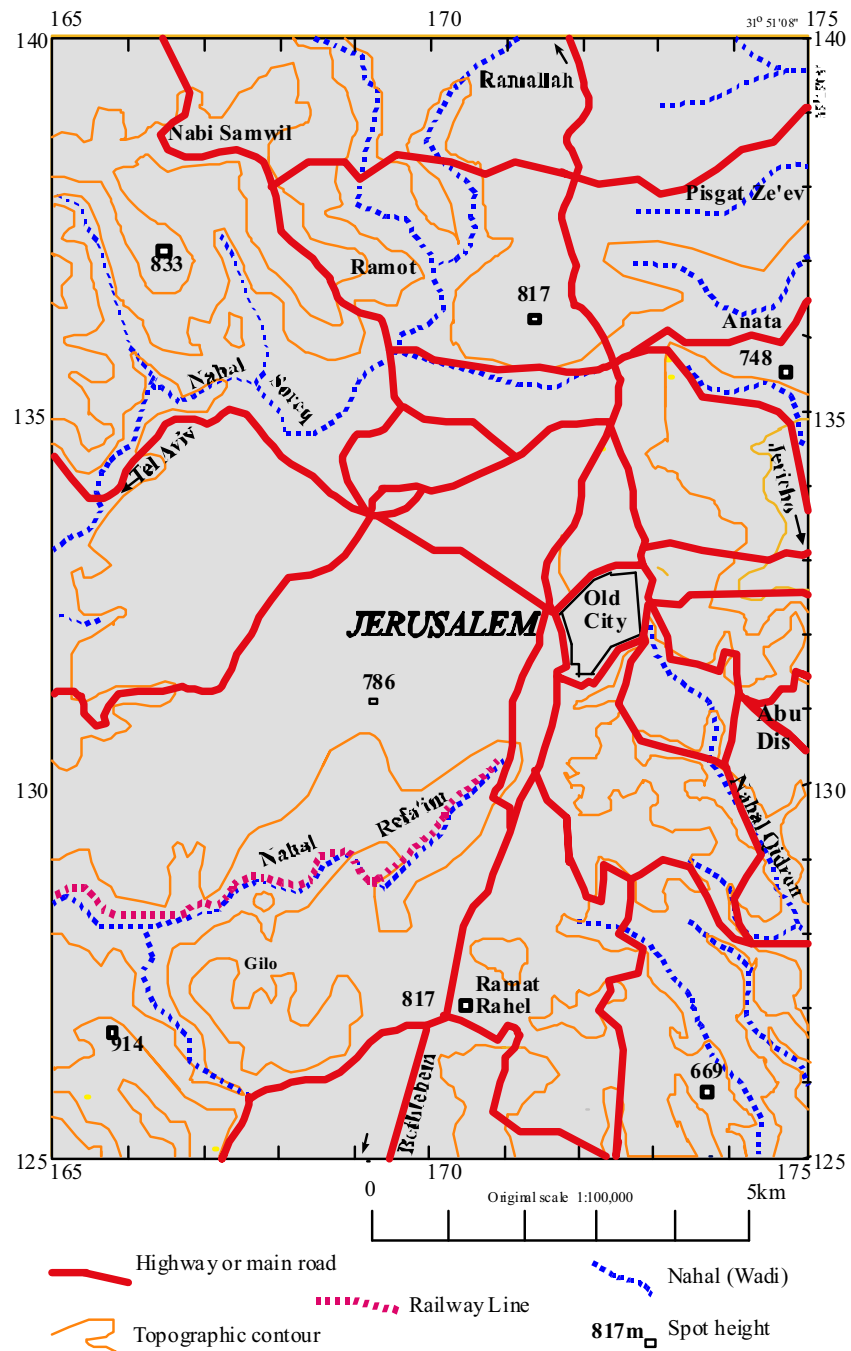


Figure 1. Topographic map of Jerusalem and vicinity.

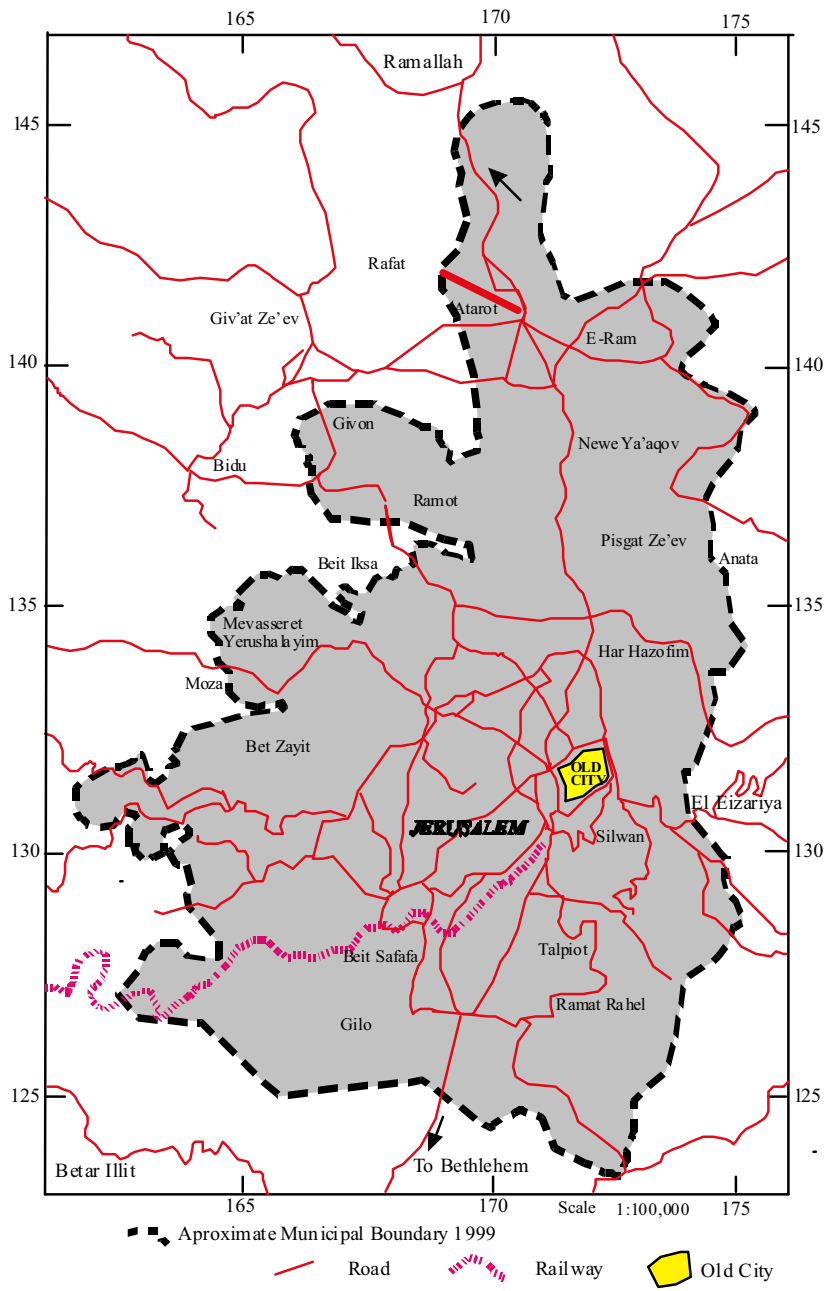


Figure 2. Municipality map of Jerusalem (1999).

The various rock types in the area were exploited for different purposes. The variety of lithologic types used in building are:

1. White, coarse crystalline limestone originally referred to as "Meleke", the stone of Kings.
2. Cream-colored micritic limestone known locally as "Mizzi Hilu" (sweet rock).
3. Red-colored limestone known as "Mizzi Ahmar" (red rock).
4. Gray crystalline dolomite known as "Mizzi Yehudi" (Jewish rock – modern times).
5. Flagstone of thin-layered limestone.

These rock types were quarried from the Judean limestone and dolomite in and around the Old City of Jerusalem.

This variety of stone gives Jerusalem its unique character. The setting sun reflected on the cream-colored limestone facade of both ancient and modern structures gives them a golden hue, giving rise to the term "Jerusalem of Gold".

Evidence of the high level of craftsmanship and organized labor in quarrying and exploiting the rocks in ancient times is seen in the Zidqiyahu Cave, known as Solomon's Quarries, located near the Damascus Gate, as well as at other numerous sites in the area (Avnimelech, 1966).

The concern to preserve historical and archeological sites has greatly impacted on modern-day infrastructure development. This is expressed in design and construction concepts that are governed by aesthetic and socio-economic concerns, not generally considered in many civil engineering projects.

Natural and man-made hazards have not bypassed this area. Although these are not obvious they can be of significant civil engineering and environmental concern. Natural phenomena such as earthquakes, landslides, karst, caves, as well as pollution of water and air, are inherent factors which nowadays must be taken into account in short and long range projects.

With the development of modern Jerusalem there has been a renewed interest in the environment and quality of life as affected by major civil engineering projects such as highways, tunnels and high-rise buildings (Arkin and Flexer, 1986). The rapid development of infrastructure and building is evidence of a vibrant modern city committed to respecting and preserving its ancient and historical past. In Israel in general and in Jerusalem in particular, ground conditions are significantly different from place to place. The rocks are mainly sedimentary and water is not an obvious part of the environment. This factor made it necessary to adapt the accepted geotechnical methods to these conditions. The success of a civil engineering project therefore relies on the availability and quality of data on the relevant ground conditions. The accurate geological evaluation of the parameters describing the rock mass is an essential

part of planning, design, and construction and is a necessary part of pre-feasibility and feasibility studies. Landmark events in the history of Jerusalem present a tale of construction, destruction and reconstruction, which had major environmental impact that is felt to this day. These events are highlighted in Appendix 1.



Figure 3. Moderate Resolution Imaging Spectroradiometer (Modis) image showing regional setting, acquired February 29, 2000.



Figure 4. Judea Mountains south of Jerusalem. Exposed formations range from the Soreq Formation in the valley to the Kefar Sha'ul Formation.



Figure 5. Judea Desert east of Jerusalem.

## **GEOGRAPHIC SETTING**

Jerusalem is located geographically at 31° 78' N and 35° 21' E within the region known as the Eastern Mediterranean (Figure 3).

The city is located in the Judea Mountains at elevations of 700-820 m above mean Mediterranean Sea level within a west-east climatic gradient that ranges from a long dry, hot summer to a short wet and cold winter. The mean annual rainfall is over 500 mm, generally occurring from October to April, compared to 600 mm in the coastal plain (Netanya) decreasing eastwards to a mean annual rainfall of less than 110 mm at the Dead Sea. The annual average temperature ranges from 8°-28°C across this gradient (Maheras, et al., 1995) with a maximum temperature that may reach up to 34°C and more in the summer and below zero in the winter. During some winters 1-3 days of snow may fall.

Jerusalem extends over the regional surface water divide in the Judea Mountains (Figures 63 and 64). This divide clearly separates the region into two distinct climatic zones. The western side of the divide is Mediterranean with the typical variety of soil and plant cover. Figure 4 shows the main geological formations on the western side of the divide. The eastern side, which is in a rain-shadow environment of restricted soil and plant cover, forms the Judea Desert (Figure 5).

The Old City of Jerusalem extends along an NE-SW oriented ridge limited to the east, west, and south by consequent drainage valleys of the Soreq, Refa'im and Qidron valleys. Modern Jerusalem has spread to the adjacent ridges in both north, south and west directions.

## **GEOLOGICAL SETTING**

In geological times the rocks in the Jerusalem area were deposited during the transgression of the Cretaceous Tethys Sea that encroached from the NW over most of the Middle East region. This sea spread out over a broad continental shelf of the Arabian-Nubian shield and was generally warm and shallow. The fauna that existed in the sea and now found as fossils within the various formations include abundant shells of microorganisms, lamellibranches, echinoderms, rudistids and gastropods. Reef structures were formed in the shallow areas (Arkin and Hamaoui, 1967). Dinosaurs that roamed the shallow mud flats left their foot prints (Avnimelech, 1962).

Continued transgression of the sea over this uniform shelf led to the deposition of a thick carbonate sequence reaching almost one kilometer in the Jerusalem area. This shelf later gradually became modified by tectonic



movements that led to the development of the anticlinal and synclinal structures. Today the anticlinal structures form the mountainous backbone of the country.

Jerusalem is situated north of the structural saddle between the NE-SW orientated Judea and Hebron anticlines (Figure 6). These asymmetric structures have a steep western flank dipping down to the foothills of the coastal plain and a shallow eastern flank that dips gradually down to the Dead Sea Rift valley (Figure 7).

Following the development of these structures and uplift, a variety of softer carbonate rocks (chalk and marl) of Senonian age and with inherent crystallinity and fossil content were deposited in the synclines and overlapping the flanks of the anticlines. These rocks also contain abundant microfossils, ammonites and fish remains (skeletons, teeth and scales). Younger sediments of Neogene and Quaternary age were generally deposited on the flanks of the anticlines and in the synclines.

The rock sequence is subdivided into three groups. The Lower Cretaceous Kurnub Group of mainly clastic rocks occurs in the subsurface core of the Judea and Hebron anticlines, only exposed in the deepest wadis (Arkin, 1976). This sequence is made up of mainly sandstone with some carbonate layers. The overlying Upper Cretaceous Judea Group carbonates form the anticlines. This group in turn is overlain by the Upper Cretaceous to Tertiary Mount Scopus Group of chalk and massive chert that generally form the flanks of the anticlines.

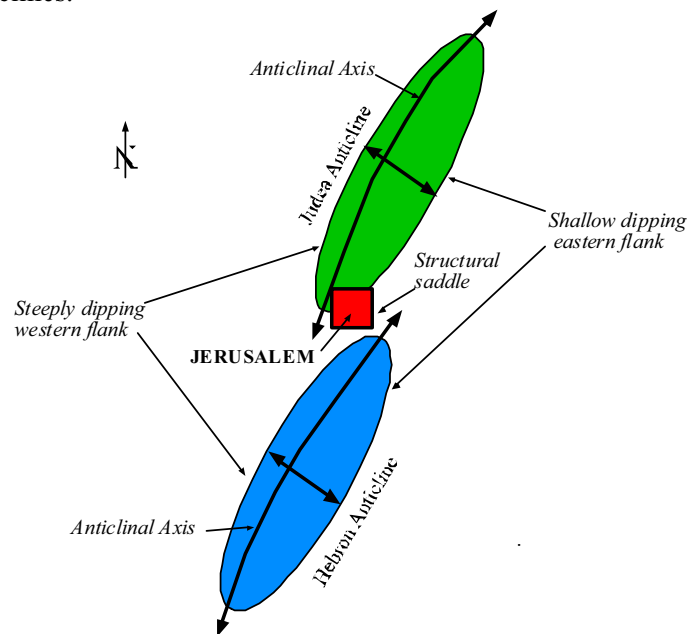


Figure 6. Schematic diagram of the location of Jerusalem in relation to the geological structure.

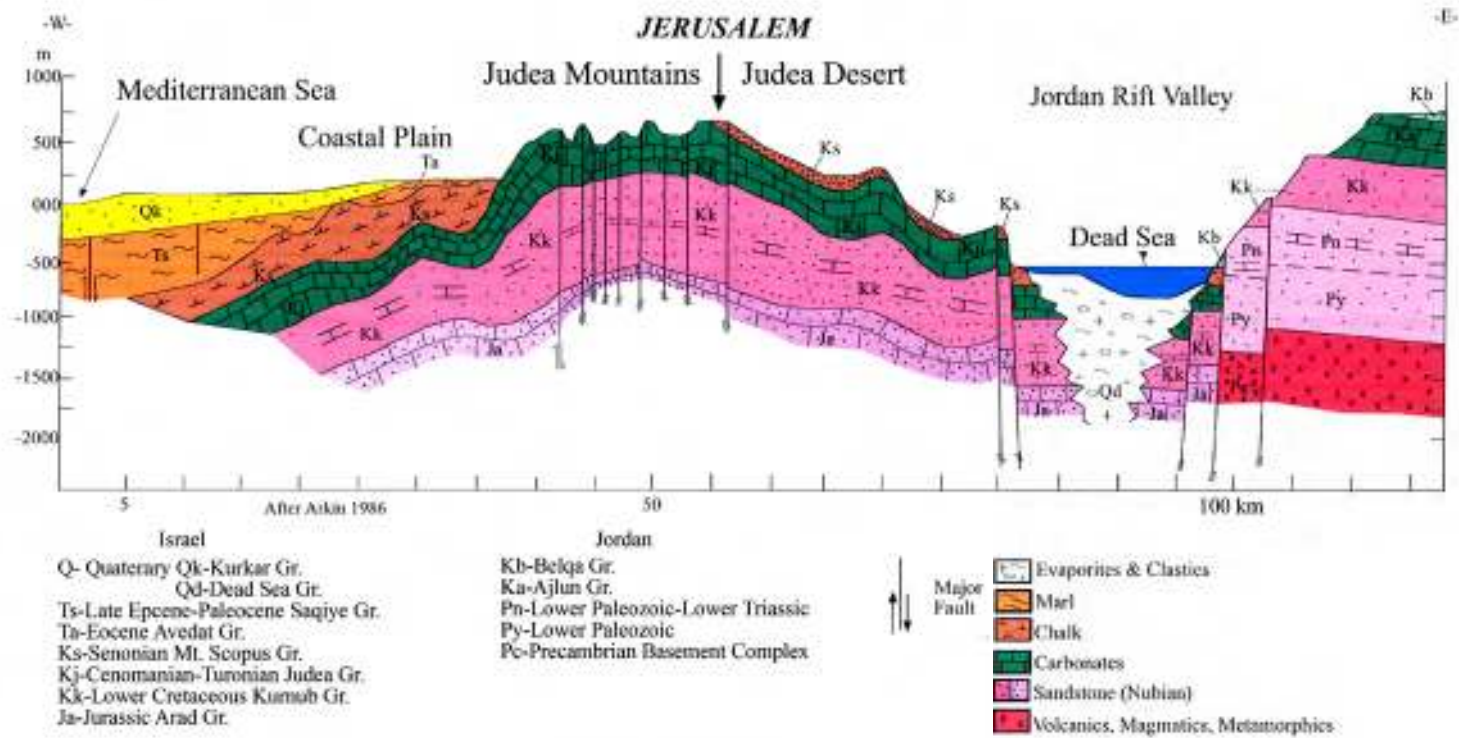


Figure 7. Schematic East-West composite geological cross section through central Israel.

The Judea and Mount Scopus groups are the main rocks exposed in the Jerusalem area. These comprise limestone, dolomite, marl, chalk and flint which are subdivided into lithostratigraphic units that are correlatable with units in other parts of the country.

The Judea Group (Arkin & Hamaoui, 1967) of Cenomanian to Turonian age reaches a total thickness of over 900 m in the Jerusalem area (Figures 8 and 9).

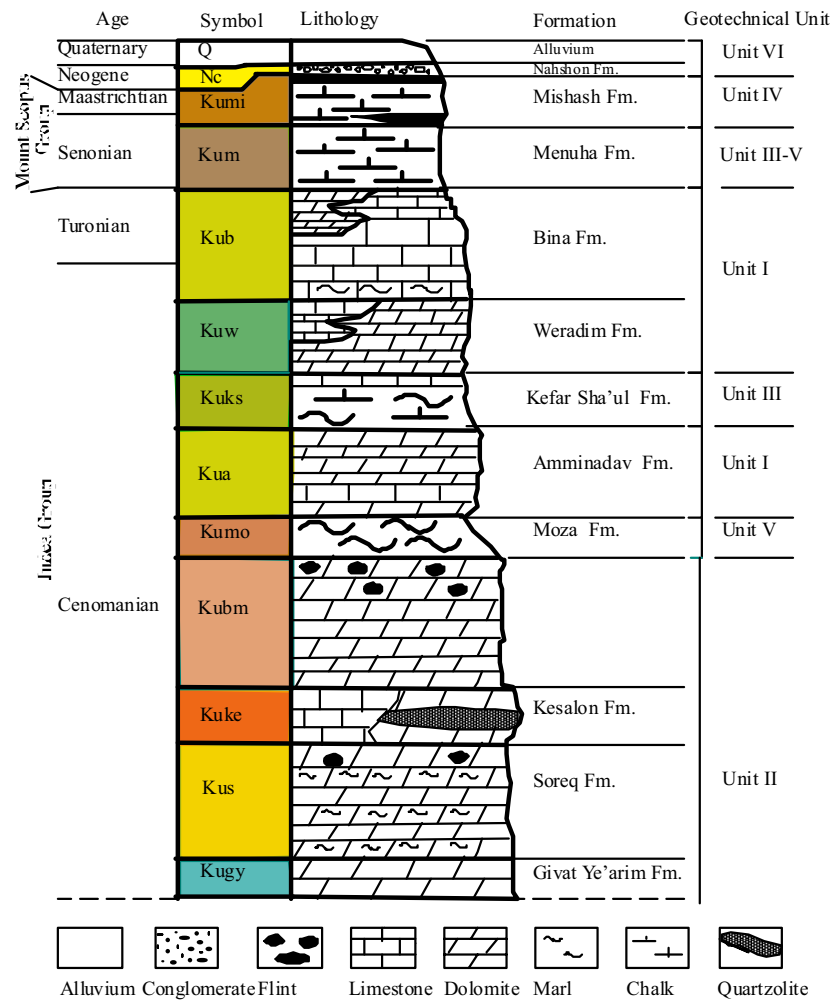


Figure 8. Stratigraphic legend of the geology in the vicinity of Jerusalem.



Figure 9. Geological map of Jerusalem and vicinity.

The group is subdivided into a lower sequence of terraced, well-bedded dolomite with minor limestone and marl and an upper more massive sequence of limestone, dolomite with some chalk and marl. The Moza Formation of marl, clay and some limestone separates these sequences and represents a key horizon with regard to understanding the structure and hydrogeology of the area (Itzhaki and Arkin, 1964). The Amminadav Formation which overlies the Moza Formation is made up of massive dolomite, porous in many places with large voids, especially along major fractures. These features make it an important

aquifer in the subsurface. The overlying Kefar Sha'ul Formation consists of well-bedded limestone, chalk and some marl. This well-bedded limestone is the main source of natural flagstone used for paving and facing stone. The Weradim Formation of hard, gray dolomite overlies the Kefar Sha'ul Formation. In the past this dolomite was quarried as a strong but dull building stone. Today it is crushed as aggregate and used in the building industry. The Weradim Formation is characterized by karst phenomena in the form of caves with stalagmites, calcite curtains and crystal clear pools such as in the Soreq caves. The top of this sequence is made up of well-bedded micritic, pale yellow limestone and thickly bedded white, coarsely crystalline limestone of the Bina Formation. These rock types have been and are being quarried today for use as polished stone and facing stone and are the basic building blocks of Jerusalem.

The overlying Mount Scopus Group of Upper Cretaceous to Paleocene in age ranges considerably in thickness, thinning out on the anticlinal flanks and in some cases, wedging out completely (Arkin, 1976). The main formation of this group around Jerusalem is the Menuha Formation consisting of white chalk mixed with clay in some areas. The chalk in some places is irregularly stained pink to pale red, giving it a particular pleasing appearance. It is often used as a facing stone. In the Hartuv area southwest of Jerusalem, these rocks are a source of raw material for the cement industry. The Mishash Formation of massive brown chert and flint overlies this chalk and around Jerusalem it is mainly found on the eastern side of the city (Arkin, 1976).

Climatic conditions and consequent weathering and erosion have imposed a distinct morphology and topography on the lithology of the various exposed rock types. The softer rocks generally form the rounded higher elevations, with broad man-made terraces. The harder rocks form the natural step-like terraces on the slopes and floors of the valleys. A gray to white caliche crust, referred to as 'Nari', developed over the softer rock. Typical Mediterranean red-brown Terra Rosa and brown to gray Rendzina soils formed on the limestones and chalks, respectively. The valleys between are filled with conglomerates and alluvium of varying thickness.

Natural marl terraces that have been intensely cultivated for several thousand years characterize the break between these two distinct morphologies. Many springs flow out over this marl and this water was used in the past to irrigate the many vineyards, olive groves and orchards planted on these terraces. Today most springs are in protected picnic areas within national parks.

Several of the rock types within the above groups have, as in the past, an important economic significance affecting the development of Jerusalem. Quarrying these rocks provides aggregates and crushed rock as well as polished and sculptured slabs.

## GEOTECHNICAL SUBDIVISIONS

Fresh rock generally appears only in road cuts and excavations. Thus to define the geotechnical characteristics of the rock types at the beginning of an infrastructural project, it is often necessary to remove the superficial cover and carry out core drillings to test the rocks.

The definition of the geotechnical characteristics and the physical and chemical properties of the rock types are based on the interaction between air, water and rock affecting the fabric of the rock. Three parameters are involved, lithology, fracture and water (Figure 10).

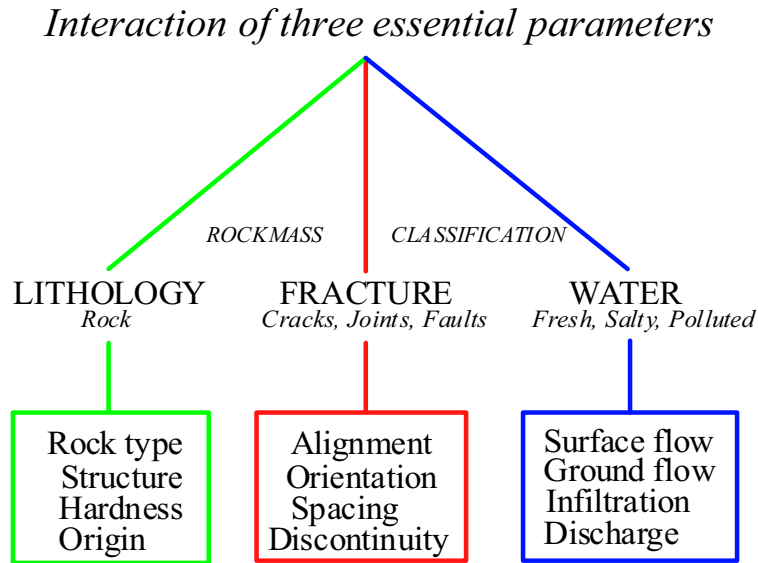


Figure 10. Factors affecting the geotechnical properties of the rock mass.

It is essential in design and construction of major civil engineering projects to determine the extent of properties such as strength and plasticity as well as the presence of discontinuities (faults, fractures and karst). These are no less relevant factors in environmental problems, particularly where remedial action is necessary.

The classification of the rock mass enables the numerical expression of the quality of the rock mass for engineering purposes. Planning of tunnels or other subsurface structures and foundation conditions are based on the geotechnical definition of the rock mass determined by the physical, chemical and mechanical properties of the rocks concerned. This enables the

determination of the size of the opening, the method of excavation, and the stability of the rock mass. All these parameters have an important impact on the economic cost of the supports necessary for the construction of a safe structure, both on the surface or underground, in the short and long term. The common methods for determining the quality of the rock mass were developed in North America and northern Europe where hard rocks (igneous and metamorphic) are dominant and groundwater are an integral part of the rock mass. In Jerusalem and Israel in general water is not a major constituent of the ground at or in the near surface. Thus it has been necessary to adapt these methods to the particular features of sedimentary rocks that build most of the country.

The main features apart from water that influence the quality of sedimentary rocks are discontinuities that include faults, fractures, bedding planes, facies changes, and geological structures. Changes in the volume of clay and sand, within the rock fabric and irregularity of grain size are also important characteristics. Discontinuities are classified according to direction, form, frequency, density, and degree of opening.

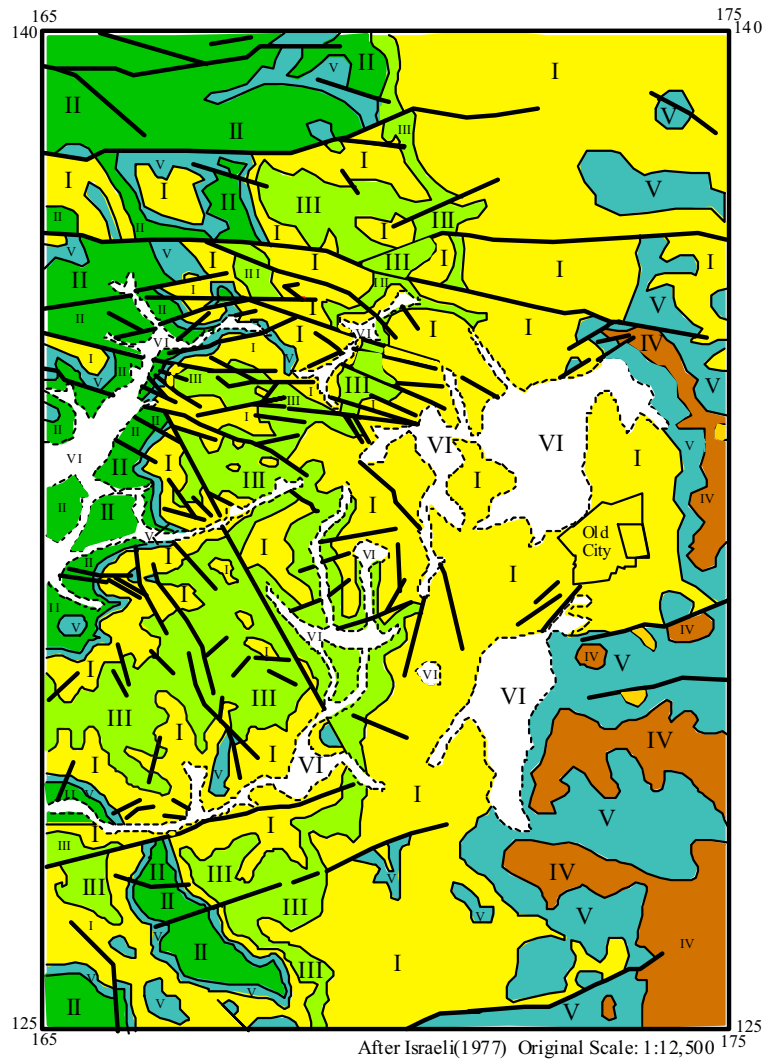
Fractures fall into two groups. Firstly, systematic fractures that are part of the regional stress regime and are characterized by continuity, and secondly, non-systematic fractures that are discontinuous and are part of the local stress relief system. These latter fractures usually disappear at depth.




The various geological formations in the Jerusalem area have been grouped together into six suggested geotechnical units of similar geotechnical properties as shown in Figures 8 and 11. Additional parameters from ongoing projects such as the Light Railway and the Jerusalem–Tel Aviv Rapid Railway may change the boundaries of these units.

Following is a description of each unit:

**Unit I. Hard limestone and dolomite.**

Unit I includes the Bina Formation (Kub), Weradim Formation (Kuw) and Amminadav Formation (Kua). These geological formations are generally comprised of hard massive to well-bedded limestone and dolomite. The ratio of Ca/Mg gives rise to a range in geotechnical properties (Table 1 ). Core recovery is very good, often up to 100%. Rock Quality Designation ( RQD: Deere at. Al. (1974) which is based on the amount of core recovered, is 70-100%, depending on the presence of fractures, bedding and karst phenomena.



<b>I-Geotechnical Unit</b>		<b>Kus - Lithological Unit</b>	
I	- Kuw, Kub, Kua	IV	- Kumi, Kum
II	- Kugy, Kus, Kuke, Kubm	V	- Kumo
III	- Kuks, Kum	VI	- Q
	Contact		Fault
			Alluvial contact

See Figure 8 for geological legend and lithological description.

Figure 11. Geotechnical map of Jerusalem and vicinity.



The Rock Mass Rating (RMR: Bieniawski 1980) is generally of good quality, 72-84, and the internal friction angle ( $\phi$ ) is high, 40°-45°. RQD, RMR and Q (Barton, et al., 1974) are classification methods of determining rock quality for tunneling purposes. Karstic features are quite common in the form of solution holes and caves often infilled with red-brown Terra Rosa soil and rock fragments. In these areas the surrounding rock is often weathered to various degrees, considerably lowering the rockmass quality. For other properties see Table 1 and the Appendix.

Table 1. Geotechnical parameters of the Amminadav, Kefar Sha'ul and Weradim formations. General values from the vicinity of Jerusalem

<b>Formation</b>	<b>Amminadav Fm.</b> Dolomite & Limestone	<b>Kefar Sha'ul Fm.</b> Marl & Limestone	<b>Weradim Fm.</b> Dolomite & Limestone
<b>Geological Symbol</b>	<b>Kua</b>	<b>Kuks</b>	<b>Kuw</b>
<b>Carbonate %</b>	79 - 100	95 - 99	98 - 100
<b>Bulk density</b> t/m <sup>3</sup>	2.21-2.77	2.34-2.45	2.34-2.67
<b>Porosity %</b>	0.25-22.36	2.96-13.29	0.18-13.29
<b>Permeability</b> md. (Millidarcy)	0.10-26.00	0.09-0.27	0.13-0.32
<b>Tensional strength</b> (2" plug) MPa	9-27	6-16	14-18
<b>Tensional strength</b> (2cm plug) MPa	5-19	5-23	13-26
<b>Point load strength</b> (Field specimen) MPa	99-251	112-147	121-217
<b>Deformation %</b> (Elasticity) MPa	0.98-1.51 3310-5940		0.85-1.93 2160-4940
<b>Sensitivity to Water</b> (Ratio dry/sat. strength)	1-1.5 (medium)	>1.5 (high)	<1 (low)
<b>Bearing Capacity</b> (Foundations) MPa	>1 (high)	0.4 (low)	>1 (high)
<b>Uniaxial Strength</b> (Schmidt Hammer) MPa	21-100	6-86	90-100
<b>Uniaxial Strength</b> (Plugs) MPa	28-111	10-60	43-140

MPa = Mega Pascal  
(Adapted from Israeli, 1977)

### **Unit II. Dolomitic limestone with interbeds of marl and quartzolite.**

Unit II is made up of the Bet Me'ir Formation (Kubm), Kesalon Formation (Kuke), part of the Soreq Formation (Kus), and the Givat Ye'arim Formation (Kugy). These formations are often evenly well-bedded with thin marl layers between beds. They generally form characteristic step-like terraces on valley slopes. Low walls of in situ stone have been built on the edge of the terraces to retain the soil developed on them. The fresh rock is generally of satisfactory to good quality Q with a value of 14-16 and an RMR of 60-80. Weathered and fractured rock is considerably poorer with Q values as low as 0.25- 0.09 and RMR of 26-49. Other properties may be found in the Appendix.

### **Unit III. Limy dolomite, dolomitic limestone and partly weathered chalk.**

The Kefar Sha'ul (Kuks) and the lower part of the Menuha Formation (Kum) make up Unit III. The rockmass consists of partly weathered rock with the degree of weathering conforming to the variations in the Ca/Mg content of the rock. The Kefar Sha'ul rock (Table 1) may be well and thinly bedded. The Menuha chalk (Tables 2 and 3) may contain varying amounts of clay. The quality of the rockmass ranges considerably from fair to good. The RMR values range from 48-55 and the Q values from 0.28-7.50. The Rock Quality Designation ranges greatly from 17-84%.

This unit includes three types of rockmass, ranging in geotechnical properties. The distribution of these is variable and interchange within a few meters. These are:-

- a) White to gray massive chalk, which may reach the hardness of limestone in places. Fossil relics and solution features with calcite infillings are present. Core recovery is good and the RQD ranges from 30-60% and is directly related to the density of fractures.
- b) White to gray and pink, massive clayey chalk with fractures infilled with clay and calcite. Core recovery and RQD range greatly. Swelling pressure ranges from 0.33 to 0.57 kg/cm<sup>2</sup>.
- c) Light yellow to brown massive marl and clay often with limonite and manganese staining. Core recovery and RQD range greatly and swelling pressure may reach 2.51 kg/cm<sup>2</sup>. Uniaxial free swell may exceed 3%.

The diversity of these rockmass types creates potential weakness areas of variable quality. They are sensitive to water with the clay fraction forming mud and the marl becoming fissile. The swelling pressure of clay ranges from 0.33-0.57 kg/cm<sup>2</sup> and can reach up to 2.51 kg/cm<sup>2</sup>. The Unconfined Compressive Strength of dry chalk can average 88.5 kg/cm<sup>2</sup> and the Modulus of Elasticity 57x10<sup>3</sup> kg/cm<sup>2</sup>. Marly chalk is considerably lower, at 13.6 kg/cm<sup>2</sup> and the modulus of elasticity is 6.8x10<sup>3</sup> kg/cm<sup>2</sup>, however under dry conditions the

rockmass is cohesive and stable. Chalk with an average unconfined compressive strength tested for instantaneous cutting rate with roadheaders in tunnelling gave the following results: 65-90 m<sup>3</sup>/hr for an MK2B medium duty roadheader and 100-125 m<sup>3</sup>/hr for an MK3 heavy duty roadheader.

#### **Unit IV. Chert, flint and silicified chalk concretions.**

Unit IV includes the Mishash Formation (Kumi) of massive brown chert and flint with silicified chalk and some phosphorite beds. This unit also includes the silicified chalk and brown flint that occurs in the upper part of the Menuha Formation (Kum). The chert and flint are essentially made up of quartz with a hardness similar to glass, and occur as discontinuous bands or individual concretions causing difficulties in drilling and excavation.

#### **Unit V. Marl and chalk**

Marl and chalk make up the main rock mass of the Moza Formation (Kumo) and parts of the Menuha Formation (Kum). The upper part of the Bet Me'ir Formation (Kubm) which underlies it, is similar to the Moza Formation, in areas around Jerusalem. Clay lenses and individual limestone beds occur in places. This rock mass is sensitive to water and disintegrates quickly. Circular slides and mudflow can occur. Geotechnical properties of the individual rock types are given in the various tables. The main feature of this unit is the disturbed Transition Zone at the contact between the overlying Amminadav Formation on the Moza Formation. The massive dolomite of the Amminadav Formation has sunk into the softer marl of the Moza Formation causing, isolated blocks to be embedded in the marl (see Hazards).

#### **Unit VI. Unconsolidated material and superficial cover.**

Unit VI is made up of clay, carbonate sand, gravel and rock fragments. The clay is generally montmorillonite, typical of Terra Rosa soil, resulting from in situ disintegration of limestone. Other clay minerals such as kaolinite and illite are found in the Rendzina soil developed on chalk. Properties of the main components of this rock mass are found in Table 4 and in accompanying tables. The rock mass is found on terraces and filling valleys. In places such as around the Old City of Jerusalem this unit is made up of rubble of archaeological origin. The unit forms a superficial cover in most places that is generally removed in infrastructure projects. However in specific areas it can be unstable, becoming a hazard (see sinkholes). Table 4 shows the geotechnical properties of soil and alluvium.

Table 2. Representative geotechnical properties of rocks in the Menuha Formation.  
(Arkin & Michaeli, 1988a,1989b,1992) Arkin et al, (1989).

PROPERTIES	CLAY	CHALK	MARLY CHALK
Specific Gravity (Gs)	2,59-2,68	2.62-2.65	2.63-2.65
Dry Density ( $\gamma_d$ ) Kg/cm <sup>3</sup>		1802-1945	1566-1795
Plasticity Index (PI) %	13.6-31		
Plastic Limit (PL) %	17.6-24.6		
Liquid Limit (LI) %	31-56		
Uniaxial Compressive Strength (Sc) MPa		15-21	8.1-12.3
Tensional Strength (St) MPa		2.71-5.2	1.97-2.48
Sonic Velocity (V) m/s		2659-3314	2243-2828

Table 3. Representative geotechnical properties of clayey chalk samples  
(Arkin & Michaeli, 1988a,1989b,1992) Arkin et al, (1989).

		Sample AG/2	Sample AG/12
Specific Gravity	Gs	2.63	2.59
<b>Plastic Limit</b>	<b>PL</b>	18	-
Liquid Limit	LL	30	-
Shrinkage Limit	SL	22	
Plasticity Index	PI	11	
Free Swell	FS	47	112
Carbonate Content	%	89	68
Cohesion	c Kg/cm <sup>2</sup>	0.22	0.35
Friction angle	$\phi^\circ$	32	25

Table 4. Representative geotechnical properties of soil and alluvium samples.  
(Arkin & Michaeli, 1988a,1989b,1992) Arkin et al, (1989).

		Sample AG/4	Sample AG/7	Sample AG/19
Specific Gravity	Gs	2.56	2.60	2.56
<b>Plastic Limit</b>	<b>PL</b>	24	19	39
Liquid Limit	LL	40	31	65
Shrinkage Limit	SL	25	20	13
Plasticity Index	PI	16	12	26
Free Swell	FSW	73	58	95
Carbonate Content	%	69	74	13
Cohesion	c Kg/cm <sup>2</sup>	-	-	-
Friction angle	$\phi^\circ$	-	-	-

## GEOTECHNICAL AND ENVIRONMENTAL CONCERNS

### Hazards

A geological hazard may be defined as a phenomenon in which the natural physical conditions present a risk that may result in damage, injury or loss of life. The end effect may be reached either through natural processes or those initiated or intensified by man. Water is considered to be the major contributing agent to instability, and its uncontrolled addition or removal from the natural environment results in the disturbance of the steady-state conditions. The equilibrium existing between the natural physical and chemical parameters such as strength, porosity, compaction and carbonate solubility occurring in the geological environment is upset.

Generally speaking, hazards may be subdivided into two broad groups. The first group includes those having their expression at the surface such as land slides and floods, and a second group which occurs mainly in the subsurface and is expressed by sinkholes, compaction or subsidence. These various phenomena are presented here in figures and photographs accompanied with explanations, using the accepted nomenclature in the geological and geotechnical literature.

The recognition, inventory and research into the geological conditions and earth processes concerned with these hazards is therefore an essential factor in the prevention, reduction of effectiveness, and remedial action required to overcome the particular hazard (Table 5).

The purpose here is to describe the type of hazard that has been recognized to date in the geological environment around Jerusalem and to point out the directions for future research into these phenomena. Appropriate remedial action can then be taken, to prevent or reduce the effect of the hazard after a detailed study and evaluation is carried out.

In many cases the trace of a fracture or fault on the surface is masked by weathering features such as nari (caliche) soil or vegetation. The trace of these features may often only be recognized as a topographic offset, step or terrace, or just a faint discontinuity in the topography. However in the subsurface and with depth faults and joints tend to be more obvious, particularly in sedimentary rocks and more commonly in carbonate rocks. The competency of the rocks plays an important role where fractures are seen to be open within the harder layers and closed within the softer ones (Figure 12).

Table 5. Earth processes causing instability relevant to areas around Jerusalem.

<b>Subject</b>	<b>Initiator</b>	<b>Geometric Changes</b>	<b>Ground conditions</b>	<b>Main process</b>	<b>Result</b>
Roads Highways Bridges Viaducts Railways	Construction Excavation Erosion	Height Slope	Soft rock Soil	Changes in stress Fracture opening Piping	Increased shear stress causing, faulting, sliding. Increased pore pressure causing flow, slides and tensional opening. Disintegration
Ground Movement Earthquakes Blasting.	Vibration Acceleration	Deformation Folding Faulting	Un-consolidated Saturated	Redistribution of blocks and particles	Reduced cohesion, Increased shear stress causing faulting and slides. Increased pore pressure, causing flow, slides, tensional opening
Cliffs Slopes Valleys	Erosion	Height Slope Rockmass	Soft, weak rock, marl, clay and sand	Stress relief opening of discontinuities	Increased pore pressure. Reduced cohesion causing deformation, flow, and slides
Dams Rivers Embankments Aquifers Floods	Rain Snow Drought	Height Slope Volume	Consolidated soft rock,	Unloading, solution swelling, opening of discontinuities.	Reduced pore pressure, stress and cohesion causing flow, creep and sliding.

Solution plays an important part in dissolving the carbonate and widening the fractures, causing an irregular configuration. The solution process begins only after several meters below the surface and this appears to involve the temperature of the solution agent and its degree of solubility. Differential opening of fractures in alternating competent and incompetent limestone units of differing hardness can be seen in a quarry face in the Bina Formation (Figure 12).

In a topography such as that of the Judea Mountains the valleys are generally steep-sided and the valley floors filled with alluvium of varying thickness. The valley sides often reflect the nature of the underlying bedrock. For example, the well-bedded dolomite and limestone of the Bet Me'ir and Soreq formations form fairly evenly spaced steplike terraces with a thin soil cover, whereas the softer marl rocks of the Moza Formation form broader terraces of good soil with moisture from seepages and springs (Figures 4,63).

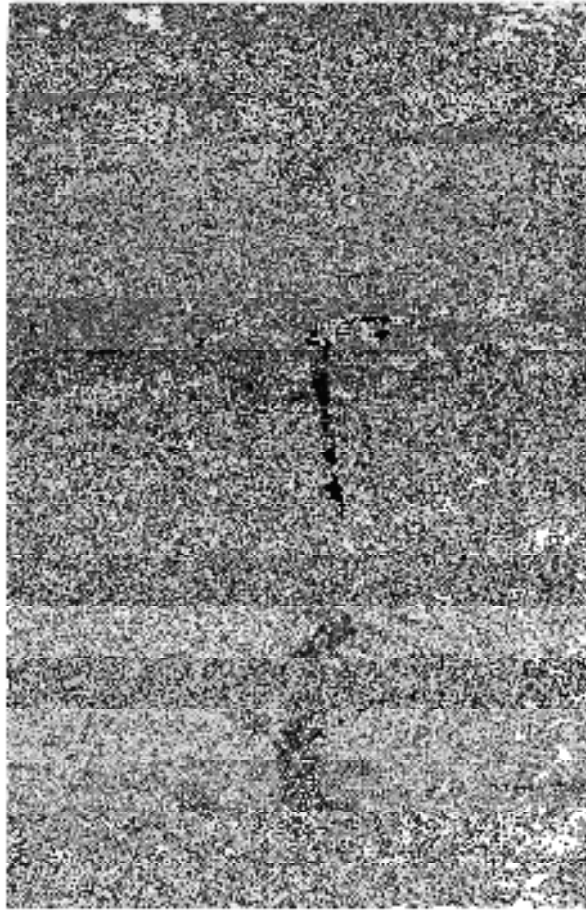
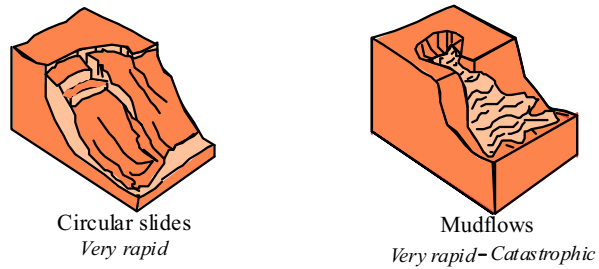


Figure12. Differential opening of fractures in layered rocks due to changes in brittleness of rock type seen in the Bina and Soreq formations.

The valley sides in places are prone to ground movement. The principle modes of rock mass failure in the sedimentary rocks around Jerusalem are shown in Figures 13 and 14. Figure 15 shows the morphology of a natural and cut cliff face and the terminology used to describe it. The resulting phenomena are seen as superficial creep of the soil cover (Figures 16 and 17), tumbling blocks in road cuts and quarries (Figures 18 and 19), dip slope failures (Figure 20), circular slides of considerable volume in the softer rocks and mudflow in marls where water is concentrated (Figures 21 and 22). Often these phenomena occur catastrophically induced by heavy rains, earthquakes or both. The relationship of these phenomena to earthquakes in the Jerusalem area are dealt with by Salamon, et al. (2003) and Katz, (2004).



Approximate rates of movement

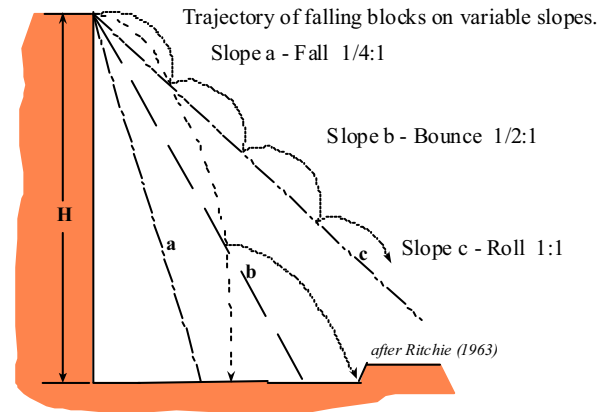
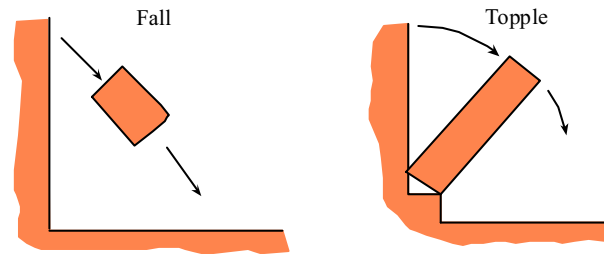
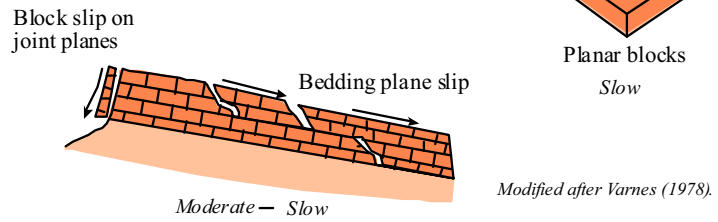
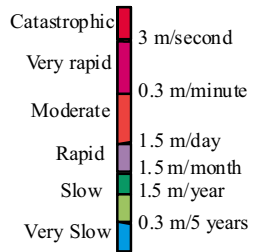


Figure 13. Principal modes of rock mass and soil failure occurring in the Jerusalem area.

Figure 14. Modes of rock fall occurring in the Jerusalem area.



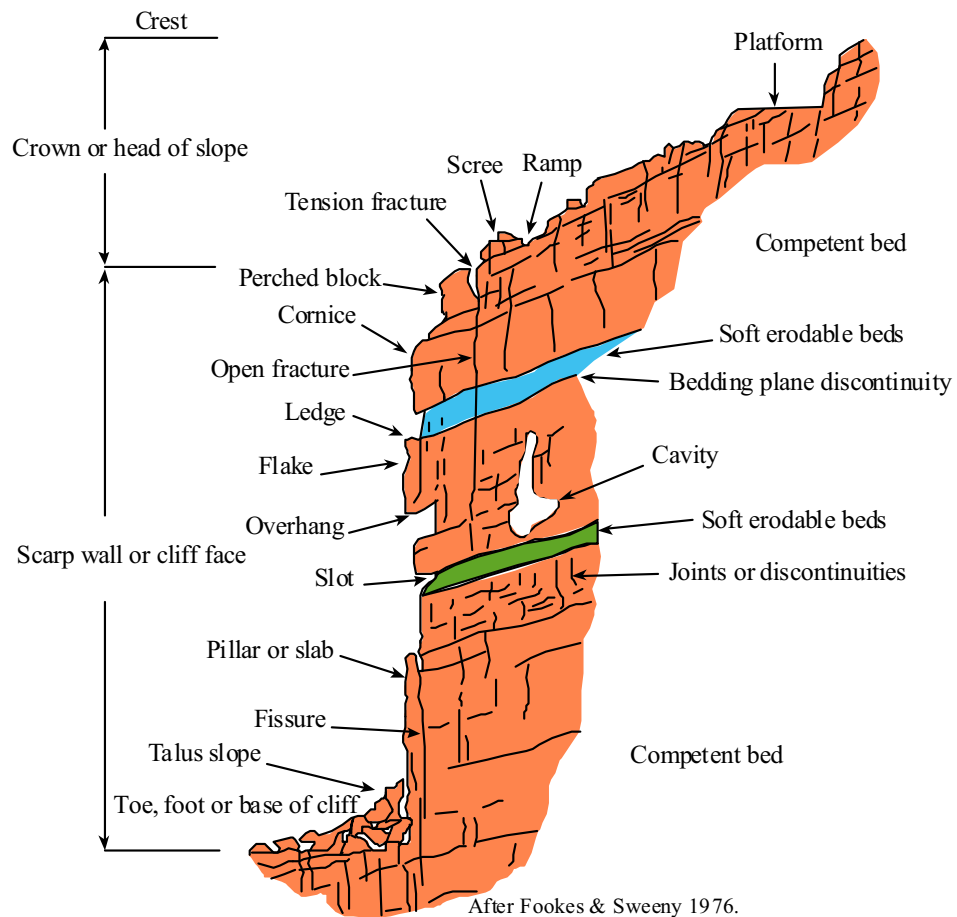


Figure 15. Schematic morphology of a cliff face or open cut wall.



Figure 16. Soil creep downslope in the Judea Mountains. Note trees tilted and bent downslope.

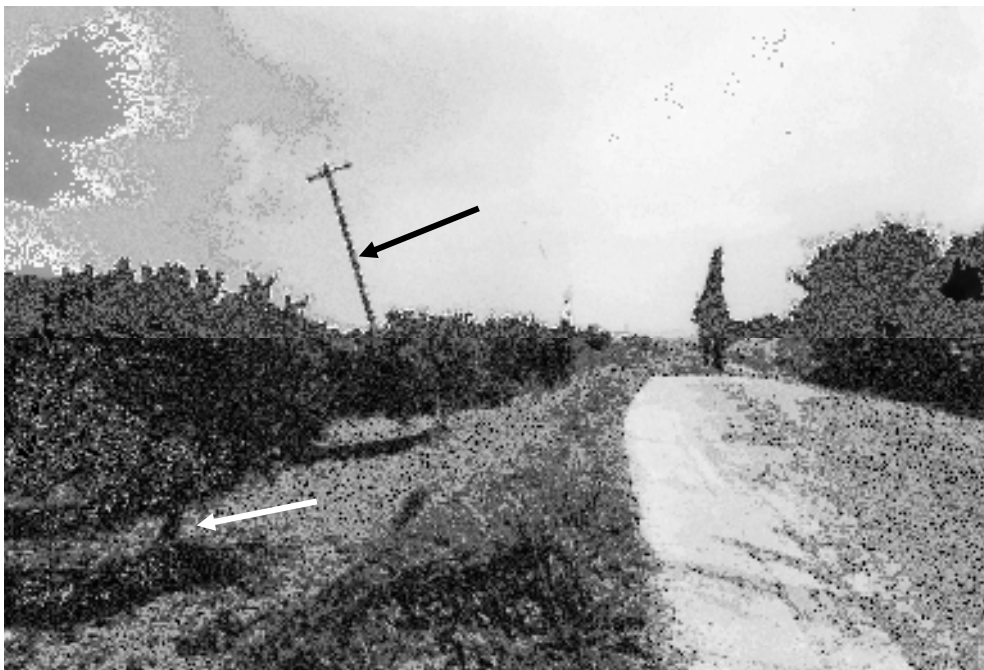


Figure 17. Soil creep downslope in the Judea Mountains. Note telephone pole and trees tilted downslope.

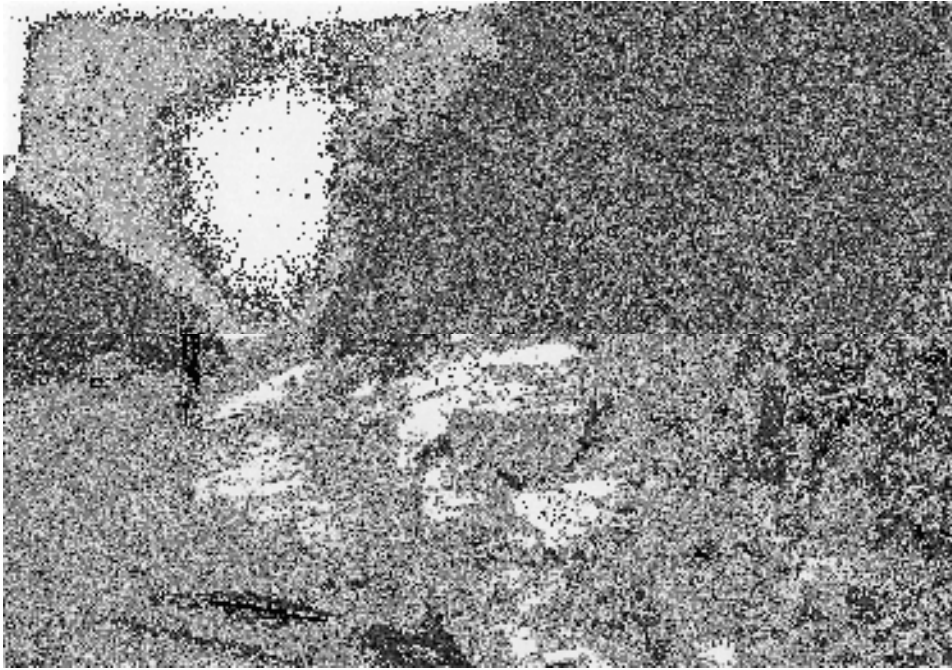


Figure 18. Rock fall in roadcut in the Soreq Formation, Jerusalem – Tel Aviv highway near Abu Ghosh.



Figure 19. Rock fall in roadcut in the Moza Formation, Jerusalem – Tel Aviv highway.



Figure 20. Dip slope failures in road cut.



Figure 21. Circular slide and scar in the Moza marl exposure ,  
Tel Aviv – Jerusalem highway.



Figure 22. Mudflow in the Moza Formation marl in a roadcut after rains.

### **Sinkholes**

Sinkholes can occur in valleys, particularly over karstic limestones. For example, in the winter of 1980 a series of sinkholes developed in both natural and artificial environments in various parts of Israel. Some were especially large, reaching several meters in diameter and reaching depths of several meters.

A sinkhole that developed near the Damascus Gate of the Old City of Jerusalem (Figure 23) serves as a good example (Arkin, 1984). It occurred in the area northwest of the gate, which was the construction site of a new junction on Road No.1 (Figure 24). The area was flat and had been reshaped several times during the past centuries as buildings were destroyed and the area filled-in with rubble and building waste. This artificially changed the topography and left “underground” openings that altered the natural drainage regime of the area. As a consequence of unusually high and concentrated rainfall, several sinkholes of various sizes appeared in the ground. The largest sinkhole was 8 m in diameter and 6 m deep.

A detailed geotechnical survey of the area (Figure 24) in the vicinity of the Damascus Gate was carried out to determine the type and depth of the fill material, the presence of karstic openings in the limestone bedrock and man-made openings such as buried cellars, water wells and aqueducts (Figure 25). Each one of these openings was considered to be a reasonable initiator of a sinkhole. Old maps of the area such as the Ordinance Survey of Jerusalem by Captain Charles W. Wilson (1864) and the *Karte Der Materiallien Zur Topographie Des Jerusalem, Deutschen Veren Zur Eroforschang Palestinas* (1904) as well as modern maps and aerial photographs were examined in detail to reveal the locations of hidden openings. A comparison of the above maps enabled the planning and execution of a geophysical refraction survey. The survey lines were chosen to provide maximum data on the thickness of the valley fill, depth to rockhead, and verification of buried water courses and openings. Auger and core drillings were then based on these results.

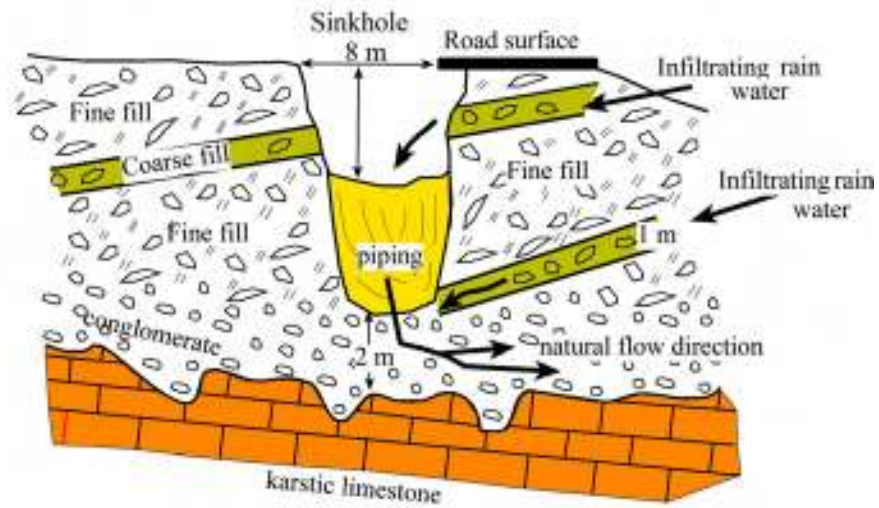


Figure 23. Damascus Gate sinkhole in artificial fill- material.

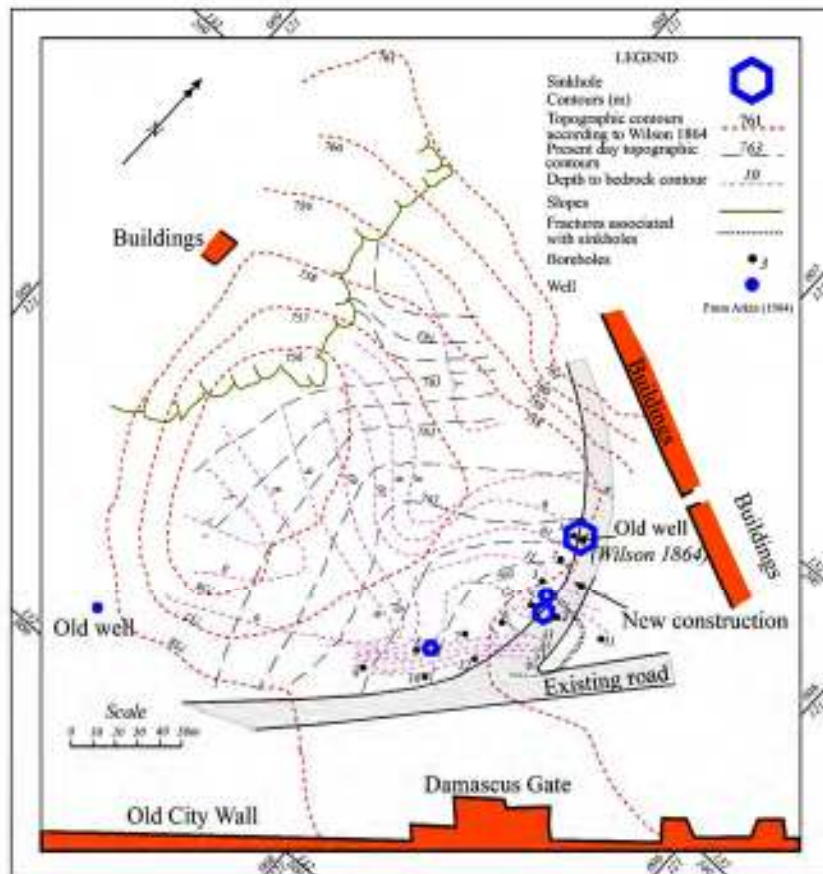


Figure 24. Geotechnical survey map of the sinkhole area near the Damascus Gate.

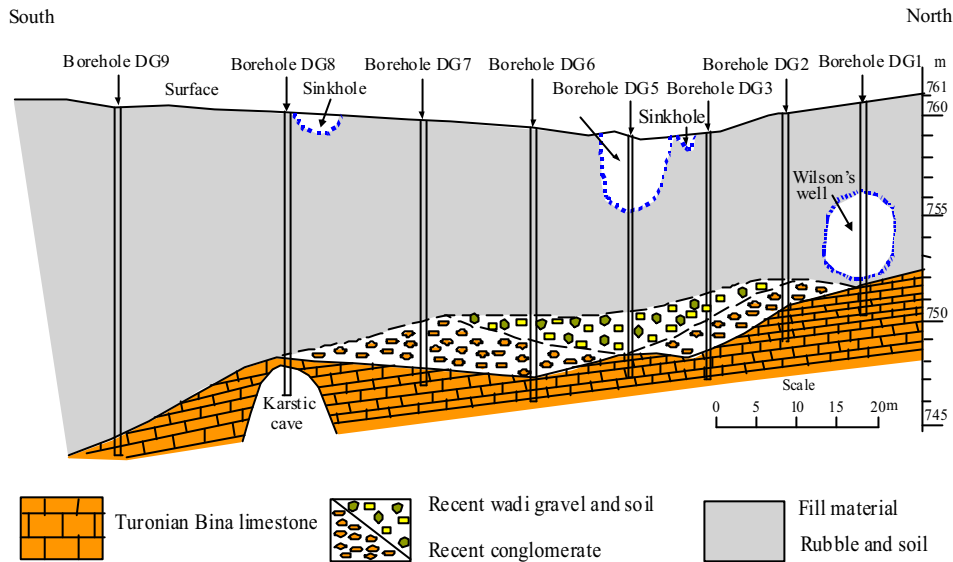


Figure 25. Geological cross section connecting boreholes. Damascus Gate.

The fill material consisted of water-sensitive clay, building waste of blocks up to 30-50 cm across mixed with fine and powdery material. A well-developed bedding and grading of the different size materials exists and the beds range in thickness up to 1.50 m. The coarse material forms well-defined beds of extremely high permeability and act as water conduits. This configuration was formed by the manner in which the material was thrown down (Figure 23).

Bedrock in the center of the area and along an ancient water course is covered by a gravel layer up to 1.50 m thick. The gravel consists of well rounded pebbles 5-10 cm across, unconsolidated and non-cemented. These layers are also highly permeable. A number of karstic holes, several meters deep and filled by Terra Rosa soil, were penetrated in the borings. The cisterns penetrated were filled with organic clay material.

Susidence began after a wet period in which 90 mm of rain fell in cycles of 2-3 days wet weather and 3-5 days dry weather. At this rate the subsurface did not have enough time to drain, causing the various clay layers to become saturated. The coarse material acted as conduits distributing the water throughout the fill.

The sinkholes are developed above the ancient water course and the intersection of permeable layers and gravel beds of opposing dips. Consequently there was a rapid increase in water content at the intersections of these layers with a subsequent increase in pore pressures and loss of strength in the clays. Piping and suction of fine material into the porous gravel beds led to the development of

concentric fractures at the surface, followed by the collapse of material and the formation of the sinkholes.

Using the data collected It was possible to delineate the unstable areas where further subsidence could affect construction. Remedial works to reduce infiltration and permeability at and around the road junction site involved excavation and recompaction. Several winters of comparable rainfall have since passed with the ground remaining stable, justifying the detailed investigation. Since this investigation the area has undergone further reshaping without these phenomena recurring.

Similar sinkholes have developed after winter floods in artificial and natural environments in other parts of Israel, such as in the coastal plain, the Haifa area and around the Dead Sea.

### **Karst**

Limestone and dolomite are particularly susceptible to solution and recrystallization and many examples are described in the literature. Solution is governed by a complex chain of reversible reactions in which the participating components are gas in the form of  $\text{CO}_2$  from the atmosphere and from within the pore structure of the rock mass, carbonic acid  $\text{H}_2\text{CO}_3$  as part of the natural water content and solid  $\text{CaCO}_3$  from the rock. The relationship between these three phases and the directions in which the reactions take place are shown in Figure 26. The amount of  $\text{CO}_2$  dissolved depends on the amount of air available for the first reaction to take place and generally varies only slightly from place to place in the free air. However the  $\text{CO}_2$  content in the pore space atmosphere of the rock mass may be far in excess of that in the free air due to local relatively high hydrostatic pressures produced by infiltration. The degree of solution of the carbonate component thus directly depends on the partial pressure of  $\text{CO}_2$  in the pore space, the  $\text{CO}_2$  content of the natural water as well as the velocity of movement of the infiltrating water, the time of contact between water and rock and the temperature of the water, pore space atmosphere and rock mass. The variations in water content and temperature in Israel, related to seasonal changes form an almost ideal environment for the above reactions to take place. During the summer fluctuations in temperature in the rock mass near the surface ranges between  $12^\circ\text{C}$  and  $16^\circ\text{C}$  and at a depth of 1.50 m or more between  $8^\circ\text{C}$  and  $13^\circ\text{C}$  (Arkin, 1986). These fluctuations above and below the temperature of the solubility of carbonate in places leads to the chemical disintegration of the carbonate and the formation of cavities. Water content during the winter and the rapid increase in infiltration inhibit the chemical reactions. The amount of contact time between water and rock is reduced due to rapid drainage. Some dissolution may take place due to lowering of temperature, however the result is mainly an erosional action clearing the flow paths for further dissolution as conditions change.



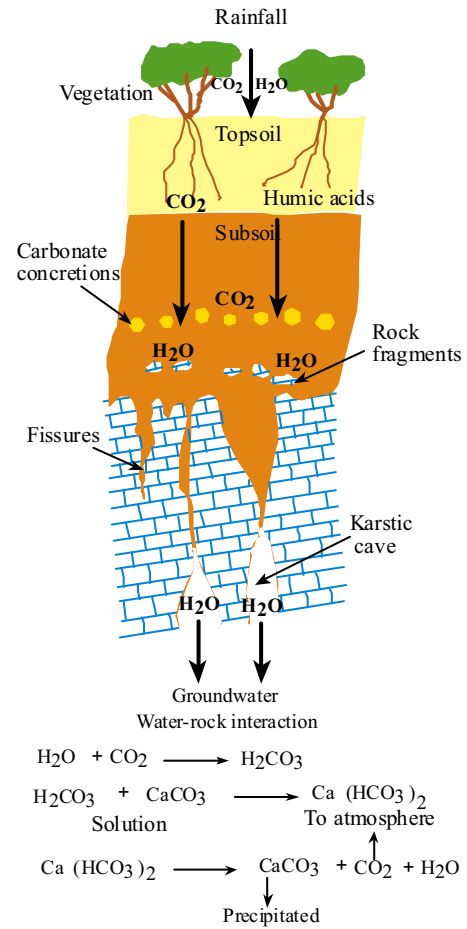


Figure 26. Schematic profile of karst processes.



Figure 27. Karstic fractures filled with red-brown soil in the Bina Formation limestone, north portal of tunnels, Begin highway, at the entrance to Jerusalem.

Over long periods of time large cavities are formed and can reach large volumes at depths below the surface, often with no evidence of their existence. Often these cavities may be filled with red-brown soil washed in from the surface (Figures 27 and 28).

Two forms of karst are relatively common in the Bina, Weradim and Amminadav formations in the Jerusalem area, which progress along bedding planes, joints and fractures.

Shallow karst is found in the limestone and dolomite at the interface of soil and rock (Figure 26). Pinnacles are formed at the interface with the spaces between them filled with soil. This type of karst usually occurs down to depths of 3-5 m and may affect shallow foundations, as was the case in the Ramot suburb of Jerusalem. In such situations, the overlying soil is usually removed to expose solid rock and the openings are filled. On exposed rock solutions can cause troughs and ridges (Rinnen-Karren) that can be over 1m wide and infilled with soil.

Deep karst in the Cretaceous dolomite and limestone in the form of large cavities such as the Soreq caves can be of large volumes with exotic features of stalagmites, stalagmites and calcite curtains. Usually these caves develop along the main fractures and joints within the rock mass and may occur to depths of over 60 m.

In historical times these features were well known and exploited in underground works such as the water tunnels and aqueducts supplying water in and around the Old City of Jerusalem (Arkin and Flexer, 1986, Gill, 1996).



Figure 28. Karstic holes in the Amminadav Formation seen as brown patches of red-brown soil filling. Herzog Street.

## Seismic Hazards

Seismology, the study of earthquakes, comes from the Greek word *SEISMOS*, which means shaking. The term was introduced by Robert Mallet in 1850 to describe earthquake movements. The first instrument for recording earthquake motion was the seismograph invented by John Milne in 1880. However it was not until 1935, when Charles F. Richter introduced a scale for measuring total energy, that major steps were taken in the advancement of the study of earthquakes. The scale he introduced is the basis in designating the strength of an earthquake.

The Richter Scale designates the total energy released on a scale of one to ten where M represents the magnitude of the earthquake. The sensitivity of the Richter magnitude (M) is described as follows:

M less than 3.5-----is recorded but not generally felt.

M 3.5 - 5.4-----felt but rarely causes damage.

M less than 6.0-----causes slight damage to well-designed buildings, and major damage to poorly constructed buildings over several hundred kilometers.

M 6.1 - 6.9-----may cause destruction up to about 100 km in areas where people live.

M 7.0 - 7.9-----major earthquake that can cause serious destruction over large areas.

M 8 or greater ----- great earthquake that can cause serious destruction over very large areas.

To have some idea of the force of an earthquake the energy equivalent in tons of TNT to magnitude gives us a measure of this force as seen below:

M4 ----- is equivalent to 1,010 tons of TNT.

M5 ----- 31,800 tons of TNT.

M6 ----- 1,010,000 tons of TNT.

M7 ----- 31,800,000 tons of TNT.

M8 ----- 1,010,000,000 tons of TNT.

M9 ----- 31,800,000,000 tons of TNT.

Before the Richter scale the only method of estimating the strength of an earthquake was by the oral evidence of those affected by it and reports in the media. In 1902 Giuseppe Mercalli introduced an intensity scale as a way of measuring or rating the effects of an earthquake at different sites. This scale was modified several times and in 1931, it was revised by the United States Geological Survey. This Modified Mercalli Intensity Scale is commonly used to describe the severity of earthquake effects. Intensity ratings are expressed as Roman numerals between I and XII from a low to a high effect. The Modified Mercalli Intensity Scale (Table 6) differs from the Richter Magnitude Scale in that earthquakes vary greatly from place

to place and that more than one Intensity value (e.g.: IV, VII) can be measured as the effects of earthquakes are felt differently in places.

Table 6. The Modified Mercalli Intensity Scale.

Scale	Description	Average Peak Velocity (cm/sec)	Average Peak Acceleration g = 9.80 m/sec <sup>2</sup>
I	People do not feel any Earth movement. A few people might notice movement if they are at rest and/or on the upper floors of tall building.		
II	Many people indoors feel movement. Hanging objects swing back and forth. People outdoors might not realize that an earthquake is occurring.		
III	Most people indoors feel movement. Hanging objects swing. Dishes, windows and doors rattle.	1-2	0.015-0.02 g
IV	The earthquake feels like a heavy truck hitting the walls. A few people outdoors may feel movement. Parked cars rock .		
V	Almost everyone feels movement. Sleeping people are awakened. Doors swing open or close. Dishes are broken. Pictures on the wall move. Small objects move or are turned over. Trees might shake. Liquids might spill out of open containers.	2-5	0.03-0.04 g
VI	Everyone feels movement. People have trouble in Walking. Objects fall from shelves. Pictures fall off walls. Furniture moves. Plaster in walls might crack. Trees and bushes shake. Damage is slight in poorly built buildings. No structural damage.	5-8	0.06-0.07 g
VII	People have difficulty standing. Drivers feel their cars shaking. Some furniture breaks. Loose bricks fall from buildings. Damage is slight to moderate in well-built buildings; considerable in poorly built buildings.	8-12	0.10-0.15 g
VIII	Drivers have trouble steering. Houses that are not bolted down might shift on their foundations. Tall structures such as towers and chimneys might twist and fall. Well-built buildings suffer slight damage. Poorly built structures suffer severe damage. Tree branches break. Hillsides might crack if the ground is wet. Water levels in wells might change.	20-30	0,25-0.30 g
IX	Well-built buildings suffer considerable damage.	45-55	0.50-0.55 g

Houses that are not bolted down move off their foundations. Some underground pipes are broken. The ground cracks. Reservoirs suffer serious damage.

- |     |   |      |          |
|-----|---|------|----------|
| X   | Most buildings and their foundations are destroyed. Some bridges are destroyed. Dams are seriously damaged. Large landslides occur. Water is thrown on the banks of canals, rivers, lakes. The ground cracks in large areas. Railroad tracks are bent slightly. | > 60 | > 0.60 g |
| XI  | Most buildings collapse. Some bridges are destroyed. Large cracks appear in the ground. Underground pipelines are destroyed. Railroad tracks are badly bent .   |      |          |
| XII | Almost everything is destroyed. Objects are thrown into the air. The ground moves in waves or ripples. Large amounts of rock may move.  |      |          |
- 

The Intensity rating of an earthquake effect does not require any instrumental measurements. Thus the seismologists can only rely on newspaper accounts, diaries, and other historical records to estimate the intensity rating of past earthquakes, for which there are no instrumental recordings. Intensities typically are greater close to an earthquake's epicenter. The Modified Mercalli Intensity Scale is important for understanding the earthquake history of a region, and estimating future hazards where little or no empirical measurements are available.

To better understand this phenomenon it is necessary to look at the anatomy of an earthquake. The focus of an earthquake is the point below the surface of the earth where the energy for the earthquake originates. The epicenter is the point on the earth's surface directly above the focus and is described by its geographic location. The vibrations produced by an earthquake can be simulated by a drop of water falling into a pond, creating concentric waves expanding out from the center (Figure 29). In the earth the waves are generated by the energy released when one block of the earth's crust moves in relation to another. The waves travel outwards from the source along the surface and through the body of the earth at varying speeds, depending on the rock types through which they move. When an earthquake occurs below the seafloor, waves known as a Tsunami are formed and spread out in concentric circles (Figure 29). Tsunamis are the most devastating, as seen recently (2005) in the Indian Ocean causing enormous damage and the loss of life of over 280,000 person. Vibrations that are generated fall into two groups: surface waves and body waves (Figure 30). Surface waves are both longitudinal (Rayleigh waves) and transverse (Love waves) and are generally the strongest, causing the most damage. Body waves are primary waves know as P-Waves, which are compressional, and secondary waves known as S-Waves, which are shear waves. P-Waves are the fastest and are first recorded by seismographs. These are followed by

the slower S-Waves. P-Waves cause displacement ahead and after the wave direction whereas S-Waves cause displacement at right angles to the direction of wave movement. Figure 31 shows examples of seismograms recorded during earthquake events in the vicinity of Jerusalem.



Figure 29. Earthquake epicenter simulated by a drop of water.

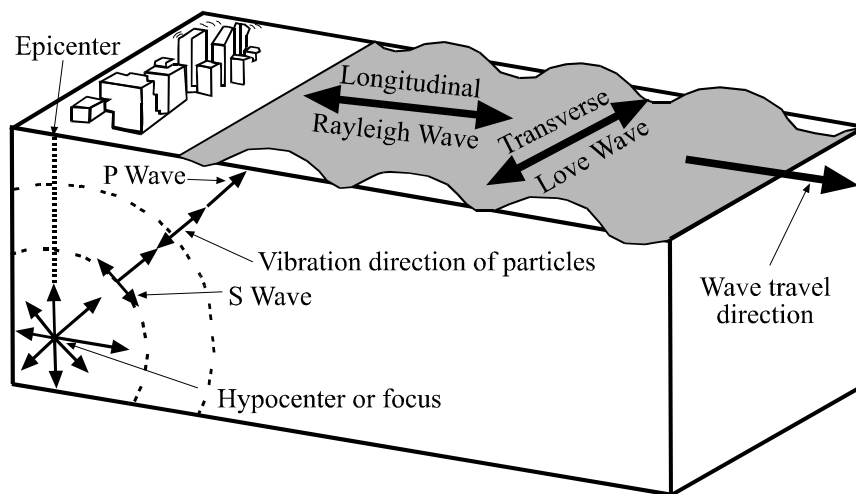


Figure 30. Seismic waves.

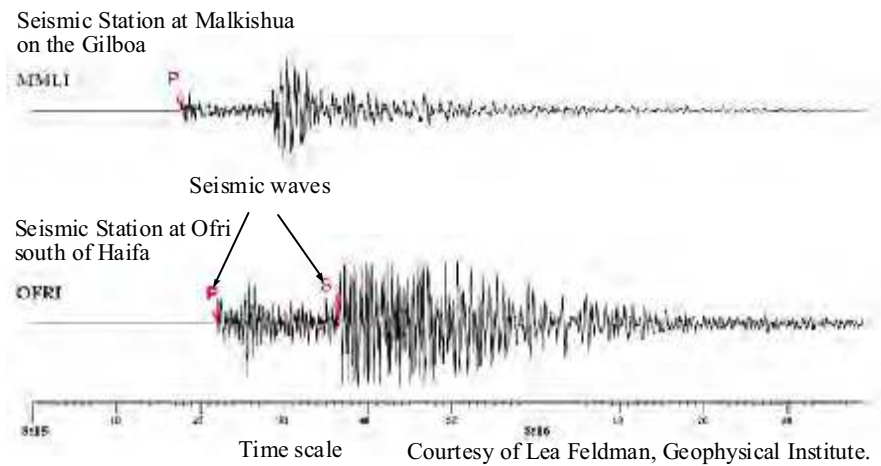


Figure 31. Typical seismograms of earthquakes recorded from stations north of Jerusalem.

References in the literature on historical earthquake events in the Jerusalem area are in many cases ambiguous regarding the damage caused. Descriptions are based on Biblical, historical, geographical and archaeological evidence. Most reports refer to some damage, mainly to important buildings of religious or political significance. For example, there are many descriptions of structural damage or collapsing walls caused to the Al Aqsa Mosque and the Dome of the Rock over the period 687-1068 CE.

These are based mainly on reports of renovations and restorations carried out at these sites. The damage in many cases can be attributed to natural decay or lack of maintenance and this damage may have been increased by an earthquake event. The Dome of the Rock is founded on bedrock whereas Al Aqsa is founded on fill material accumulated through the ages. This difference in the type of bedrock and the type of damage emphasizes the importance of knowing the foundation conditions of a particular site regarding a seismic event. The relationship between earthquake acceleration versus intensity for different foundation conditions is shown in Figure 32 and may be applied to the Jerusalem area.

In the vicinity of Jerusalem earthquake events have occurred with intensities of III-V on the Modified Mercalli Scale. These are classified as low to medium earthquakes equivalent in most cases to vibrations of a passing heavy vehicle. Table 7 gives a list of important historical events and major destructive earthquakes in Israel and adjacent areas since 64 BCE that have been felt in Jerusalem.

Table 7. Important historical events

<b><u>Date</u></b>	<b><u>Location</u></b>	<b><u>Result</u></b>
64 BCE	Jerusalem	Damage to temple and city walls.
31 BCE	Galilee and Judea	30,000 people and animals killed in Judea.
30, 33 CE	Jerusalem	Slight damage
115CE	Syria, Caesarea.	Possible tidal wave damage.
306 CE	Jerusalem, Caesarea	Damage from Tsunami Tidal wave.
363 CE	Palestine, Jordan	Severe damage at many sites.
419 CE	Palestine, Jordan	Jerusalem damaged; Antipatris destroyed; many towns and villages destroyed.
447 CE	Gadara	Thermal baths destroyed, many killed.
631 CE	Palestine	Aftershocks for 30 days. Widespread damage.
749 CE	Palestine	Severe; tens of thousands of deaths at Capernaum, Sussita, Tiberias Gadara thermal baths: damage in Scythopolis, Jerusalem, Pella, Jerash. Philadelphia. Tsunamis in Mediterranean & Dead seas.
1033 CE	Jordan Valley	Severe earthquakes for 40 days, at Ptolmias, Jerusalem, Tiberias, Jericho, Hebron.

In general earthquakes of major significance in the Jerusalem area are not common. Those recorded or mentioned in various sources were of a relatively small scale. The events were generally recognized in the damage caused to walls and foundations of mainly religious sites and recorded in their annals. The largest earthquake having a direct effect on Jerusalem occurred in the Dead Sea Rift valley in July 1927. This earthquake, with an estimated strength of M6.25, struck Jerusalem and caused moderate damage in Lod, in the coastal plain west of Jerusalem. Damage occurred in the Old City and on the Mount of Olives, causing some injured and deaths. Shalem (1947) shows photographs of the damage from this earthquake.



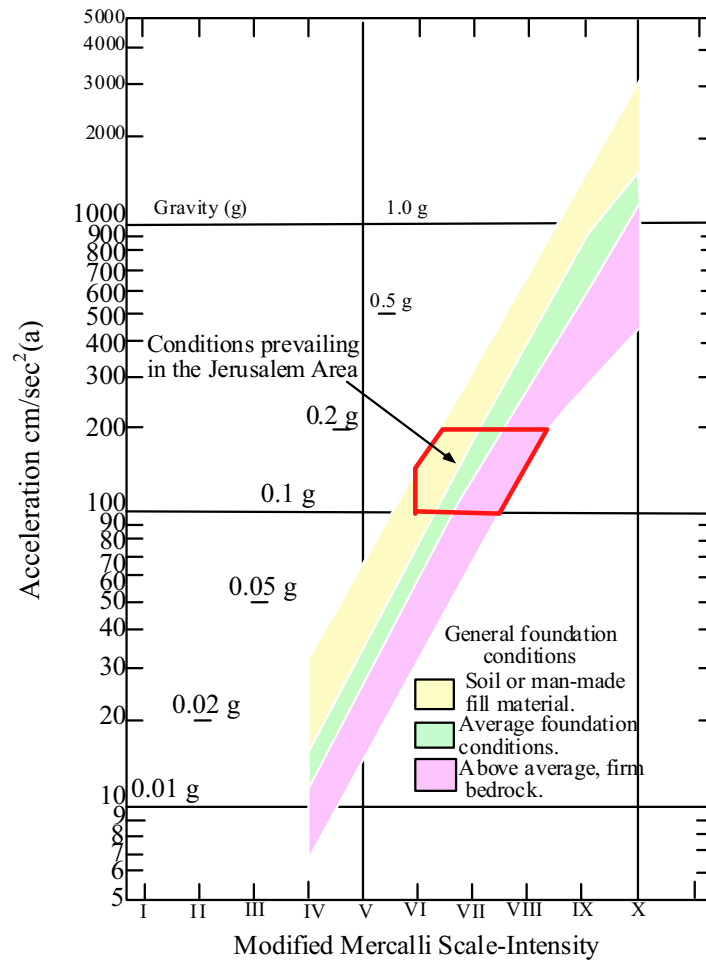


Figure 32. Earthquake accelerations versus intensity for foundation conditions (after Leeds, 1973).

Various studies and evaluations of potential seismic activity that may affect construction in Jerusalem recommend that an acceleration of 0.1-0.2 g be taken into account in most engineering projects (Figure 32). A detailed study of the earthquake hazards in Jerusalem has been presented by Salamon et al. (2003). This work indicates potential areas of seismic risk, taking into consideration rock types, topography, landforms and evaluation of seismic intensities as a result of the 1927 earthquake.

The 1927 earthquake that struck this area received world wide attention. The following is a selection of reports on the earthquake that appeared in some major American newspapers.

**Los Angeles Times. Tuesday July 12, 1927:**

Hundreds hurt in earth shock. Church of Holy Sepulcher suffered ground tremor. Felt in Cairo, worst toll in country region. 26 killed, 30 injured. Damage to post office, Zionist Executive Building, Government House. After quake Jerusalem streets filled with excited crowds refused to enter homes. Tremor felt in Australia.

**San Francisco Chronicle. Wednesday 13 July, 1927:**

Twenty towns damaged by long series of tremors. Hundreds injured, most casualties in Transjordan. Jerusalem in terror, fearing shock recurrence; Bridges down. British Air Force Depot at Amman Destroyed; Many casualties when Nablus Bazaar falls.

**San Francisco Chronicle. Wednesday 15 July, 1927:**

Palestine Quake toll set at 670 dead, 3000 hurt, \$2 Million damage Biblical city of Nablus in ruins; rescue parties at work; many of injured dying. New suburbs suffer, Talpiot, Beth Israel. Baghdad Synagogue collapsed.

**Time Magazine. 25 July 1927 Volume X no.4:**

“The holy land trembled and was shaken last week from Jerusalem to Jericho and very largely along the banks of Jordan. 670 persons died, not one of these reputedly a US citizen nor Jew. Although no Jew was killed in Palestine last week many were rendered homeless by the destruction of their houses, and students at the Institute of Jewish Studies in Jerusalem found most of its buildings unsafe or utterly shaken. Manhattan dry goods merchant cabled \$25,000 to Palestine, instructing that it be used for feeding and caring for earthquake sufferers without distinction of race or creed”.

**Quarries**

Since the Stone Age stone is and has been the main building material in this region. In the beginning stones were collected and placed one upon the other to build fences, protective walls and crude buildings. As time progressed the methods of obtaining the raw material to provide cut, and crushed stone became more efficient and economically sustainable. Today Jerusalem’s unique architecture developed from the structures previously built through the ages, and exemplified by the superb Herodian masonry and buildings. The stone raw material was in most cases obtained from quarries around Jerusalem with only specific stone such as marble and granite imported from other areas. Figure 33 shows the ancient quarries and excavations of limestone and dolomite in and around the Old City of Jerusalem.

Construction in modern Jerusalem is based mainly on limestone and dolomite in all its forms. The material is crushed for aggregate, cement, lime and carbonate sand as well as for all types of masonry. Limestone in particular is used today as polished stone resembling marble and as cut and dressed stone for facing buildings (Figures 35 and 36). Municipality by-laws that originated during British Mandate



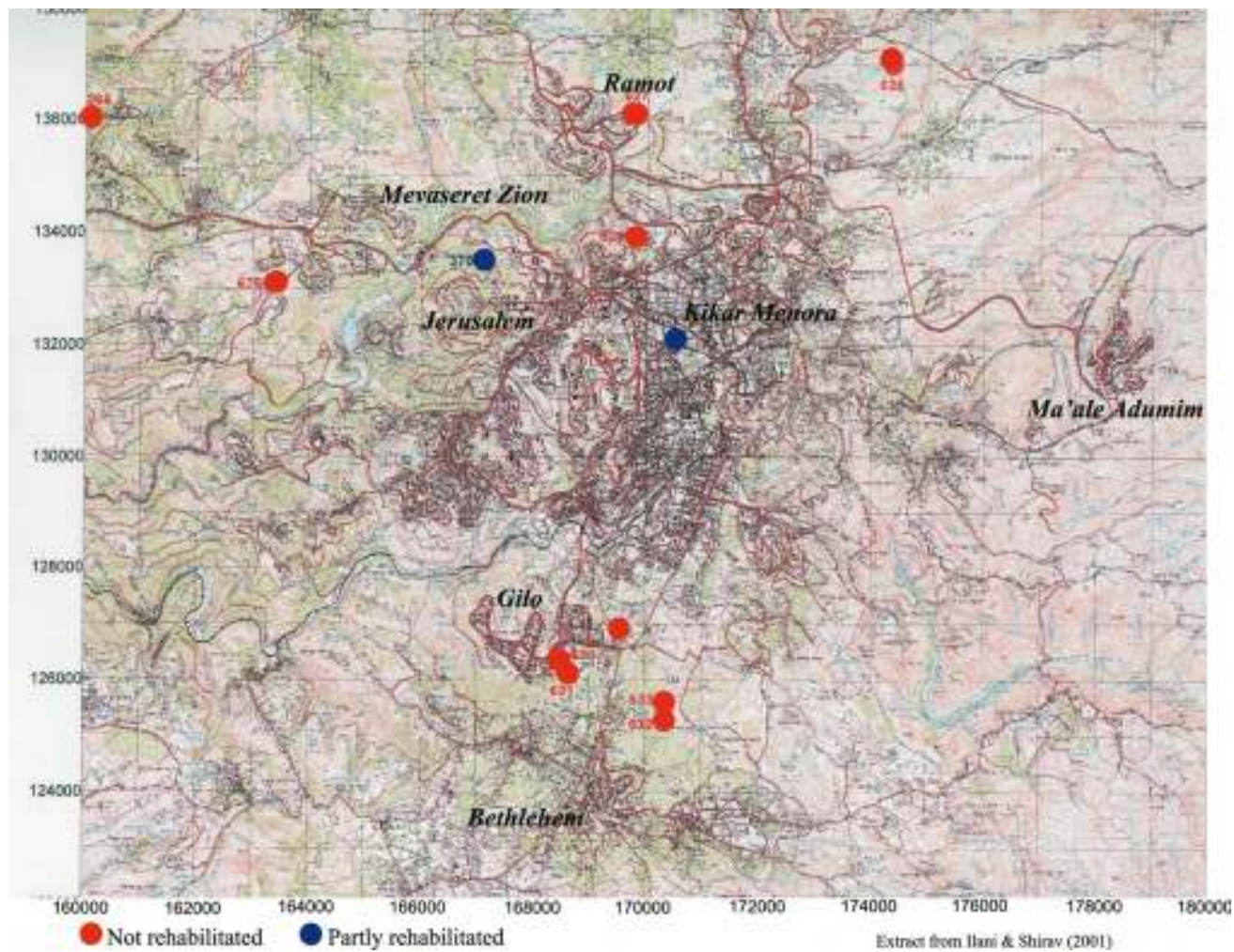


Figure 34. Abandoned quarries within the Jerusalem municipality.

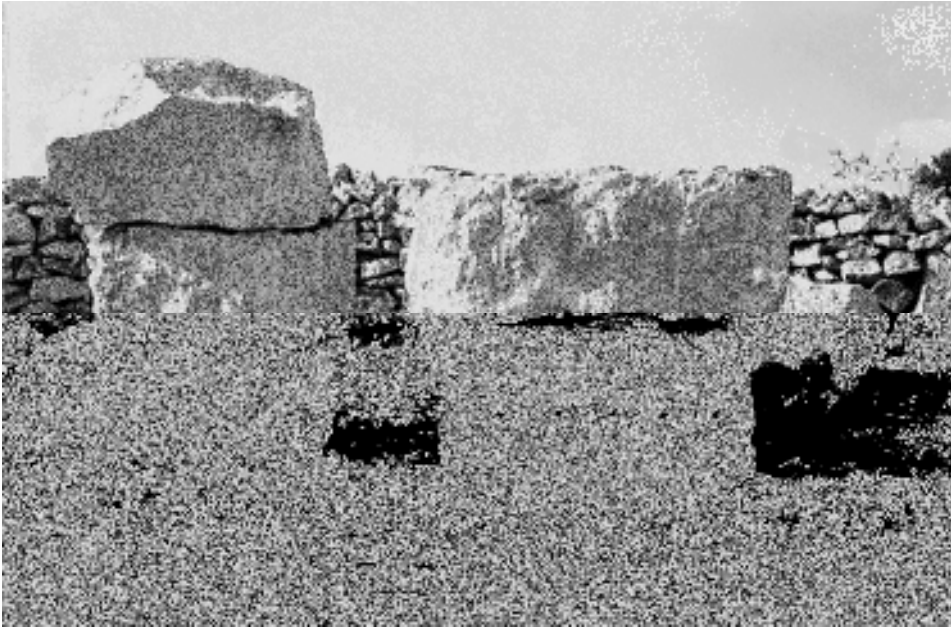


Figure 35. Bina limestone blocks used as “marble”. Note line of drillholes showing method of quarrying.

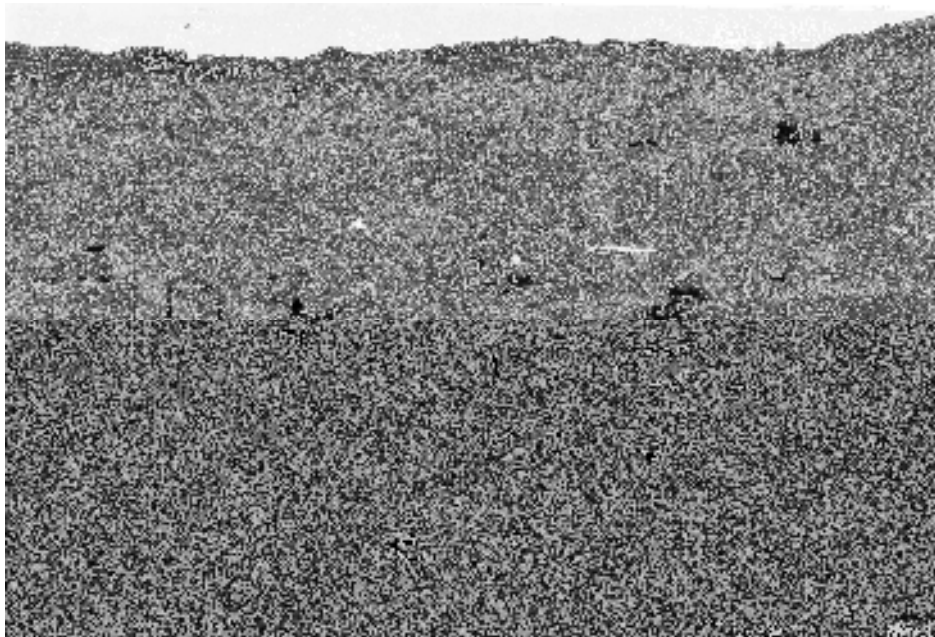


Figure 36. Quarry face in Bina limestone south of Jerusalem.

## CASE HISTORIES

### Tunnels and Viaducts

In the past few years a number of surveys have been carried out for building tunnels, viaducts and major highways in the Jerusalem area. The Gilo and Mount Scopus projects are good examples of these and their case histories are discussed below. The geology in the area consists of sedimentary rocks of limestone, dolomite and marl of the Judea Group of Upper Cretaceous age. These rocks form part of the eastern flank of the Judea anticline that dips some 10° towards the Jordan River Rift valley (Figures 7 and 9). Steeper inclinations are found near faults and local folds.

Table 8. Tunneling classifications and methods used around the world.

CLASSIFICATION	SYMBOL	TYPE	PARAMETERS	PURPOSE	APPLICATION
Rock Load Factor		qualitative	rock load	rock quality	tunnels
Stand-up Time		qualitative	rockmass behavior in time	structural defects & stand-up time	tunnels
New Austrian Tunneling Method	NATM	Qualitative ground classification	behavior under load & monitoring	ground conditions, excavation and supports	tunnels
Rock Quality Designation	RQD	quality index	NX core recovery	index for identifying low quality zones	general & tunnels
Rock Structure Rating	RSR	qualitative rating	geological & structural	rockmass quality for support	mainly tunnels
Rock Mass Rating Geomechanics	RMR	qualitative rating	mechanical & fracture data	definition of rock mass for engineering practice	tunnels, slopes, chambers, foundations
Q- System	Q	quantitative assessment	rockmass, geological, mechanical, and water conditions	numerical assessment for design	underground excavation
Size-Strength Quality		quality index	strength & fracture spacing related to block size	rock mass character	underground excavation & ground control
International Society for Rock Mechanics	ISRM	qualitative	lithological, structural & mechanical	simplified geotechnical	general purpose
Modified Basic Rock Mass Rating	MBR	quantitative rating	strength, fracture density & water	indicator of competence disregarding opening	mainly hard rock mining & excavation

The Gilo project of tunnels and a viaduct connecting them, as part of Road No. 60, giving access to Gush Ezion south of Jerusalem, are a good example of the procedures followed during the various stages of a major civil engineering project of this kind. The design of the Gilo project, which consists of two tunnels and a viaduct, began in 1987 (Figure 37).

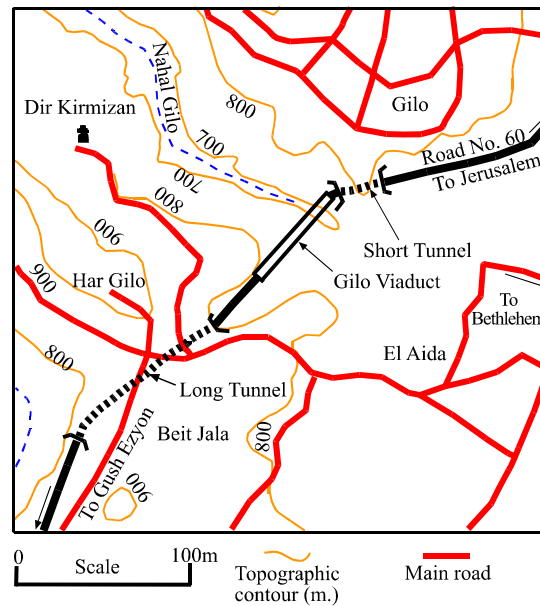


Figure 37. Gilo Project location map.

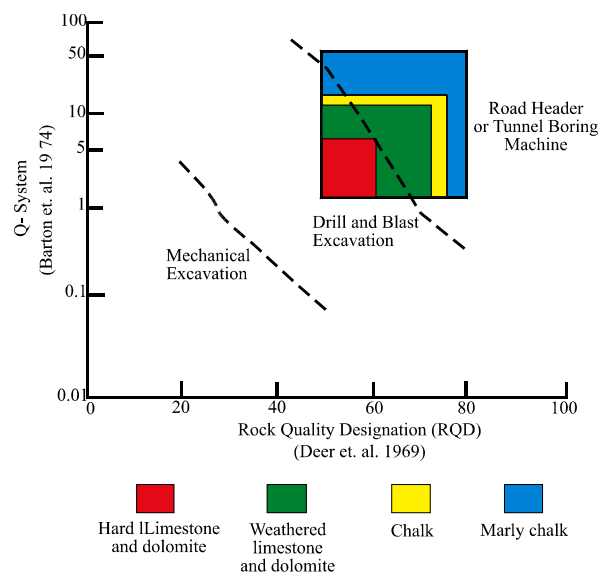


Figure 38. Tunneling method in various lithologies around Jerusalem according to rock mass quality.

Excavation of the short tunnel began in July 1992 and was completed in March 1993. Excavation of the long tunnel began in September 1993 and was completed in May 1995. Evaluation of the rock mass for both tunnels began with geological mapping followed by core drilling. The data gained was processed by the "Q" System of Barton, et al., (1974) and Rock Quality Designation (RQD) of Deere, et al., (1969). The quality of the rock was also evaluated using the Rock Mass Rating (RMR) of Beiniawski (1976). These methods use measurable and descriptive parameters which take into account the fracture system, measuring the continuity, spacing, degree of roughness of the fracture plane and the type of material filling them. This data formed the basis for design and constituted a guide to the tunneling method that was applied to the different lithologies around Jerusalem (Figure 38). The effect of water on the cohesion and friction angle of chalky marl of the Kefar Sha'ul Formation is shown in Figure 39.

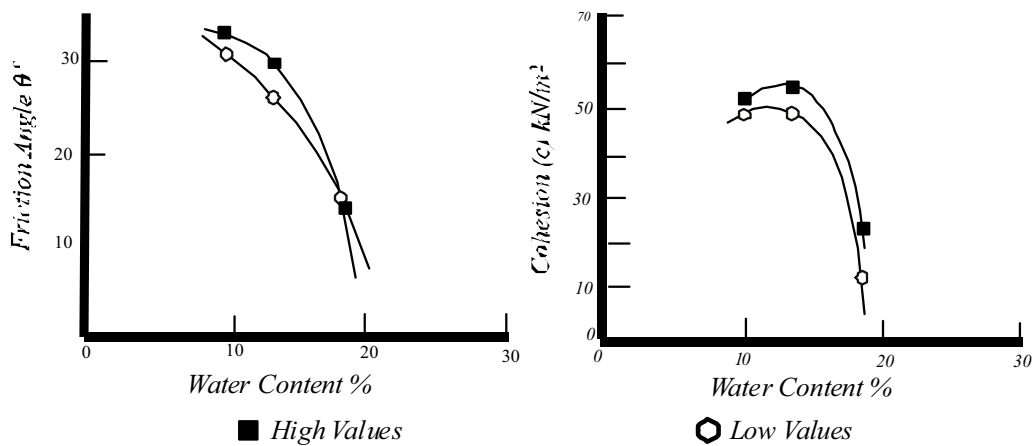


Figure 39. Cohesion and friction angle in relation to water content in the chalky marl unit of the Kefar Sha'ul Formation in the Gilo Short Tunnel.

The comprehensive geological and geotechnical survey included mapping of the alignment, borehole exploration, geophysical surveys, that included Resistivity and Ground Penetrating Radar followed by laboratory tests, all carried out prior to excavation.

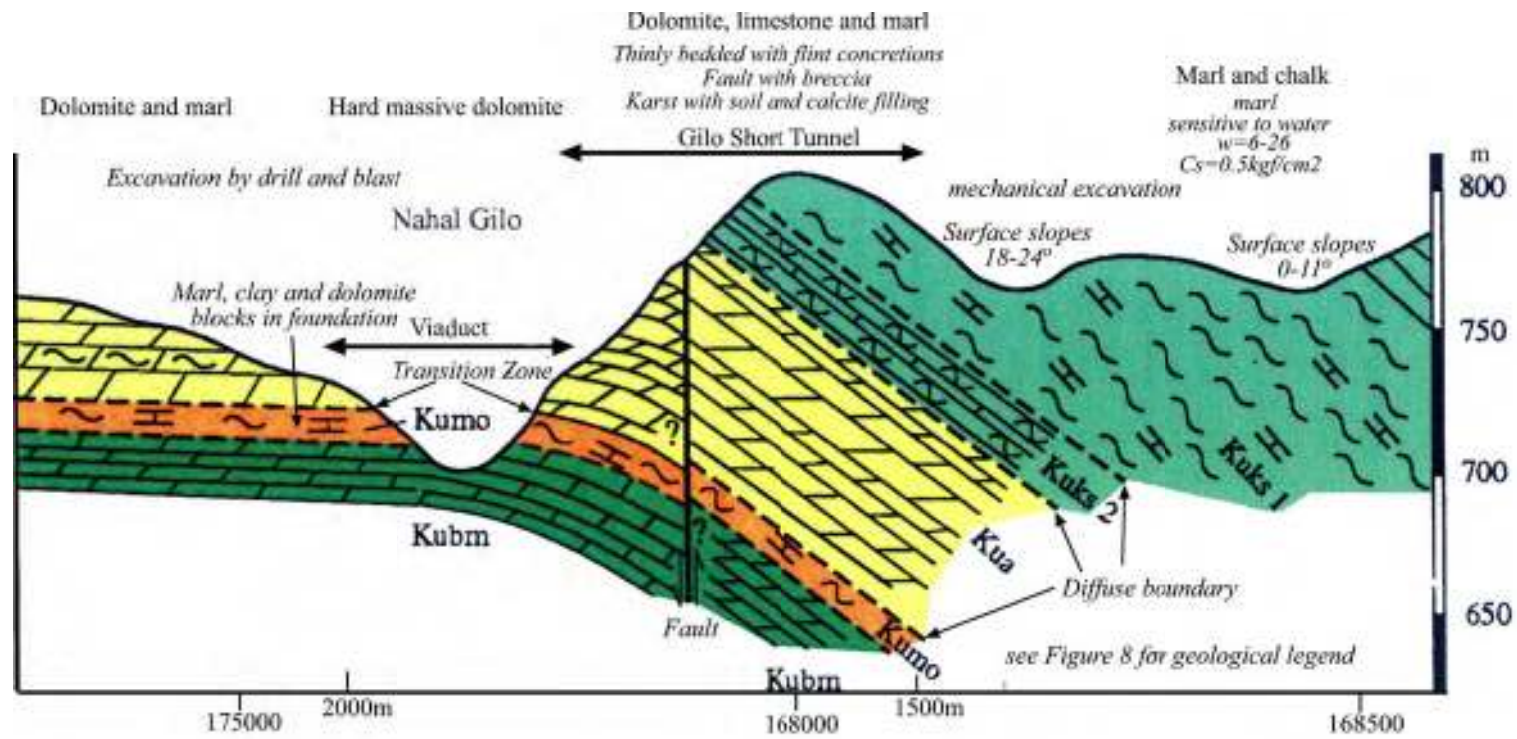


Core samples from the boreholes provided the physical and mechanical parameters that included Specific Gravity (Gs), Density ( $\gamma_d$ ), Plasticity Index (PI), Porosity (n), Permeability (k), Friction Angle ( $\theta$ ), Cohesion (c), Shrinkage Index (SI), Compressive Strength (Sc), Tensile Strength (St), Modulus of Elasticity (E), Poisson Ratio ( $\nu$ ), Core Recovery (%), Rock Mass Designation (RQD), Rock Mass Quality (Q), and Ultrasonic Wave Velocity (V).

### **Gilo Short Tunnel**

The Gilo Short Tunnel passes mainly through the Kefar Sha'ul and the upper part of the Amminadav formations (Figures 40, 41, 42 and 43). The Kefar Sha'ul Formation consists of two units: a lower unit of well-bedded limestone and marl and an upper unit of massive chalk and marl. The thickness of the exposed formation is 50-60 m. Several clay layers occur in the upper part of the formation. The common clay minerals are montmorillonite and illite. The clay minerals are associated with both the chalk and marl and are dispersed within the rock mass. Highly varied swelling phenomena were identified within the rock mass, ranging from non-swelling chalk containing small amounts of clay to clayey chalk with moderate swelling pressures of 0.24-1.4 kg/cm<sup>2</sup> and to higher swelling pressures of 6.2-9.8 kg/cm<sup>2</sup>. This non-uniform spread of swelling pressure throughout the rock mass is quite different from that described in the literature. Testing for swelling pressure was carried out because of the infiltration of sewage water from a spill at the surface above the tunnel. This water entered the tunnel along fractures above a clay bed during construction.

Monitoring of possible increase in swelling pressure, which may have affected the tunnel walls and the shotcrete support, was carried out for a long period post construction by installed convergence meters and extensometers at depths of 9 m and 13 m into the walls and roof of the tunnel in the area of the clay beds. No significant deformation was measured attesting to the reliability of the support structures. The rock mass of the formation was evaluated as having an RMR of 40-60 and Q of 0.75-12.5, representing a poor to satisfactory quality.



52 Figure 40. Geotechnical cross section of the Gilo Short Tunnel alignment.



Figure 41. View of the north portal of the Gilo Short Tunnel in the Kefar Sha'ul Formation during construction.



Figure 42. Gilo Short Tunnel south portal in the Amminadav Formation.



Figure 43. Gilo Short Tunnel work face in the Lower Unit of the Kefar Sha'ul Formation chalky limestone.

The Amminadav Formation consists of hard limestone and dolomite, occurring in beds of 0.50 –1.00 m in thickness. Karst phenomena and fissuring appear locally. The thickness of the formation ranges between 50 m. and 90 m. The rock mass of the formation is evaluated as having an RMR = 60-80 and  $Q = 16-14$  for the massive dolomite, with lower values for fractured and weathered dolomite.

#### **Gilo Long Tunnel**

The Gilo Long Tunnel (Figure 44) passes mainly through the Amminadav Formation. Karst phenomena in the form of open fractures and cavities mostly filled with brown clay soil and rubble are found in places (Figures 45 and 46). The lower part of the formation shows collapse structures and blocks of dolomite, partly weathered and imbedded in the underlying marl of the Moza Formation. This zone is referred to as the Transition Zone and ranges in thickness from 5 to 10 m (Figures 47 and 48). The zone occurs regionally, and is easily recognized in outcrops by the indistinct contact between the two formations and the accompanying collapse structures. The condition of the rock mass in this zone is difficult to predict since there is a rapid change from hard dolomite and weathered soft “sandy” dolomite to marl or clay. Excavation in this zone was carried out after horizontal probe drilling to test conditions in advance of the work face. The overall rockmass quality along the tunnel alignment was calculated as  $Q = 2.5-24$ , which conformed to a rock mass of fair to good quality.

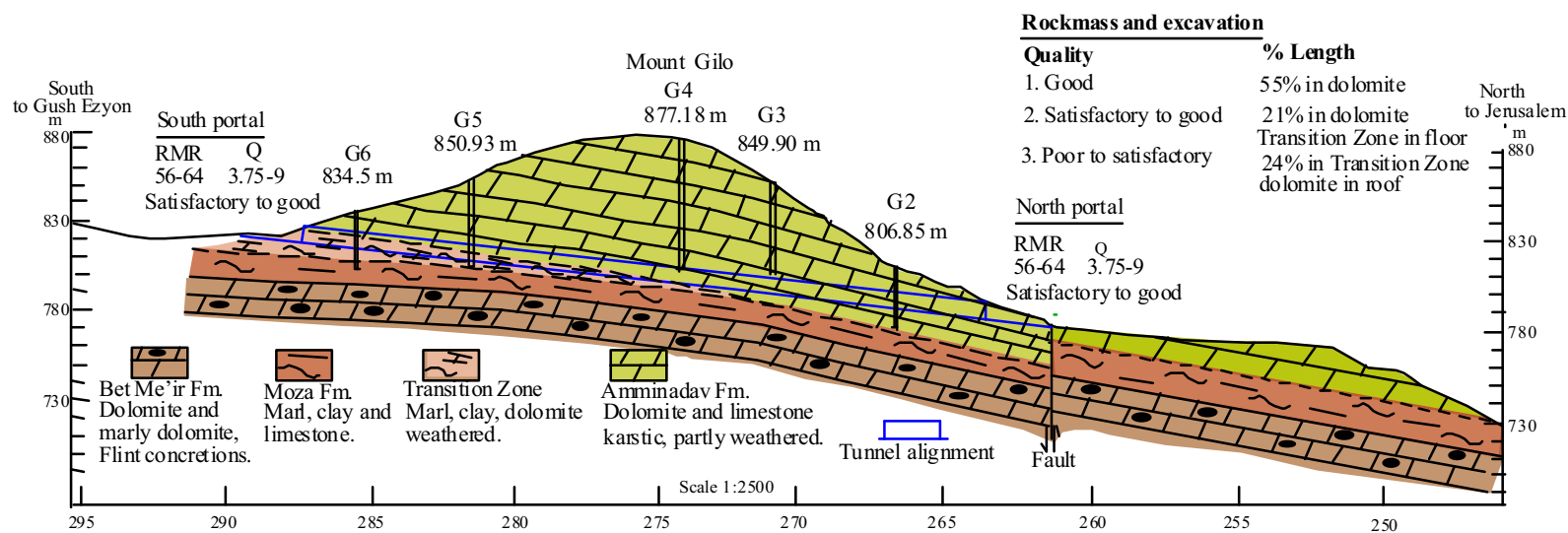


Figure 44. Geotechnical cross section along the Gilo Long Tunnel.

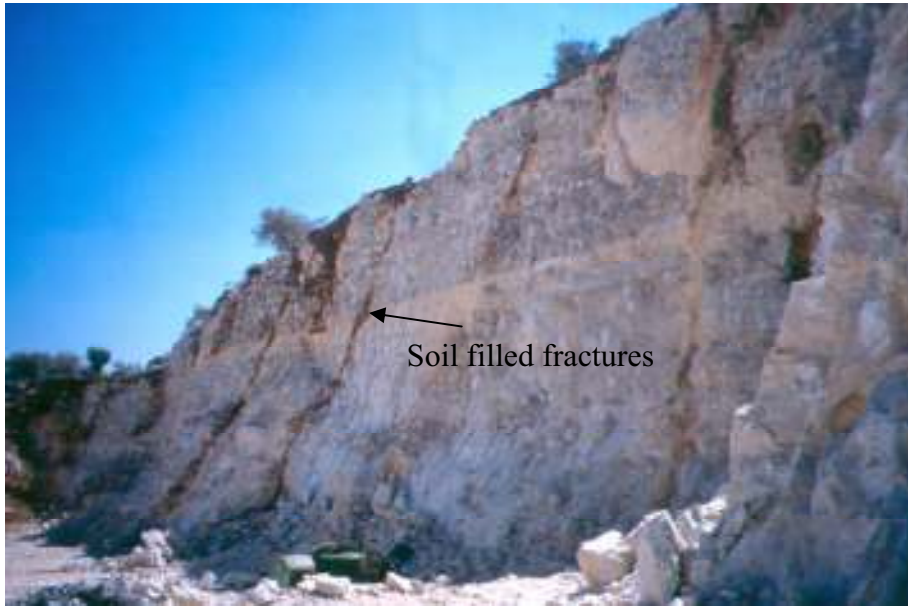


Figure 45. Karstic fractures at the north entrance to the Gilo Long Tunnel.



Figure 46. Gilo Long Tunnel at the start of the north portal.

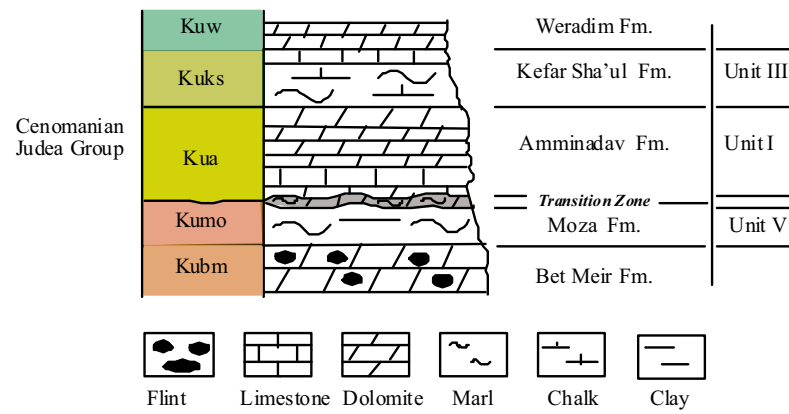


Figure 47. Columnar geological section showing position of the Transition Zone.



Figure 48. Dolomite block in the Transition Zone.

However this quality was reduced locally in areas within the Transition Zone. The areas in which this zone is found at the surface or in the underground should be investigated in detail at sites where other engineering projects are planned. Direct shear tests on the “sandy” dolomite yielded an internal friction angle  $\Phi$  of  $33^\circ$  and cohesion of 27 kPa. Granulometric tests defined the grain size between silt and sand. The internal friction angle of the massive dolomite was close to  $\Phi$  of  $45^\circ$  and the cohesion was close to 35 MPa. The uniaxial strength of the massive dolomite was between 100 and 200 MPa. Open fractures and large karstic voids filled with Terra Rosa soil of mainly expansive montmorillonite occurred in places along the alignment. Rockmass evaluation of quality gave a range in Q between 0.004 and 0.06 and an RMR between 10 and 90. This combination of soft material and voids in massive rock caused a problem in the geomechanical definition of the rock mass.

The method of excavation in both tunnels was drill and blast with a boomcutter used in soft areas. The rate of excavation ranged from 2 to 5 m/day at the face. The supports in both tunnels were steel arches and shotcrete along the whole length of the tunnel, with spacing between arches ranging from 0.5 m to 2 m, according to the quality of the rock.

The values of Q and RMR of the rock mass of dolomite, defined as reasonable to good along part of the route in the two tunnels, were found to be lower during excavation due to the unpredictable conditions in the Transition Zone. In these places the number of supporting steel arches was increased and the spacing reduced.

The main lesson to be learned from this is that in areas of rapid local lithological changes that are not readily recognized in the field or in boreholes, it is necessary to relate to the documentation from other projects in a similar geological situation. The number of exploratory boreholes should be increased significantly along the suggested tunnel route to be better prepared for excavation.

### **Gilo Viaduct**

The Gilo Viaduct spans Nahal Gilo and connects between the short and the long tunnel. The viaduct is 350 m long and at its maximum height is 50 m above the bed of Nahal Gilo (Figures 49 and 50). It is made up of 5 columns and 2 end members connecting the viaduct at each end to the rock foundations. Figure 51 shows one of the columns. The foundations for each column and the end members received special attention since these are sensitive points in the construction of the viaduct and of its stability.



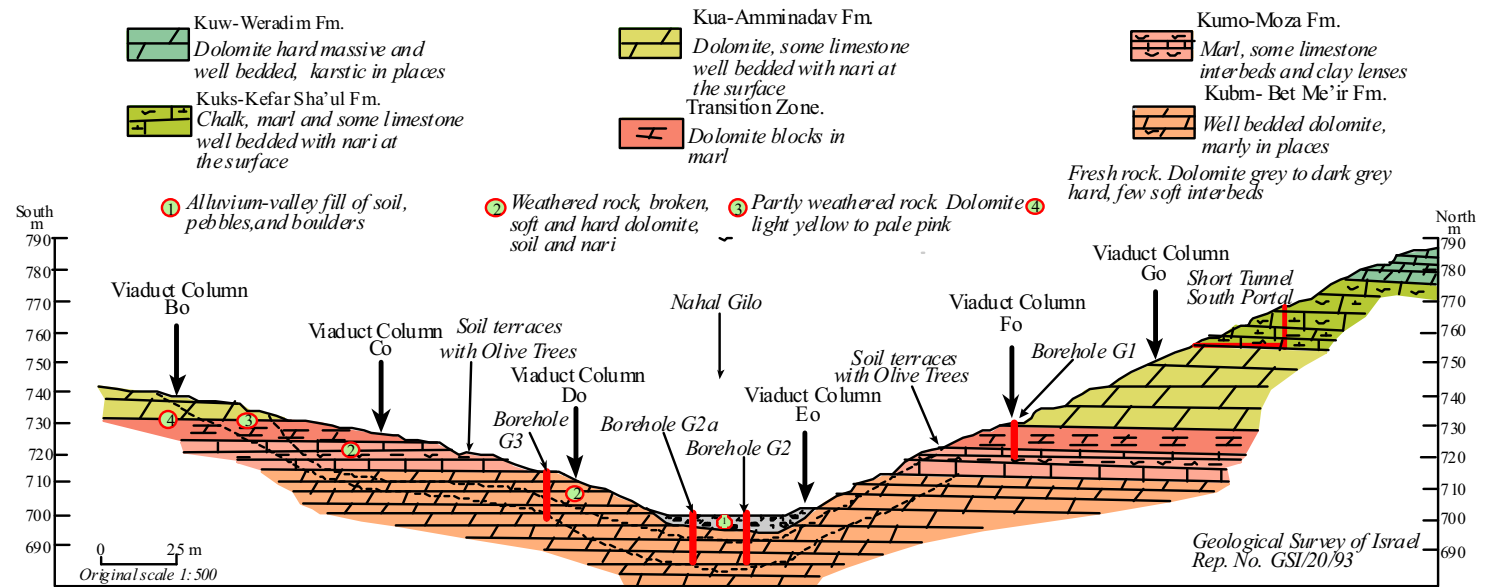


Figure 49. Geological cross section along the Gilo Viaduct alignment.



Figure 50. Gilo Viaduct during construction.

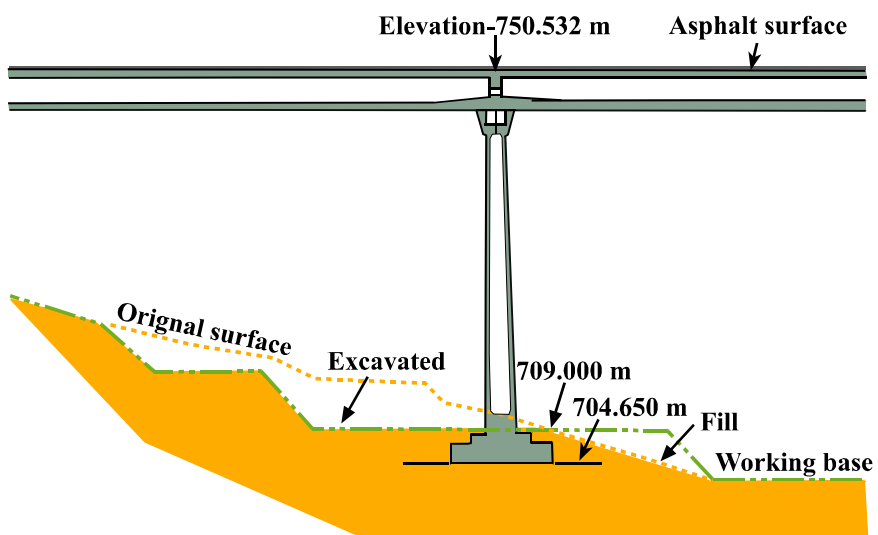


Figure 51. Gilo Viaduct-column Do.



Figure 52. Foundation pit Do.



Figure 53. Foundation pit Do. Drilling exploratory and grouting holes.



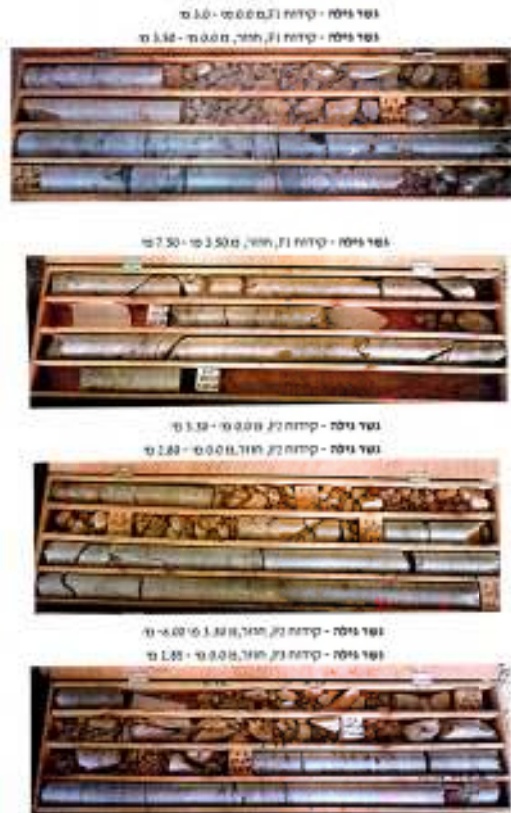


Figure 55. Gilo Viaduct Foundation Fo. Boreholes F1 F2 F3 core.

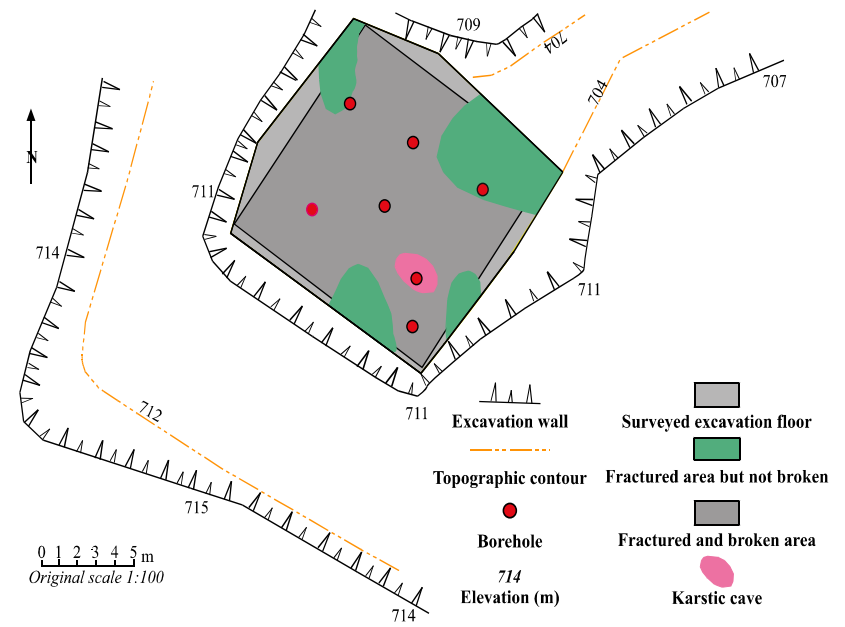


Figure 56. Gilo Viaduct foundation pit Do. Map of fractures and karst zones.

### **Mount Scopus Tunnel**

The Mount Scopus tunnel provides an example of tunneling in a different rock type from that described above. The tunnel is excavated through the N-S trending ridge between Mount Scopus and the Mount of Olives. The ridge ranges in elevation from 750 to 840 m above mean Mediterranean Sea level, built of carbonate rocks that are part of the regional water divide separating the Mediterranean drainage basin from the Dead Sea drainage basin. Along the western side of the ridge the slopes are generally short and slope up to 12°. On the eastern side the slopes are generally longer and steeper, ranging between 12° and 15°. Rainfall to the west of the divide may reach an annual average of up to 500 mm and more whereas on the eastern side it drops rapidly towards the Judea Desert to less than 200 mm within a few kilometers. Snow may cover the top of the ridge several days during some winters. The regional groundwater table in this area is at a depth of several hundred meters below the tunnel level. Therefore water was not considered to be a major problem in excavation.

The tunnel site is located between the Mount Scopus University Campus and the Augusta Victoria Hospital (Figure 57). The general direction of the tunnel is E-W and allows easy access to the town of Ma'ale Adummim. Excavation was in chalk, marl and some clay of the Senonian Menuha Formation (Figures 8, 9 and 11) which is inclined 5°-10° in a southeastern direction as part of the eastern monoclinical flank of the Judea anticline. The chalks are generally massive, occurring in the upper and lower parts of the Menuha Formation. Marl and clay lenses are found in the middle section of the formation. Lateral facies changes from chalk to marl with variable amounts of clay along the alignment characterize the rock mass. As a result of this it was difficult to establish a correlation between boreholes. To overcome this a detailed micro-paleontological examination was made of samples from each borehole and this enabled good comparison between the boreholes.

Investigation began May 1993 with geological mapping and geotechnical evaluation of the rock types at the site. Five initial boreholes were made to obtain full cores and samples for testing, using a hydraulic rig and water to obtain full cores of 67 mm diameter. An additional two boreholes were drilled using a Failing 1250 rig to obtain a core of 80 mm diameter. Drilling with air was mandatory for these boreholes to enable retrieving in-situ cores of undisturbed rock with a natural water content. This was necessary for evaluating the swelling pressures in the clayey material. Figures 58 and 59 show a summary of data from a typical borehole. The total data was summarized in a geotechnical cross section along the tunnel alignment given in Figure 60.

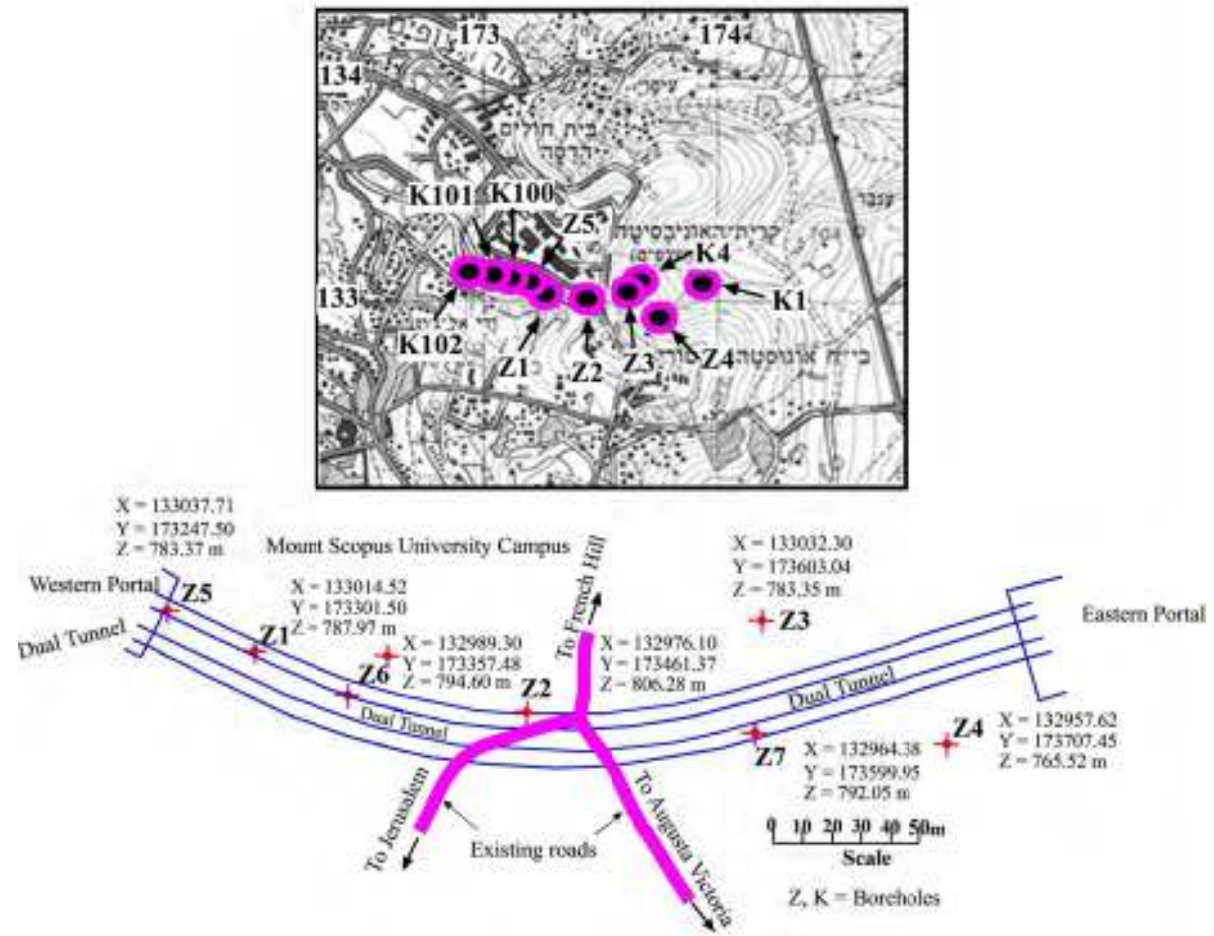


Figure 57. Location of the Mount Scopus Tunnel and exploratory boreholes.

REMARKS	GEOTECHNICAL PROPERTIES																	LITHOLOGY	STRATIGRAPHY							
	Q	c	φ	Sc	Is	St	n	CaCO <sub>3</sub> % MgCO <sub>3</sub>	IR Residue	PI	LL	PL	SL	v	E	k	V		γ <sub>d</sub>	G <sub>s</sub>	R.O.D #	CORE #	DEPTH	UNITS	FORMATION	AGE
	MPa	MPa	°	MPa	MPa	MPa	%	%	%	%	%	%	%	%	MPa	rad	m/s	kN/m <sup>3</sup>					m			
Med. chalk white.	0.11																									
Chalk white; fractures 60°, 70°, 90° dip with calcite and limestone.	0.85-1.17			6.02	1.71	39.56									4.35	2283	1578	2.61								
Marly chalk white; fractures 50°, 90°, dip with limestone.				7.07	1.47	39.28									1.59	2216	1596	2.63								
Chalk white; fractures 60°, dip with some limestone.				6.89	1.53	40.89									1.24	2279	1573	2.64								
Marly chalk light brown massive; fractures 20°, 40°, 50°, dip, limestone, see manganese; silicates.	0.6-0.6			8.19	1.67	34.81									1.24	2328	1661	2.63								
Chalk white; fractures 30°, 50°, 60°, 90°, dip, some limestone, fossil relics.	1-1.5			8.09	1.57	38.91									2.31	2343	1528	2.64								
				17.67	1.89	24.71									0.37	2812	2043	2.63								
				14.23	1.00	17.33									0.17	2117	2027	2.61								
	1-1.5			8.09	1.70	40.09									0.48	2341	1600	2.59								
Chalk marly light grey. Med. dark grey, brownish, limestone. Chalk white, massive.	1.3			11.63	1.80	37.33									0.21	2314	1858	2.58								
	0.83			16.18	1.61	21.03									0.08	2670	2049	2.63								
	0.84			12.58	1.13	21.33									16.36	3220	2097	2.63								
Chalk marly, white, light grey; pink; fractures 0°, 90°, 80°, dip, limestone.	0.39-0.67			11.18	1.19	28.51									0.57	2828	1816	2.63								
	0.58			18.65	1.20	21.33									0.17	3426	2028	2.66								
Chalk white; fractures 80°, dip, calcite 2 mm wide, silicates.	0.18																									

- c - Cohesion
- φ - Friction angle
- Sc - Compressive strength
- St - Tensile strength
- Is - Point load strength index
- n - Porosity

- PI - Plasticity index
- LL - Liquid limit
- SL - Shrinkage
- E - Modulus of elasticity
- v - Poisson ratio
- 1 MPa = 10.197 Kgf/cm<sup>2</sup>

- K - Permeability
- V - Ultrasonic wave velocity
- γ<sub>d</sub> - Dry density
- G<sub>s</sub> - Specific gravity
- R.Q.D - Rock quality designation
- Q - Rock mass quality
- CORE % - Core recovery

- Limestone
- Dolomite
- Marl
- Clay
- Chalk
- Flint
- Fossil
- Kent
- L - Limestone
- M - Manganese

BORING NO - HYDRAULIC  
 BORING METHOD - CORE DRILLING  
 DIAMETER - 97 mm  
 CONTRACTOR - L.M.M.  
 DATE - April 1981

GEOLOGICAL SURVEY  
 REP No. : G S / 18 / 81  
 COORDS : 179 07 41 / 13 03 52  
 ELEVATION : 763.33 m  
 DEPTH : 30 m.

66 Figure 58. Mount Scopus Tunnel, Borehole Z4.



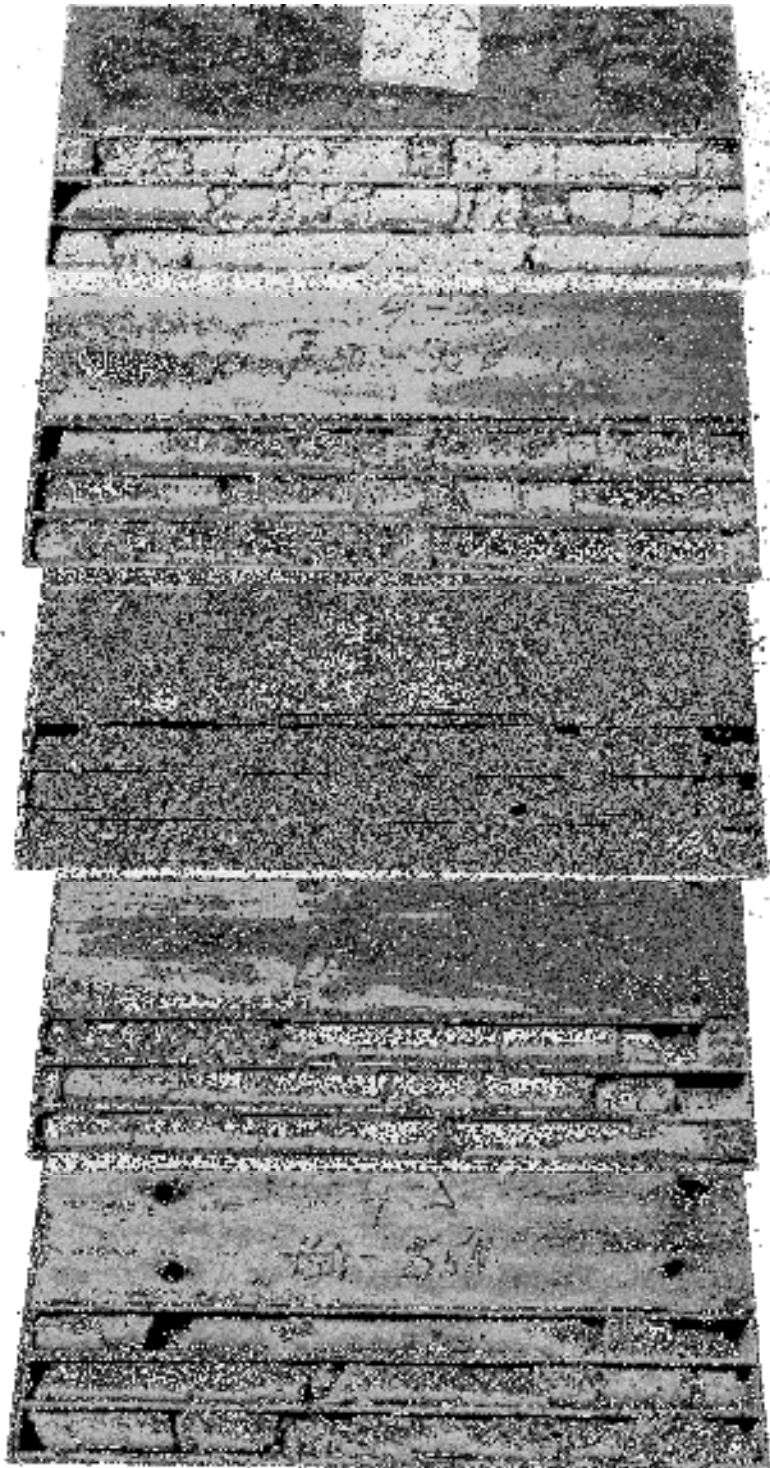


Figure 59. Mount Scopus Tunnel, Borehole Z4. Photo of borehole core recovery.

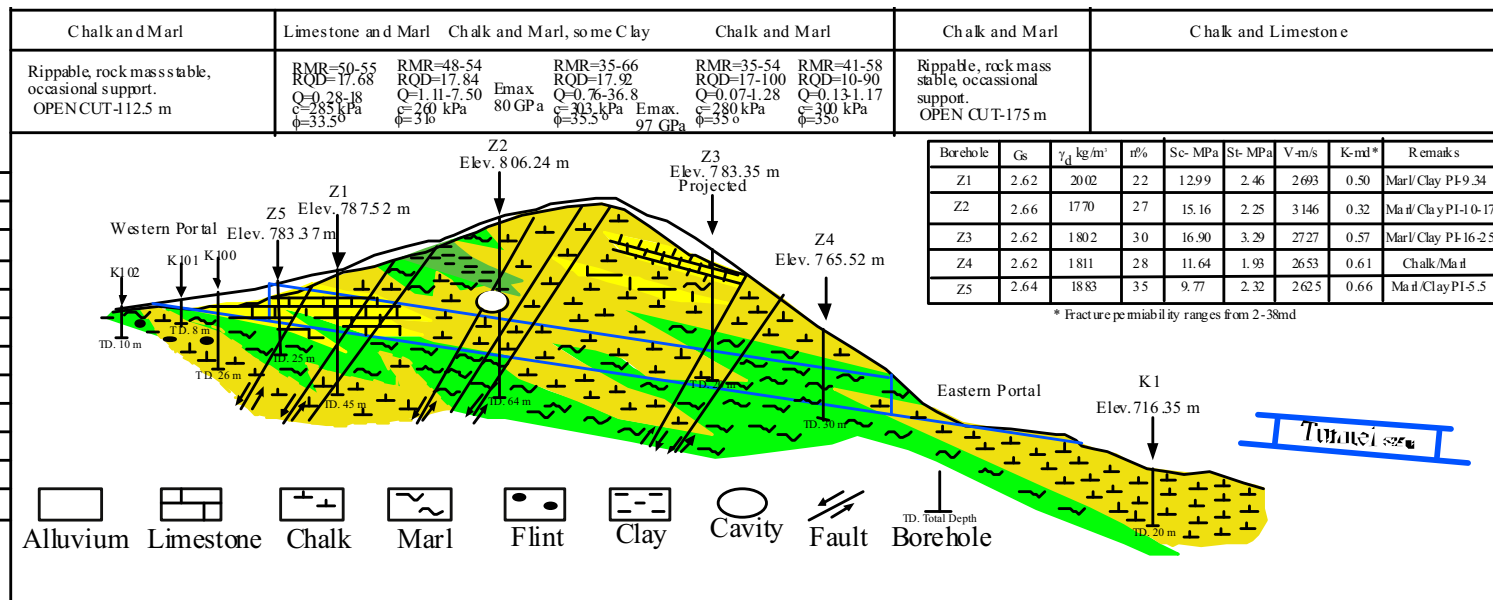


Figure 60. Geotechnical cross section along the Mount Scopus Tunnel alignment.

The plasticity of the rock types containing clay was summed up in Figure 61 and the suggested method of excavation according to the rockmass classification was shown in Figure 62. Additional boreholes denoted by the letter K were drilled along the approach roads to the tunnels on both the eastern and western sides to provide data for the construction of retaining walls in the soft chalk.

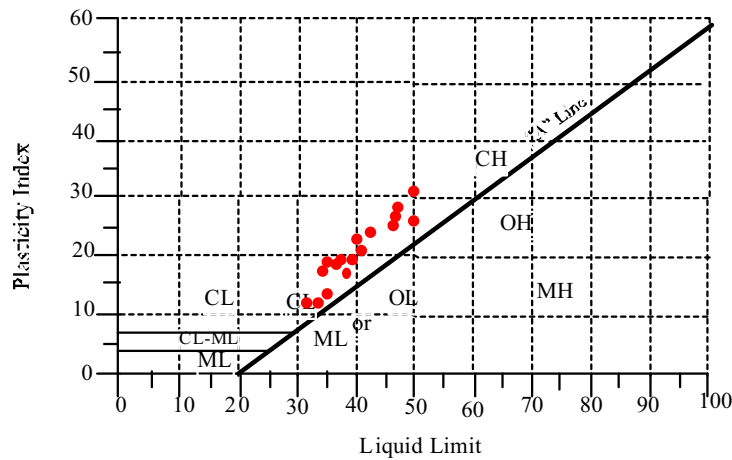


Figure 61. Plasticity chart for clay in the Menuha Formation marly chalk at the Mount Scopus Tunnel site.

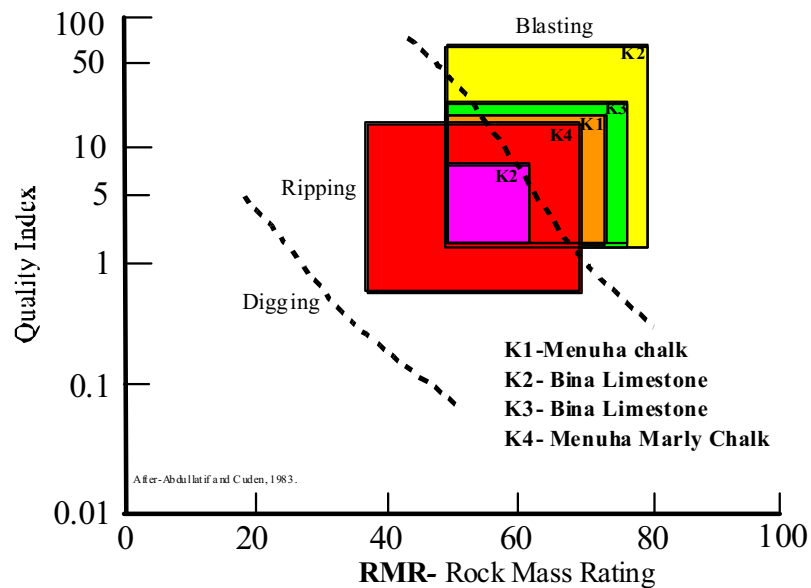


Figure 62. Suggested excavation method according to rock mass classification.

The hard chalk has a compressive strength of 11.7-33.2 MPa and a tensile strength of 2.12-4.5 MPa. The soft chalk has a compressive strength of 10.9-22.6 MPa, and tensile strength of 1.48-1.96 MPa. The limestone within the formation has a compressive strength of 30.8-77.3 MPa. The clay component is smectite with some kaolinite, the former being sensitive to water. Where clay occurs the Plasticity Index ranges from 11-26 (Figure 61) and swelling pressure may reach as high as 0.246 MPa. The overall rockmass classification has a Q range of 0.35-3.8 and is as high as 11.3 in places. The RMR ranges from 35-66, representing a poor to good rock mass. The support structures used were shotcrete and steel arches.

Tests on chalk and soft limestone samples with regard to the method of excavation indicated ideal conditions for the use of a roadheader tunneling machine. The samples tested had an average strength of 18.9 MPa and indicated an estimated instantaneous cutting rate of 65.90 m<sup>3</sup>/hr for a medium duty roadheader or 100-125 m<sup>3</sup>/hr for a heavy duty machine. The final performance during construction compared favorably with the parameters achieved during the investigation. The overall method of excavation with regard to quality rating and rock mass rating is shown in Figure 62.

## **WATER SUPPLY**

### **General**

Water supply to Jerusalem in the early years is assumed to have been from the nearby Gihon perennial spring in the upper Qidron valley that flows out at the foot of the City of David. The rocks from which the Gihon flows consist of fractured, karstic limestone and dolomite of Turonian age. Additional water was obtained by collecting rainwater in cisterns and pools, some shallow hand dug wells, as well as via aqueducts. In the latter case water flowed to the city from perennial springs located at higher elevations 11.5-18.5 km south of Jerusalem.

During the British Mandate (1917-1948) the British Army supplied Jerusalem with water by pumping directly from the Arruba Pool (see chapter Aqueducts following) through a metal pipe. Since 1918 the Lower Aqueduct ceased to supply water to Jerusalem. The British Mandatory Government also installed pumping stations at Solomon's Pools in 1923 and at three springs in Wadi Qelt, east of Jerusalem: Ein Farah in 1928; Ein Fawwar in 1931; and Ein Qelt in 1935. A 60 km long 18" diameter pipe line was laid in 1936, joining Jerusalem with the Rosh Ha'ayin (Hayarqon) springs in the coastal plain. Since 1948 three additional pipe lines have been laid and fed from wells pumping from the two subaquifers of the Judea Group aquifer west of the Judea Mountains.

In rainy winters when the water level in Lake Kinneret is high 5% and more of the total water supply to Jerusalem is supplied via the National Water Carrier. During the past fifty years groundwater in Jerusalem and vicinity has been pumped from the Lower Judea Group Subaquifer from wells mainly west of Jerusalem and these are shown in Figures 63, 64, 65 and 67. Discharge from these wells ranges between 58 and 334 m<sup>3</sup>/h, however some wells have been shut down due to contamination. The Gihon Water Company nowadays supplies the water throughout the city and is also responsible for sewage disposal.

## **GROUNDWATER**

Groundwater in Jerusalem and vicinity occurs in the phreatic, karstic and fractured Judea Group aquifer. West of the Judea Mountains the aquifer is mostly confined. The aquifer consists of a complex of Cretaceous dolomite and limestone with some thin marl and clay layers. For a detailed description of these rocks and formations see Figure 8. The Moza Formation of marl, clay and some limestone and the marly facies of the Bet Me'ir Formation within the rock sequence separates the aquifer into two main subaquifers: the Upper and the Lower Subaquifers (Shachnai, 1980) shown in Figure 63. In some areas the marly Kefar Sha'ul Formation separates the Upper Subaquifer into two secondary subaquifers (Shachnai, 1980). The thin marl layers of the Soreq Formation separate the Lower Subaquifer into a several secondary subaquifers. The thickness of each main subaquifer is approximately 400 m, however the Upper Subaquifer is thinner in many places due to erosion. Numerous perched springs flow out of the Upper Subaquifer where the Moza Formation acts as an aquiclude and daylight at the surface.

The groundwater flow in the region is controlled by the geological structure of the Judea anticline. The Lower Judea Group Subaquifer around Jerusalem has been penetrated by more than twenty boreholes (Table 9) from which a groundwater contour and a isochloride map have been prepared. (Figures 64, 65 and 66). These maps demonstrate that groundwater enters the area from the northeast along synclinal folds and splits into two directions, one from northeast to southwest and the other eastwards, forming the local groundwater divide.

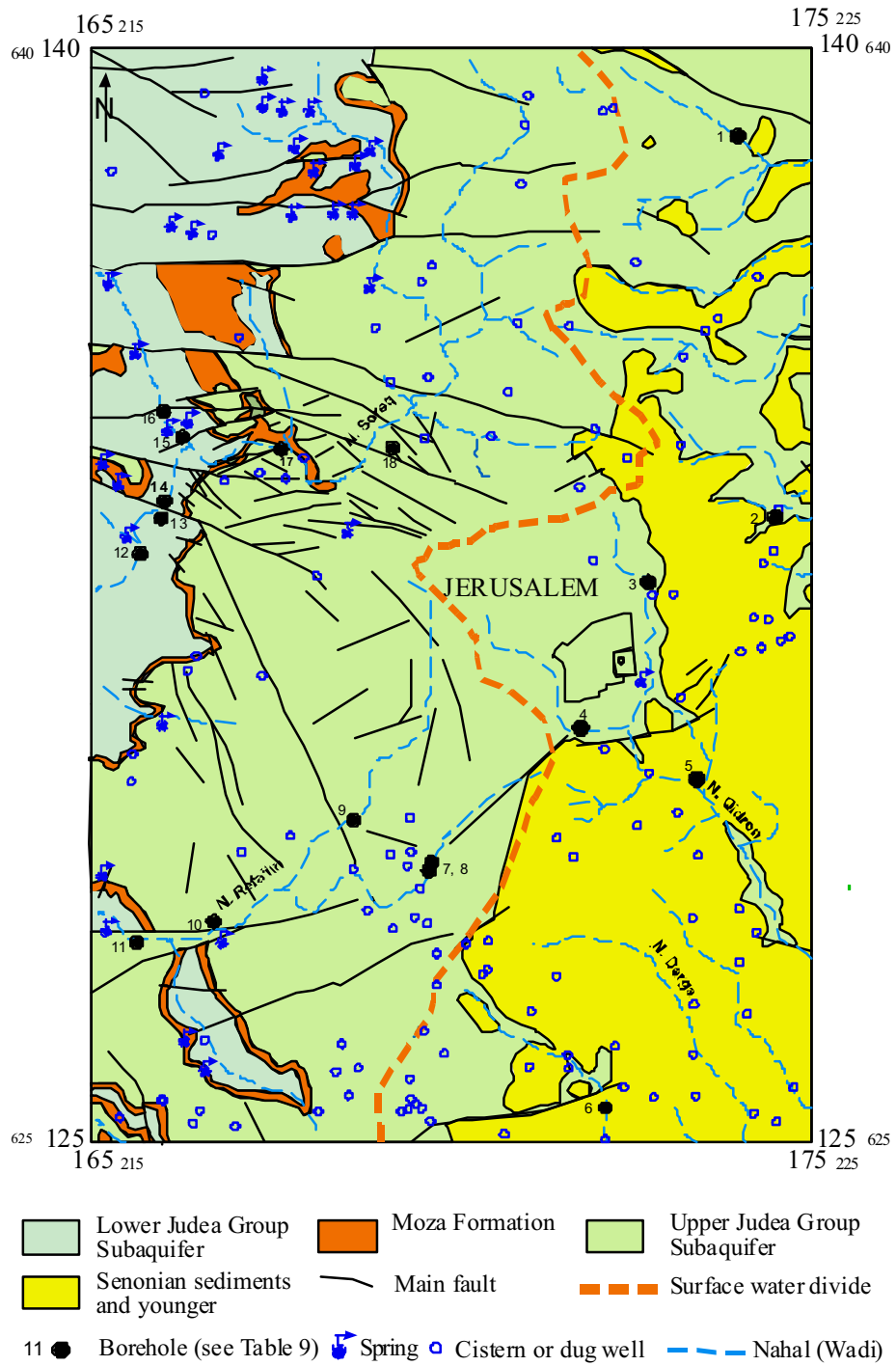


Figure 63. Hydrogeological map showing subaquifers, boreholes, springs and cisterns.

Table 9. Groundwater elevations, Cl and NO<sub>3</sub> in the Lower Judea Group Subaquifer.  
(After Baida and Guttman 1985, Hydrological Service 2007)

Well Number on the map	Well name	Coordinates	Groundwater elevation (+m) (March 1984)	Cl (Mg/l) (April-May 1985)	NO <sub>3</sub> (Mg/l) (May 1985)
1	Yerushalayim 11	17411/13876			
2	Yerushalayim 7	17445/13340			
3	Yerushalayim 5	17291/13271	362	28	15.3
4	Yerushalayim 4	17170/13070	420	32	14.4
5	Yerushalayim 14	13745/13000			
6	Yerushalayim 6	17217/12559	223 (2/84)	25	
7	Yerushalayim 2	16980/12877			
8	Yerushalayim 3	16980/12877	422	28	10.8
9	Yerushalayim 1	16880/12950	480	37	15.2
10	En Kerem 16	16685/12805		39	18.3
11	En Kerem 17	16571/12777	450		
12	En Kerem 15	16552/13282	478	39	17
13	En Kerem 2	16608/13363	(482-4/83)	28	14.4
14	En Kerem 14	16623/13402	477	43	
15	En Kerem 9	16641/13475		28	
16	En Kerem 18	16610/13515			
17	En Kerem 10	16782/13466	486	39	
18	En Kerem 12	16910/13456	498	57	
On Figures 65, 66	El Eizariya 1	17660/13200	13 (2/84)	28	
On Figures 65, 66	En Kerem 5	16146/13379	476		
On Figures 65, 66	En Kerem 7	16160/13166	408		
On Figures 65, 66	En Kerem 8	15902/13372	498		
On Figures 65, 66	En Kerem 11	16305/13085	436		
On Figures 65, 66	En Kerem 1	16490/13193	472	43	
On Figures 65, 66	En Kerem 4	16416/13117	459	57	15
On Figures 65, 66	En Kerem 6	16226/13006	429	36	
On Figures 65, 66	En Kerem 13	16465/12791	443	39	
On Figures 65, 66	Herodion 2	17092/11933	328	25	

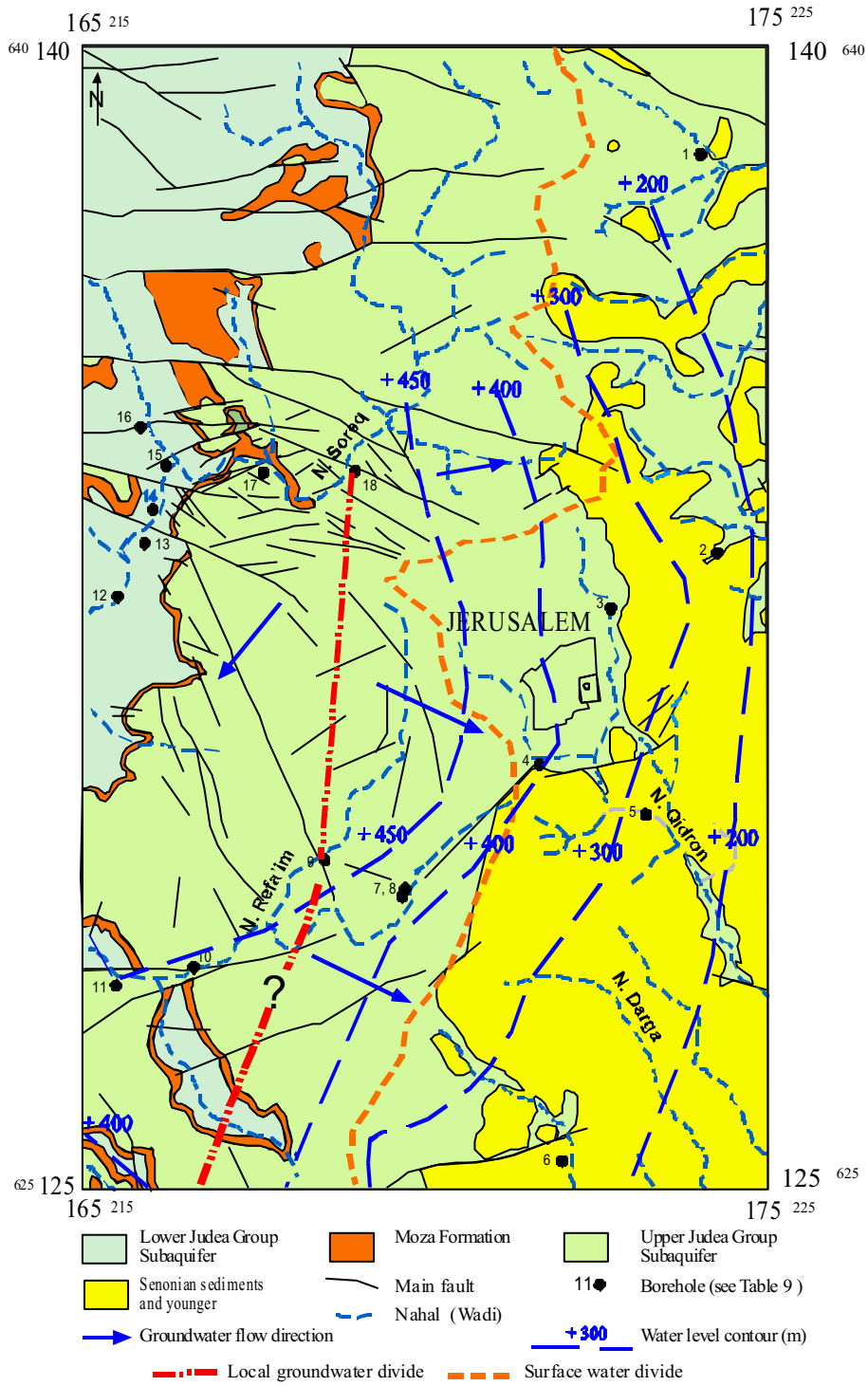


Figure 64. Jerusalem groundwater contour map of the Lower Judea Group Subaquifer (March 1984).





Groundwater elevations in the Lower Subaquifer near this groundwater divide range between 420 and 490 m above mean Mediterranean sea level, becoming lower towards the east by 226 m in the Yerushalayim 6 well (March 1984) and 13 m in the El Eizariya 1 well (March 1984). The depth to water level from the surface near the groundwater divide is generally between 100 and 200 m and fluctuates between 3 and 26 m in the different wells throughout the year.

The chemical analyses presented in Table 10 and the isochloride map (Figure 66) indicate high quality fresh water. The low value of cation and anion concentrations show that the water source is located in the recharge area and is from precipitation of rain and occasional snow. The amount of recharge is approximately 30% of the total yearly precipitation of an annual average rainfall of 500 mm (Ecker, 2000).

Table 10. Chemical analyses (mg/l) of waters from the Upper and the Lower Judea Group subaquifers.

Water source and subaquifer	Ca	Mg	Na	K	Cl	SO <sub>4</sub>	HCO <sub>3</sub>	NO <sub>3</sub>
En Kerem 15 – well. (Lower) <i>Hydrological Service 26/9/93.</i>	77.0	29.4	23.0	1.8	43.0	21.0	18.15	23.0
Ein Se'adim-spring. (Upper) <i>Mekorot Co. 14/12/95.</i>	87.5	44.7	20.5	2.1	42.9	7.5	405.1	1.3

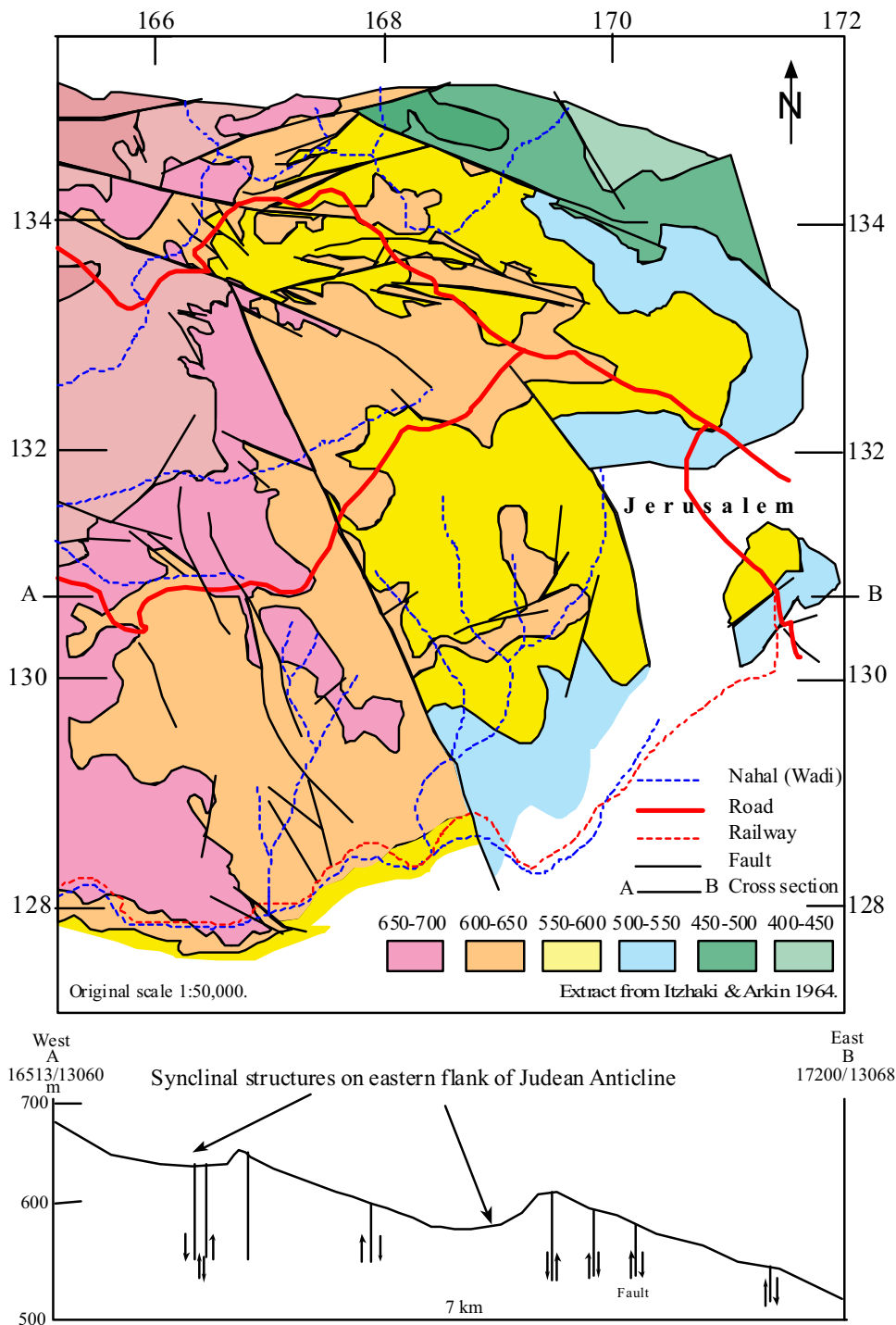


Figure 67. Structural contour map (m) and structural cross section on base Moza Formation (kumo).

### Cisterns and pools

In the mid 20<sup>th</sup> century, before the appearance of boring machines, the water supply to Jerusalem was from springs, rainwater and floodwater collected in cisterns and pools, some shallow dug wells and water imported via aqueducts and pipe lines.

The hydrogeological map (Figure 63) shows the location of many of the present-day cisterns and dug wells. In early times cisterns were excavated in places where water was needed regardless the geological formations. Today 34 cisterns are found on the Temple Mount. The largest three cisterns are located near the El Aqsa Mosque and have a volume of 12,000 m<sup>3</sup>, 8,000 m<sup>3</sup> and 5,000 m<sup>3</sup>, respectively (Hecker, 1965).

During King Herod's time (37-4 BCE) some 15 pools and reservoirs were excavated to collect rainwater, aqueduct water and floodwater within and in the vicinity of the actual walls of the Old City (Avitsur, 1992). Today these pools are not in use and most are filled with rubble or covered with soil. Table 11 shows pools from the First and the Second Temple times as well as those of Herod's time not in use today. Six thousand cisterns with a total capacity of 500,000 m<sup>3</sup> (Avitsur, 1992) existed in Jerusalem towards the end of the Ottoman Rule (1517-1917).

In 1948, the Jewish Quarter of the Old City contained 1,053 cisterns with an approximate capacity of 1,000,000 m<sup>3</sup> (Hecker, 1965).

Table 11. Pools and water reservoirs not in use today.

Name	Dimensions	Period	Remarks
Upper Pool.	23 m deep.	First Temple.	In the Old City.
Sedeh Koves.		First Temple ?	Near Ein Rogel.
Birket El Hamra.			Known also as the Siloam Pool. Supplied by the Gihon Spring.
Miriam Pool.		Second Temple.	
Sultan's Pool.	73,920 m <sup>3</sup> capacity. (Avitsur, 1992).	Herodian.	In the Ben Hinom Valley. Largest pool.
Mammilla Pool.	97 m x 60-65 m x 6.5 m.	Herodian.	In the upper Ben Hinom Valley. Fed by floodwater and by the Upper Aqueduct. In use till 1948.
Israel Pool.	110 m x 38 m x >26 m.	Herodian.	In the Old City.

Bet Hisda Pool.	45 m x 6 m x 11 m.		In the Old City. Known also as the Probatica Pool.
Amegdalon Pool.	95 m x 44 m x 6-7.5 m.	Herodian.	In the Old City. Known also as The Tower or the Hezekiah Pool. Supplied by gravity from the Mammilla Pool.
Hesterotion Pool.		Herodian.	Discovered in the 19 <sup>th</sup> century.

### Aqueducts

Since the time of the Second Temple (2<sup>nd</sup> century BCE), water was imported to Jerusalem mainly by an aqueduct system (Figure 68). It was collected from perennial springs issuing from the lower part of the Upper Subaquifer close to the Moza Formation. Three pools, called “Solomon’s Pools”, (locally named El Burekh pools) acted as the main reservoir of the system from which water flowed by gravity to Jerusalem. The pools are hydraulically connected and contain more than 180,000 m<sup>3</sup> of fresh water (Mazar, 1989). They are located 11.5 km south of the Temple Mount at elevations of 765 m, 785 m, and 800 m above mean Mediterranean sea level.

These pools are fed by floods, nearby springs, as well as by the two Herodian Biyar and Arruba aqueducts which carry water from springs located south of the pools. The Biyar aqueduct, 4.7 km long, begins at the El Biyar spring at an elevation of 890 m and connects the pools via two tunnels (one of them is 2.8 km long) and two channels. The Arruba aqueduct is 39 km long and supplied water to the second pool from springs located at elevations of 820 m to 840 m. This system also included a pool of approximately 20,000 m<sup>3</sup> capacity constructed by the Roman governor, Pontius Pilatus (26-36 CE).

Water was brought to Jerusalem from the above pools by two main aqueducts:

a. **The Lower Aqueduct** was built during Hasmonean rule at the time of the Second Temple. It began at Ein Eitam, below the lowest pool, at an elevation of 765 m. It is 21 km long and terminated at the Temple Mount at an elevation of 735 m. Water was supplied to the aqueduct from the pools as well as from the nearby spring of Ein Faruje. This enabled a continuous flow throughout the year (Mazar, 1989). The aqueduct winds through the topography, crossing like bridges and passing through two tunnels. One tunnel, 360 m long, is located under the city of Bethlehem and the other, 423 m long, passing through the Armon Hanaziv ridge (Jebel Mukkaber). This aqueduct was in operation up to the end of the Ottoman rule and was repaired many times during its history (Figures 69 and 70).

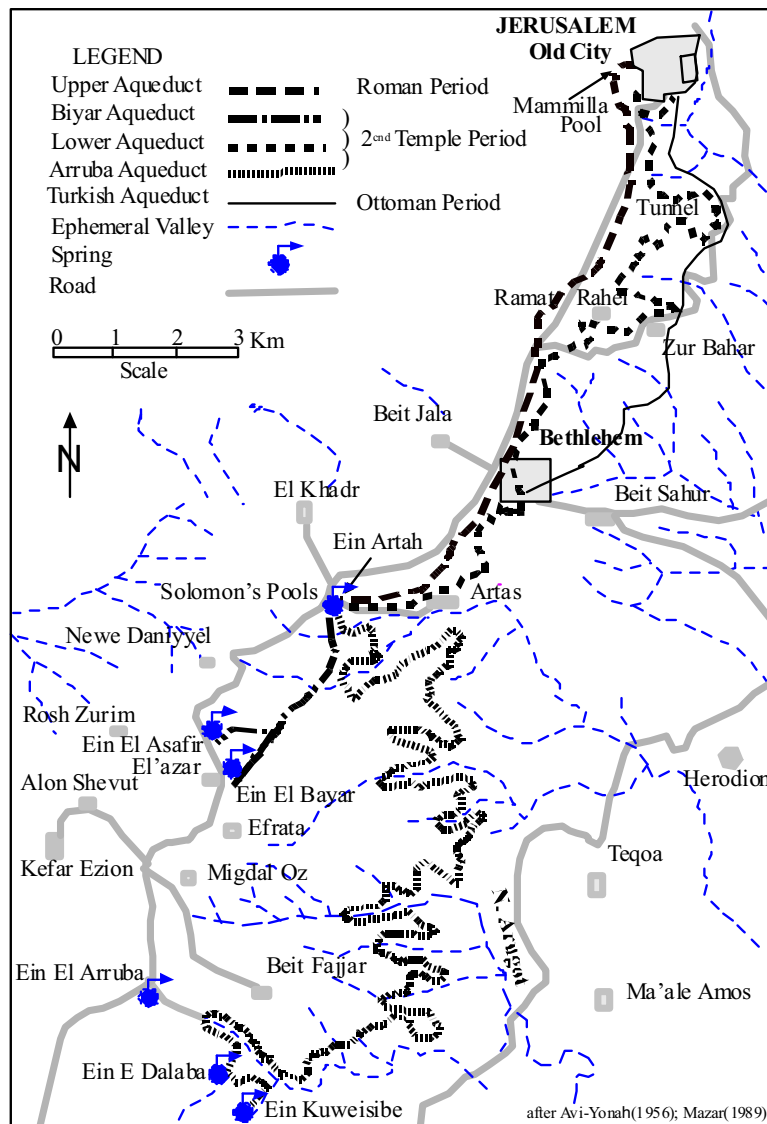


Figure 68. Ancient aqueduct network supplying water to Jerusalem.

b. **The Upper Aqueduct** was built by King Herod (37-4 BCE) and is 14 km long. It began at the upper pool of Solomon's Pools at an elevation of 800 m and terminated in Jerusalem at an elevation of 760 m. A bridge more than 2 km long was built over the 35-40 m deep valley north of Bethlehem (Amit, 1994) to maintain the elevation of the aqueduct as high as possible. The bridge was later destroyed. The aqueduct was rebuilt 200 years later by the Roman Tenth Legion, using a ceramic pipe acting as a siphon instead of a bridge to cross this valley.



Figure 69. The lower aqueduct located on the southern side of Mt. Zion, partly broken and showing the installed Ottoman clay pipe.



Figure 70. The lower aqueduct between the Sultan's Pool and the Temple Mount located on the western side of Mt. Zion. An Ottoman clay pipe is installed in the aqueduct.

## WASTE MATERIALS

### Sewage

Five main watersheds exist in Jerusalem and vicinity (Figure 71). Two drain westwards to the Mediterranean Sea through Nahal Refa'im and Nahal Soreq and the other three, Nahal Og, Nahal Qidron and Nahal Darga, drain eastwards to the Dead Sea.

Sewage control along these watersheds began during Ottoman times some 100 years ago. Remnants of the system are seen as channels paved with bricks and clay pipes that still exist in East Jerusalem. The sewage system was designed to flow by gravity except at three locations where pumping was required. Part of this old system in the Muslim and Christian Quarters of the Old City was replaced in recent years to provide a cleaner environmental area to encourage tourism (Jad et al., 1996).

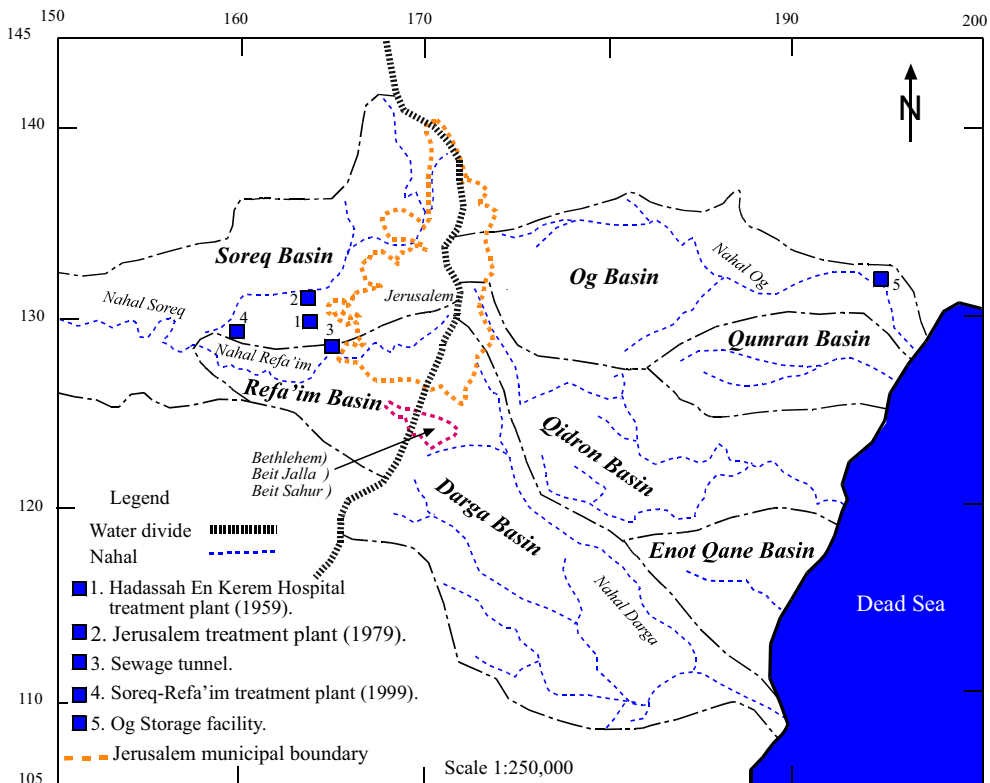


Figure 71. Drainage basins and sewage treatment plants in the Jerusalem area.



### **Western Drainage System**

The current situation in Jerusalem and vicinity with regard to liquid sewage disposal is confined mainly to the watersheds of Nahal Refa'im and Nahal Soreq. Nahal Refa'im drains sewage from the southwestern part of Jerusalem and from Har Homa, Beit Jala and western Bethlehem. The sewage from Beit Jala and western Bethlehem drains to the valley through a pipeline donated by the German government.

Sewage from Har Homa, Zur Bahr and Umm Zuba will be treated by a plant using the membrane method. The effluents will be used to irrigate public parks in Jerusalem (M. Blum personal communication, 2005).

Before the construction of the sewage treatment plants in Nahal Soreq raw sewage flowed untreated along Nahal Soreq over fractured rocks of the Judea Group aquifer (Figure 63). There is no evidence, as yet, to where infiltrating sewage flows in the underground. It seems possible that some deviates towards the Dead Sea, at the local groundwater divide, with the rest flowing westwards.

Nahal Soreq drains the sewage of northwestern Jerusalem (Figures 63 and 71) as well as that of several villages in the neighborhood. In 1959 the first sewage treatment plant was built in the upper part of Nahal Soreq specifically to treat sewage from the Hadassah Hospital in En Kerem. Twenty years later, in 1979, another treatment plant with a capacity of 13,000 m<sup>3</sup>/day was constructed near the existing plant in En Kerem to treat the sewage from Jerusalem. The treated sewage was released through a 6 km long pipe into Nahal Soreq and flowed over rocks of the Lower Judea Group Subaquifer to the confluence with Nahal Refa'im. By 1994 the plant could not absorb the total flow of the sewage that had increased to 22,000 m<sup>3</sup>/day (Hazut et al., 1995). The surplus untreated sewage flowed from the plant along the valley floor over the Judea Group limestone and dolomite.

A major treatment plant in Nahal Soreq built to serve both valleys was completed in 1999. The flow from Nahal Refa'im has been diverted since 1999 through the 2.1 km long tunnel into the Nahal Soreq system. The sewage from both valleys is collected in a pipeline that terminates at the treatment plant. The first stage capacity of the plant is 100,000 m<sup>3</sup>/day and will be followed by a second stage of 135,000 m<sup>3</sup>/day. It is estimated that a flow of 100,000 m<sup>3</sup>/day will be reached during 2008-2010. By 2030 it is estimated that a flow of 135,000 m<sup>3</sup>/day will be reached (Hazut et al., 1995). The treated sewage will be released through a single pipeline by gravitation outside the Judea Mountains, to be used for irrigation in the coastal plain.

### **Eastern Drainage System**

The eastern drainage system follows Nahal Og, Nahal Qidron and Nahal Darga, which collect sewage from the eastern parts of Jerusalem and several peripheral villages (Figure 71). In some sections it flows over the Menuha and Ghareb formations of mainly chalk and some marl which act as aquicludes preventing percolation into the aquifers below.

In Nahal Og the sewage flows along the valley floor into a filtration plant that removes large materials. It continues through a pipeline to a reservoir in the vicinity of the Dead Sea which is intended for irrigation purposes in the area.

Nahal Qidron drains the sewage of the central and southeastern parts of Jerusalem, Bethlehem and Beit Sahur (Figure 71). The untreated sewage flows eastwards along the valley floor over rocks of the Upper Judea Group Subaquifer and rocks of the Senonian and Ghareb formations. During the rainy season the flow reaches the Dead Sea. The effluents are today diverted to the Og storage facility near the Dead Sea and used to irrigate date plantations in the area.

Nahal Darga, south of Nahal Qidron, drains the sewage from the villages and towns south of Jerusalem. The sewage flow does not reach the Dead Sea. The area to the east of these town and villages is a nature reserve and therefore it is planned to divert future flows into the Nahal Qidron and the Nahal Og storage facilities.

### **Solid Waste**

As a rule solid waste is laid out on the surface. The solid waste from west Jerusalem is accumulated near the village of Abu Dis, east of Jerusalem, where it is spread out and covered with soil. The solid waste from the Arab villages around Jerusalem is generally laid out on bare terrain or in valleys with no infrastructure (Jad et al., 1996). In these areas it may be partly treated, burned or covered with soil or in some areas left untreated.

## BIBLIOGRAPHY AND REFERENCES

- Abel, F. M., 1967. *Geographie de la Palestine, Paris. p. 505*
- Abels, Z., Arbit, A., 1995. The City of David Water Systems. The Faculty of Printing Techniques, *Hadassah College of Technology, Jerusalem.*
- Aisenstein, B., 1965. Some observations on deconsolidation of limy rocks on steep slopes. *Proc. 6<sup>th</sup> Int. Conf. Soil Mechanics. pp. 439-441.*
- Aisenstein, B., David, D., Wiseman, G., 1966. Mechanical properties of some marls in Israel. *1st Cong. Rock Mechanics, Lisbon. pp. 393-397*
- Amiran, D.H.K., Arieh, E., Turcotte, T., 1994. Earthquakes in Israel and adjacent areas: Macroseismic observations since 100 BCE. *IEJ, Vol. 44, pp. 260-305.*
- Amit, D., 1994. New data for dating the aqueducts of Jerusalem. In: The hundred booklet of Ariel. Part B. pp. 57-64. *Ariel Publishing House Jerusalem (in Hebrew).*
- Arkin, Y., 1963. Composite section of the Judea Group (Jerusalem area). *Isr. Geol. Surv. Publ.*
- Arkin, Y., 1967. Jerusalem-Bet Shemesh: Geological cross sections. *Isr. Geol. Surv. Publ.*
- Arkin, Y., 1973. Geological map of Greater Jerusalem on a scale 1:50,000 with explanatory notes. *Atlas of Jerusalem.*
- Arkin, Y., 1976. Geological map of Jerusalem and vicinity. Scale 1:50,000. *Survey of Israel Publ., reprinted in 1985 and 1997.*
- Arkin, Y., 1978. Lithostratigraphic dictionary of geological mapping units in Israel. In: Steps in the Geology of Israel. *Tel Aviv Open University Publ. 17 p.*
- Arkin, Y., 1980. A survey of karst phenomena, western Judea Mountains. *Isr. Geol. Surv. Rep. No. MM/5/80, 30 p. (in Hebrew).*
- Arkin, Y., 1980a. Ground subsidence (sinkhole) near the Damascus Gate, Nevi'im-Zanhanim Junction, East Jerusalem. *Isr. Geol. Surv. Rep. MM/3/80, 27p. (In Hebrew).*
- Arkin, Y., 1984. A Sinkhole near the Damascus Gate, Old City of Jerusalem. *3<sup>rd</sup> Int. Symp., on Land Subsidence, Venice, Proc. pp. 565-574.*
- Arkin, Y., 1986. Geotechnical factors influencing marl slopes in Israel. *Ph.D. Thesis, University of London, UK. Isr. Geol. Surv. Rep. GSI/27/86, 386 p.*
- Arkin, Y., 1988. Disintegration of marl slopes in Israel. In: *Environmental Geology and Water Science 11:1:5-14. Elsevier. pp. 5-14.*
- Arkin, Y., 1989a. Geotechnical cross section, bridge alignment Road No. 4 Nahal Gilo. *Isr. Geol. Surv. Rep. GSI/21/89. 13p.*

- Arkin, Y., 1989b. Moza-Rupin environmental impact: geology, geotechnics and hydrology. *Isr. Geol. Surv. Rep. GSI/58/89*, 32 p.
- Arkin, Y., 1989c. Stability of slopes in Upper Cretaceous chalks in Israel. *Proc. Int. Chalk Symp. Brighton Polytechnic*. 8 p.
- Arkin, Y., 1989d. Preliminary geological and geotechnical survey of proposed tunnel site , Weizmann-Herzl Junction, Road No.4 Jerusalem. Rep. GSI/38/89, *Isr. Geol. Surv.* 21 p.
- Arkin, Y., 1992. Geotechnical aspects of tunneling in the Jerusalem Area. *11<sup>th</sup> Conf. Mineral Engng., Nahariyya*.
- Arkin, Y. and Bartov, Y., 1982. Geological maps-types and Application. In: Maps and Map Reading. (eds.) Kadmon, N. and Shmueli, A. ( in Hebrew) *Keter Jerusalem*.
- Arkin, Y. and Braun, M., 1967. Correlation table of lithostratigraphic units in Israel. *Isr. Geol. Surv. Publ.*
- Arkin, Y. and Braun, M., Starinsky, A., Hamaoui, M., Raab, M., 1965. Type sections of Upper Cretaceous formations in the Jerusalem-Bet Shemesh area. Strat. Sect. No. 1. *Isr. Geol. Surv. Publ.* 42 p.
- Arkin, Y. and Hamaoui, M., 1967. The Judea Group (Upper Cretaceous) in central and southern Israel. *Isr. Geol. Surv. Bull. No. 42*. 17p.
- Arkin, Y. and Flexer, A., 1986. Engineering Geology in Israel. *Isr. Journ. of Earth Sciences*.
- Arkin, Y. and Gavish, E., 1995. Har Gilo Tunnels-geological aspects, civil engineering with a view to the future. *10<sup>th</sup> National Conf. Of Engineers. Tel Aviv. Pp.187-199.(in Hebrew)*.
- Arkin, Y., Kafri, U., Michaeli, L., Mimran, Y., 1987. Geological and geotechnical survey along Road No. 4 Jerusalem-Gush Ezion, Har Bet Gilo tunnel alignment. *Isr. Geol. Surv. Rep. GSI/5/87*. 32p.
- Arkin, Y. and Michaeli, L., 1988a. Exploratory drilling and geotechnical classification of the rock mass at the site of tunnels, Route N<sup>o</sup>. 60. Jerusalem-gush Ezion, Har Gilo Section. *Geol. Surv. Isr. Report GSI/40/88*. 81p.
- Arkin, Y. and Michaeli, L., 1988b. Borehole investigation and engineering geological rockmass classification of tunnel sites, Road N<sup>o</sup>. 4. Jerusalem-Gush Ezion, Bet Gilo section. *Isr. Geol. Surv. Rep. GSI/40/88*. 86p.
- Arkin, Y. and Michaeli, L., 1989a. Exploratory drilling for detailed design Gilo tunnels, G6,G7,G8, Route No. 60. *Geol. Surv. Isr. Rep. GSI/6/89*. 34p.

- Arkin, Y. and Michaeli, L., 1989b. Strength and consistency of artificial clay-carbonate mixtures: Simulation of natural sediments. *Engine. Geol.* 26. pp. 201-213 Elsevier.
- Arkin, Y. and Michaeli, L., 1989c. Exploratory boreholes for detailed planning of Gilo tunnels, G-6, G-7, G-8, Road N° 60, Jerusalem-Kefar Ezion. *Isr. Geol. Surv. Rep. GSI/46/89*, 18 p.
- Arkin, Y. and Michaeli, L., 1989d. Exploratory geological and geotechnical survey of proposed tunnel, Haft Circle, Moza-Bet Hakerem Junction, Road No. 1 Jerusalem. *Isr. Geol. Surv. Rep. GSI/18/89*, 24p.
- Arkin, Y. and Michaeli, L., 1990. Exploratory boreholes Herzl-Weizmann Junction tunnel, Road No. 4 Jerusalem. *Isr. Geol. Surv. Rep. GSI/16/90*, 59p.
- Arkin, Y. and Michaeli, L., 1992. Geological and geotechnical site investigation of proposed tunnel alignment Herzl-Weizmann Boulevard Junction, western entrance to Jerusalem. *Isr. Geol. Surv. Rep. GSI/9/9*, 36p.
- Arkin, Y. and Michaeli, L., 1993. Tunnel site investigation, summary of geotechnical data (Road No. 60 Jerusalem-Gush Ezion). *Isr. Geol. Surv. Tech Rep. TR/GSI/20/93*. 29p.
- Arkin, Y. and Michaeli, L., 1993a. Monitoring possible deformational movements in the Gilo Short Tunnel. *Isr. Geol. Surv. Rep. GSI/32/93*, 49p.
- Arkin, Y. and Michaeli, L., 1994. Geology and geotechnology of the Gilo Short Tunnel. *Isr. Geol. Surv. Current Res.* 9:11-15.
- Arkin, Y. and Michaeli, L., 1997. Geological and geotechnical survey of the northern foundation site, Gilo Viaduct. *Isr. Geol. Surv. Rep. TR-GSI/12/97*, 43p.
- Arkin, Y., Michaeli, L. and Liberman, A., 1994. Har Hazofim tunnel additional boreholes Z6 and Z7. *Isr. Geol. Surv. Rep. TR-GSI/22/94*, 56p.
- Arkin, Y., Michaeli, L. and Rosen, A., 1989. Swelling features in the Kefar Sha'ul Formation, Gilo Short Tunnel Jerusalem. *Isr. Geol. Surv. Rep. GSI/52/89*, 31 p.
- Arkin, Y., Michaeli, L., Wolfson, N., 1993. university road approaches to the Har Hazofim Tunnel, borehole investigation. *Isr. Geol. Surv. Rep. GSI/19/93*, 39 p.
- Arkin, Y., Michaeli, L., Wolfson, N., 1993. Gilo Viaduct borehole investigation. *Isr. Geol. Surv. Rep. GSI/20/93*.

- Arkin, Y., Michaeli, L., Wolfson, N., 1993. Har Hazofim Tunnel, University road geological and geotechnical site investigation. *Isr. Geol. Surv. Rep. GSI/18/9*, 62 p.
- Arkin, Y., Mimran, Y., 1983. Geology of the rock mass in Israel with relevance to tunneling. Discussions in the use of the underground in Israel. *Ministry of Energy and Infrastructure, Jerusalem*.
- Avitsur, S., 1992. Water Resources in the Land of Israel. *Avshalom Inst. Tel Aviv (in Hebrew)*.
- Avi-Yonah, M., 1956. Ed. The Book of Jerusalem; Its Natural Conditions, History and Development from Origins to Present Day. Vol.1. *The Bialik and Dvir Publ. House, Jerusalem (in Hebrew)*.
- Avnimelech, M., 1962. Dinosaur tracks in the Lower Cenomanian of Jerusalem. *Nature Vol. 196. No. 4851. 264p*.
- Avnimelech, M., 1963. Discovery of Dinosaur tracks of Lower Cenomanian age in Beit Zeit, west of Jerusalem. *Isr. J. Earth Sci., Vol. 12. No. 1. Proceed. 80-81*.
- Avnimelech, M., 1966. Influence of geological conditions on the development of Jerusalem. *Bull. Amer. School Oriental Res. No. 181*.
- Bahat, D., 1989. Atlas of Jerusalem, *Jerusalem*.
- Baida, U., 1983. Follow-up hydrological report in sensitive areas for 1982/83. Be'er Sheva, En Kerem – Jerusalem, Jordan valley, Judea and Samariya (YO"SH), Shuni, Tireli. *Water Planning for Israel (Tahal) 01/83/52 April. Tel Aviv*.
- Baida, U. and Guttmann, Y., 1985. Follow-up hydrological report in sensitive areas in the Judea Group Aquifer for 1984/85. Be'er Sheva, En Kerem – Jerusalem, Jordan valley, Judea and Samariya (YO"SH), Shuni, Tireli, Modi'in, Ajur (Lower Aquifer). *Water Planning for Israel (Tahal) 01/85/65 March. Tel Aviv*.
- Baida, U., Zukerman, H., 1992. Jerusalem area. Exploitation and development possibilities of the groundwater resources in the Cenomanian aquifer. Hydrogeological examinations and numerical model. *Water Planning for Israel (Tahal), 01/92/10. Tel Aviv*.
- Barton, N., Lien, R., Lund, J., 1974. Engineering classification of rock masses for the design of tunnel support. *Rock. Mech. Vol. 6. No. 4. pp. 189-236*.
- Bartov, Y. and Arkin, Y., 1975. The geological photomap of Israel, on a scale of 1:500,000. *Isr. Geol. Surv. Publ.*
- Bartov, Y., Arkin, Y., Lewy, Z., Mimran, Y., 1981. Regional stratigraphy of Israel: A guide to geological mapping. *Isr. Geol. Surv. Publ. pp. 38-41*

- Bell, F. G., 1977. A note on the physical properties of the chalk. *Eng. Geol. Vol. 11. No. 3. pp. 217-225.*
- Bieniawski, Z. T., 1976. Rock mass classification in rock engineering. In: Z.T. Bieniawski (ed.) *Exploration for Rock Engineering, Balkema, Rotterdam. Vol. 1. pp. 97-106.*
- Bieniawski, Z. T., 1980. Rock classification: State of the art and prospects for standardisation. *Transport Research Record 783. Nat. Acad. Sci. Washington.*
- Bieniawski, Z. T., 1989. *Engineering Rock Mass Classification: John Wiley & Sons. 251p.*
- Bishop, A. W. and Blight, G. E., 1963. Some aspects of effective stress in saturated and partly saturated soils. *Geotechnique, Vol. 13. pp. 177-197.*
- Blake, G.S., 1936. The stratigraphy of Israel and its building stones. *Govt. of Palestine Print. and Stationery Office. 133p.*
- Blankenhorn, M., 1905. *Geologie der Naeheren Umgebung von Jerusalem. Zeitschr.Deutsche Palestina Ver. Vol.28.*
- Clark, A. R., Walker, B. F., 1977. A proposed scheme for classification and nomenclature for use in the engineering description of Middle Eastern sedimentary rocks. *Geotechnique, Vol. 27. No. 1. pp. 93-99.*
- Coates, D.F., 1964. Classification of rocks for rock mechanics. *Inst. Rock Mechanics and Mining Sci. Vol. 1, pp. 421-431.*
- Dan, J., 1977. The distribution and origin of Nari and other lime crusts in Israel. *Isr. J. of Earth Sci. Vol. 26, No. 2. pp. 68-83.*
- Deere, D. U., Merrit, A. H., Coon, R. F., 1969. Engineering classification of in situ rock. *Tech. Rep. AFWL-TR-67-144, Airforce Weapons Lab., New Mexico.*
- Deere, D. U., Lien, R., Lunde, J., 1974. Engineering classification of rock masses for the design of tunnel supports. *Rock Mechanics. Vol. 6. No. 4. pp.189-239.*
- Ecker, A., 2000. Contribution of saline waters in the Avedat and Mount Scopus groups aquitard to the Judea Group aquifer in the Yarqon-Be'er Sheva Basin. *Isr. Assoc. Water Resour. Ann. Meet., Akko, May 2000; Abstr. pp. 3-6.*
- Emery, J. J., 1976. *Creep on Slopes. Mechanics of Rock Slides and Avalanches, Elsevier, NY.*
- Flexer, A., 1968. Stratigraphy and facies development of the Mt. Scopus Group (Senonian-Paleocene) in Israel and adjacent countries. *Isr. J. Earth Sci Vol.17. pp. 85-114.*

- Fink, M., 1963. Hydrologic report on the groundwater horizon in the Jerusalem Corridor. *Water Planning for Israel (Tahal)*, Tel Aviv, July.
- Fischbein, A., Foner, H.A., Levy, R., Fischer, I., Brenner, S., Ganor, E., 1996. Urban atmospheric concentrations of lead, manganese and particular matter in central Jerusalem. In: Preservation of Our World in the Wake of Change, *ISEEQS Publ. Jerusalem. Vol. VIb, Ed. Y. Steinberger*, p. 605-607.
- Foner, H. A., 1990. The distribution of petrol-derived lead in Israel. *Sci. Total Environ.* 93; 43-50.
- Foner, H. A., 1993. Lead pollution in Israel. *Water Sci. Tech.* 27(7-8); 253-262.
- Fookes, P. G., Higginbottom, I. E., 1975. The classification and description of near-shore carbonate sediments for engineering purposes. *Geotechnique*, Vol. 25. No. 2. pp. 406-411.
- Fookes, P. G. and Sweeny, M., 1976. Stabilisation and control of local rock falls and degrading rock slopes. *Quart. J. Engineer. Geo.* 9:37-55.
- Gafni, G., 1978. Survey of abandoned quarries in Israel. Land Registration and Nature Reserves for *The Quarry Rehabilitation Fund*.
- Ganor, E., Foner, H.A., 2001. Mineral dust concentrations, deposition fluxes and deposition velocities in dust episodes over Israel. *J. Geophys. Res. – Atmospheres*, 106, D16, 18,431-18,437.
- Gavish, E., Arkin, Y., Hazor, Y., 1995. Problematics in rockmass classification of underground openings in the lower part of the Amminadav Formation. *Isr. Geol. Soc. Meet. Zikhron. (Abstract)*.
- Gavish, E., Hazor, Y., Arkin, Y., 1996. Adaption of imperical classification methods (Q & RMR) for tunneling in bedded rock: lessons from the Gilo Tunnel. *Isr. Geol. Soc. Meet. Elat*.
- Geddis, James. D., 1977. (ed.) Large Ground Movements and Structures. *Pentach Press, London*.
- Gilat, A., Wolfson, N., Michaeli, L., Arkin, Y., 1992. Eastern ring road geological and geotechnical survey. *Isr. Geol. Surv. Rep. GSI/22/92*, 61 p.
- Gill, D., 1996. The Geology of the City of David and its Ancient Subterranean Waterworks. *Excavations at the City of David 1978-1985, Vol. IV. QEDEM, The Hebrew University of Jerusalem*.
- Gillot, J. E., 1968. Clay in Engineering Geology. *Elsevier*.
- Ginzburg, D., 1972. Quarries and quarrying for building materials in Israel. *Rep. GSI/MP/536*, 32 p.



- Ginzburg, D., Ecker, A., Rosensaft, M., 1998. Computerized database of earth science maps from Israel and neighboring countries. *Geol. Surv. Curre. Res.* 11, pp. 51-52.
- Grinwald, Z., 1980. Water in Israel. *I.W.W.A. Tel Aviv*.
- Hazut, E., Sivan, E., Adir, S., 1995. Jerusalem and vicinity sewage treatment project. *Water Assoc. Water Engineers (Israel)*. Vol. 20. pp. 22-24 (in Hebrew).
- Hecker, M., 1965. Jerusalem water supply in ancient times. In: Book of Jerusalem Vol.1. 191-218.
- Hoek, E. and Bray, J., 1974. Rock slope engineering. *Inst. Min. and Met . London .*
- Hydrological Service 2007. Data from the water well inventory.
- Ilani, S., Shirav, M., 2001. Abandoned quarries in the Jerusalem and Bet Shemesh sheets, 1:50,000. Geology and environmental survey as an infrastructure for their rehabilitation. *Isr. Geol. Surv.Rep. GSI/5/2001*. (in Hebrew).
- Israeli, A., 1977. Geological-engineering properties of rocks in the Jerusalem area and geotechnical map on a scale of 1:10,000. *M.Sc. Thesis Hebrew University Jerusalem*.
- Itzhaki, Y., Arkin, Y., 1964. Geological map of Israel (structural), 1:50,000 Jerusalem-Bet Shemesh sheet. *Isr. Geol. Surv. Publ*.
- Jad, I., Qumsieh, V., Hosh, L., 1996. Environmental Profile for the West Bank. Vol. 6 Jerusalem District. *Applied Res. Inst. Jerusalem, Bethlehem*.
- Karte Der Materialien Zur Topographic Des Alten Jerusalem Gezeichnet von Oberlehrer August Kummel Barmen, und Herausgegeben Vom. *Deutschen Verein Zur Erforschung Palestinas 1904*.
- Katz, O., 2004. Landslide hazard evaluation of slopes during earthquakes, in the municipality of Jerusalem. *Isr. Geol. Surv. Rep. GSI/12/04*. (In Hebrew) 34 p.
- Kirkby, M. J., 1978. (ed.): Hillslope Hydrology. Chichester, *Wiley*. 389 p.
- Leeds, D. J., 1973. The design earthquake. In: Moran, D. E., Slosson, J. E., Stone, R. O. and Yalverton, C.A. (eds), *Geology, Seismicity and Environmental Impact. Assoc. Eng. Geol. Sp. Pub. Los Angeles*. pp. 337-347.
- Legget, R. F., 1973. *Cities and Geology. McGraw-Hill N. Y.*
- Lerman, S., 1995. Jerusalem sewage. Solutions for sewage treatment in the Western Basin. *Water. Assoc. Water Engineers (Israel) Vol.20*. pp. 27-42. (in Hebrew).

- Maheras, P., Kutiel, H., Gkika, S., 1995. Relations entre les precipitations Malte et les indices de circulation en Mediterranee durant la derniere periode seculaire. *Pub. Assoc. Int. climatol.*, 8, 320-326.
- Mazar, A., 1989. Aqueduct network to Jerusalem. In: Old Aqueducts in Land of Israel. *Yad Ben Zvi Edition*. pp. 169-204. (in Hebrew).
- Mimran, Y., Honigstein, A., Arkin, Y., Rosenfeld, A., Michaeli, L. and Hatzor, Y., 1996. The use of ostracod biostratigraphy in the geotechnical evaluation of the Santonian chalk for the proposed Mount Scopus tunnel. *Isr. Geol. Surv. Current Res.*, Vol., 10. Jerusalem. pp. 138-142.
- Minster, Z., 1981. Evaluation of potential quarrying for building materials in the Jerusalem Corridor. *Isr. Geol. Surv. Rep. GSI. MPBK/429/81*.
- Morgenstern, N. R., Eigenbrod, K.D., 1974. Classification of argillaceous soils and rocks. *J. Geotech. Eng. Div. ASCE. Paper 10885*. pp. 1137-1156.
- Mosely, P. M., 1981. Slopes and slope processes. *Prog. Physc. Geogr.*, Vol. 5. No. 1. pp.114-122.
- Olivier, H. J., 1979. A new engineering-geological rock durability classification. *Eng. Geol.*, Vol. 14. No. 1. pp. 255-279.
- Perath, I., 1984. Stone Building and Building Stone in Israel, a Historical Review. *Isr. Geol. Surv.* 97 p.
- Picard, L., 1938. The Geology of new Jerusalem. *Hebrew Uni., Jerusalem Geol. Dept.*, B. 2,1. 12p.
- Picard, L., 1943. Structure and evolution of Palestine *Hebrew Uni., Jerusalem Geol. Dept.* 135p.
- Rahn, H. P., 1986. Engineering Geology. An Environmental Approach. *Elsevier*. 589p.
- Ritchie, A., 1963. Evaluation of rockfall and its control. Highway Research records, USA, 17, 13-28.
- Rosen, A., 1989. Preliminary estimates of the swelling problem in the marly chalk of the Kefar Sha'ul Formation, Route No. 60 Jerusalem-Gush Ezion road tunnels at Har Gilo.
- Rosen, A., Arkin, Y., Michaeli, L., 1993. Jerusalem-Mount Scopus Tunnel Rep. No. 4. Deformation measurements while tunneling. *Isr. Geol. Surv. Rep. TRGSI/31/93*, 13 p.
- Russell, K. W. 1985. The earthquake chronology of Palestine and northwest Arabia from the 2<sup>nd</sup> through the mid-8<sup>th</sup> century AD. *Bull. American Schools Oriental Res.* 260, pp. 37-59.
- Salamon, A., Katz, O., On, C., 2003. Earthquake risk in Jerusalem. *Isr. Geol. Surv. Rep. GSI/21/03*, 39 p. (In Hebrew).
- Selby, M. J., 1982. Hillslope materials and processes. *Oxford Uni. Press*

- Shachnai, E., 1980. Yarqon Taninim-Be'er Sheva Basin. Updating the hydrogeological model. *Water Planning for Israel (Tahal)*, 01/80/12. 59 p.
- Shalem, N., 1927. La Creta Superiore nei dintorni di Gerusalemme. *Bull. Soc. Geol. Ital.*, Vol. 47, fasc. 1.
- Shalem, N., 1947. Landslide in the Hebron district. *Engineer. Architects Union Paper*, Vol. 8. pp. 29-32.
- Shaw, S.H., 1947. Southern Palestine, geological map on a scale of 1:250,000 with explanatory notes. *Govt. of Palestine, Govt. Printer*.
- Stowe, R., 1997. Reflection of Earthquakes on Early Arab Jerusalem. *Depart. of Land of Isr. Studies, Bar Ilan University*, 1374580-7.
- Szechy, K., 1977. The Art of Tunneling. *Hungarian Acc. Sci.* 891p.
- Terzaghi, K., 1946. Rock defects and loads on tunnel supports. In: *Rock Tunneling with Steel Supports*, R.V. Proctor and T.L. White, Commercial Shearing, Inc.
- Terzaghi, K., 1950. Mechanics of landslides in application of geology for engineering practice. *Geol. Soc. Amer. N.Y.* pp. 83-123. *Berkley Volume*.
- Terzaghi, K., 1962. Stability of steep slopes in hard unweathered rock. *Geotechnique*, Vol. 12. pp. 251-270.
- Terzaghi, K. and Peck, R. B., 1967. *Soil Mechanics in Engineering Practice*. NY. Wiley and Sons.
- Tourtlot, H. A., 1977. Geologic origin and distribution of swelling clays. *Assoc. of Engng. Geol. Bull.*, Vol. 11. No. 4. pp. 259-275.
- Varnes, D. J., 1978. Slope movement and processes. In Schuster, R. L. and Krizele, R. J. (eds.) *Landslide Analysis and Control*. Washington DC. *Nat. Acad. of Sci. S.R.* 176. pp. 11-23.
- Vilnay, Z., 1970. Jerusalem, The Capital of Israel, A: the Old City. *Ahiever Press, Jerusalem*.
- Voight, B., 1968. On the functional classification of rocks for engineering purposes. *Int. Symp. Rock Mechanics Madrid*. pp. 131-135.
- Wilson, W. Charles., 1864, Ordinance Survey of Jerusalem. *Royal Engineers*.
- Yair, A., 1971. Geomorphological processes on marl slopes Jerusalem *Studies in Geography*. 2, pp. 156-190.
- Zaruba, Q. and Mencl, V., 1969. Landslides and their control. *Elsevier*. 214 p.
- Zaslavsky, D. and Kassif, G., 1965. Theoretical formulation of piping mechanism in cohesive soils. *Geotechnique*, Vol. 15. No. 3. pp. 305-316.

**Appendix I. Landmark events in the history of Jerusalem**

A tale of construction, destruction and reconstruction

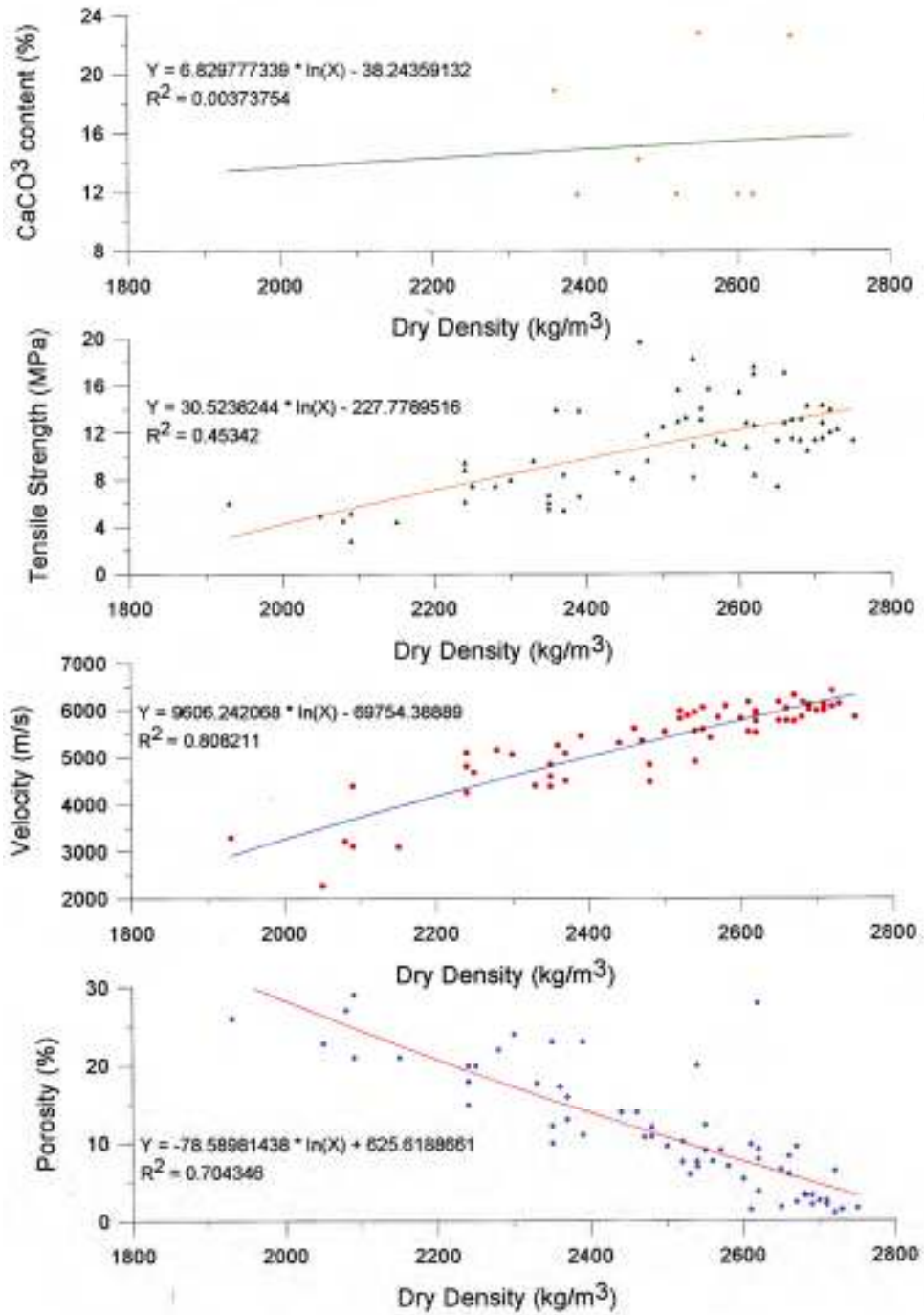
<b>DATE</b>	<b>EVENT</b>	<b>INITIATOR</b>
<b><u>Before Common Era (BCE)</u></b>		
<b>4000</b>	Oldest records on Jerusalem Canaanite rule.	Egyptian Hieroglyphs.
<b>1150</b>	Jerusalem conquered.	Judah, Judges 1,8.
<b>1004</b>	Jerusalem declared Capital of First Israelite Kingdom.	King David.
<b>954</b>	First Temple constructed on Mount Moriah.	King Solomon.
<b>586</b>	Israel divided into Israel and Judea. Jerusalem captured by the Babylonians and First Temple destroyed.	King Nebuchadnezar.
<b>536</b>	Second Temple constructed.	Ezra and Nehemia.
<b>537</b>	Persian conquest.	
<b>332</b>	Greek conquest.	
<b>165</b>	Jerusalem liberated from Hellenistic rule.	Judah the Maccabee.
<b>141</b>	Maccabean rule.	
<b>63</b>	Roman conquest.	
<b>20</b>	Second Temple enlarged.	King Herod.
<b><u>Common Era (CE)</u></b>		
<b>70</b>	Jerusalem captured and Second Temple destroyed by Romans.	Emperor Titus.
<b>135</b>	Bar Kochba revolt crushed.	Emperor Hadrian.
<b>136</b>	Jerusalem renamed Aelia Capitolina and Judea renamed Palestine.	
<b>323</b>	Byzantine conquest.	
<b>326</b>	Jesus' crucifixion and burial site identified and true cross relics found.	Empress Helena.
<b>335</b>	Church of the Holy Sepulcher constructed.	Helena's son Constantine the Great.
<b>614</b>	Persian conquest, Holy Sepulcher Church destroyed.	
<b>628</b>	Byzantine re-conquest.	
<b>629</b>	Holy Sepulcher Church reconstructed and relics restored.	Emperor Heraclius of Byzantium.
<b>638</b>	Arab conquest, Jerusalem surrenders 6 years after Mohammed's death.	Muslim Caliph Omar.
<b>691</b>	Dome of the Rock constructed.	Caliph Abd el-Malik.
<b>709</b>	Al-Aqsa Mosque constructed.	

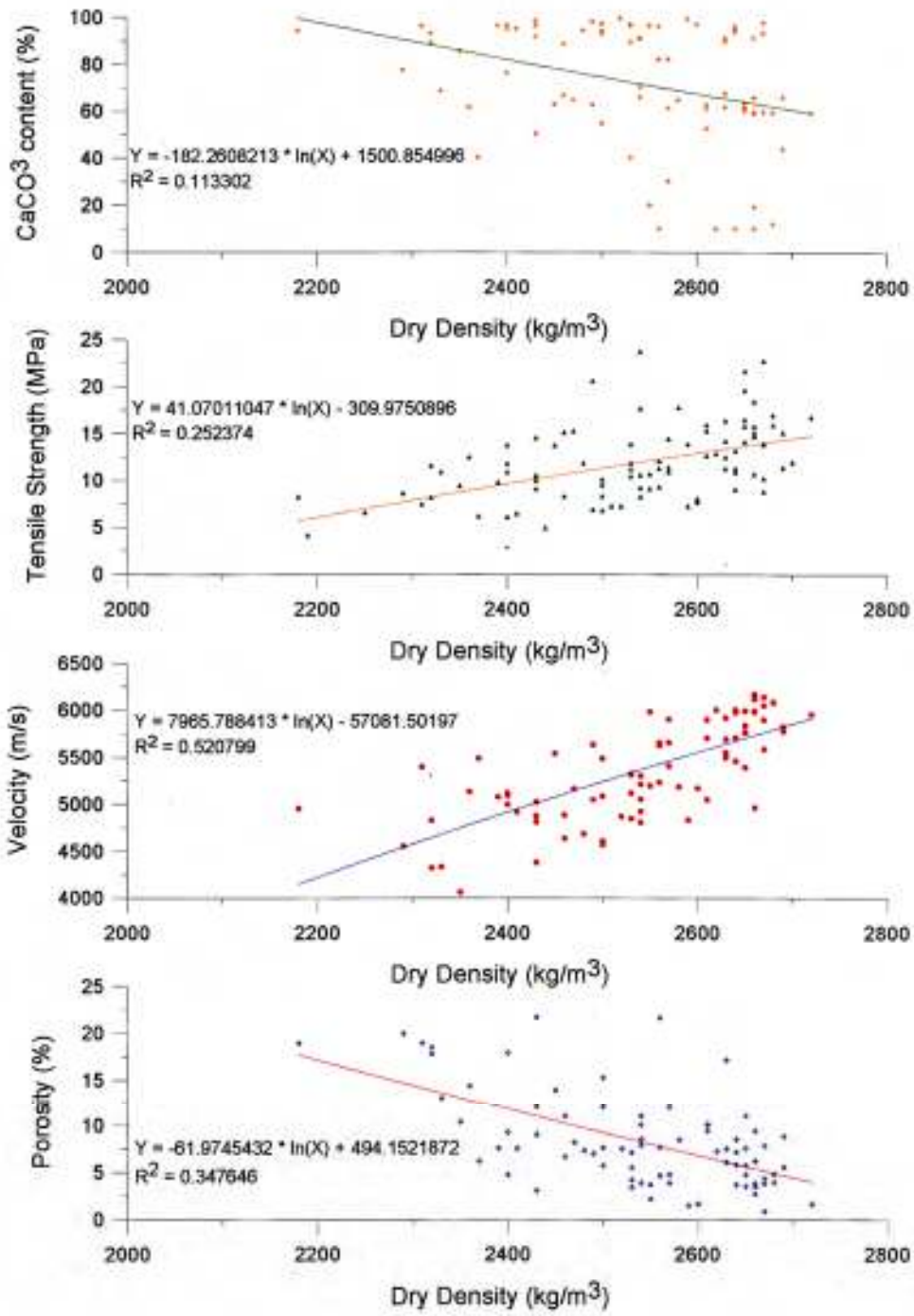
<b>1009</b>	Holy Sepulcher Church destroyed sparking First Crusade.	Muslim Caliph Hakim "The Mad".
<b>1072</b>	Turkish conquest.	
<b>1092</b>	Arab conquest.	
<b>1099</b>	Crusaders first conquest and Latin kingdom of Jerusalem established.	
<b>1187</b>	Arab conquest.	
<b>1229</b>	Crusader re-conquest.	Frederick II.
<b>1244</b>	Arab conquest from Egypt.	Khwarezmyians.
<b>1219</b>	Franciscan Order established. Jerusalem walls destroyed.	St. Francis of Assisi. Mamluke Sultan. Malik al-Muathan of Cairo,
<b>1516</b>	Turkish conquest by Ottomans and Jerusalem captured by Ottomans.	Sultan Selim I the Grim.
<b>1537</b>	Walls rebuilt with 7 Gates.	Ottoman Sultan Suleiman the Magnificent.
<b>1541</b>	The Golden Gate sealed for fear of war with Holy Roman Emperor.	Charles V.
<b>1701</b>	Rabbi Judah the Pious arrives with 1500 disciples. Construction of Hurva Synagogue.	Rabbi Judah Pious.
<b>1721</b>	Hurva Synagogue destroyed.	
<b>1818</b>	Jews constitute largest ethnic group in Jerusalem. British explorer Richardson.	Palestine Exploration Fund.
<b>1831</b>	Egyptian conquest and rule.	Mohammed Ali.
<b>1841</b>	Turkish re-conquest.	
<b>1864</b>	Landmark Hurva Synagogue and Memorial Arch reconstructed.	Sir Moses Montifiore.
<b>1917</b>	British occupation and Jerusalem liberated from Ottoman Rule.	British General Allenby.
<b>1922</b>	British mandate.	
<b>1947</b>	British relinquish mandate.	
<b>1948</b>	Jerusalem declared capital of the State of Israel. War of Independence. East Jerusalem and Old City captured by Jordan. Hurva Synagogue destroyed.	
<b>1967</b>	6-Day War Old City of Jerusalem captured and Jerusalem united. Laws Protecting Holy Places passed by Knesset, Israel Parliament.	
<b>1989</b>	The Citadel Museum in King David's Tower. 3000 yrs. Inauguration.	
<b>2000</b>	New Era of rebuilding and construction of modern Jerusalem.	

**Appendix II.** Conversion Table, English-Metric (SI units)

<b>Quantity</b>	<b>Customary Unit</b>	<b>SI equivalent</b>
Acceleration	ft/s <sup>2</sup>	0.3048m/s <sup>2</sup>
Area	ft <sup>2</sup>	0.09290m <sup>2</sup>
	in <sup>2</sup>	645.2mm <sup>2</sup>
	mi <sup>2</sup>	2.590km <sup>2</sup>
	acre	0.4047hectare
Energy	ft.lb	1.356J=1.356x10 <sup>7</sup> ergs
Force	kip	4.448kN
	lb	4.48N=4.48x10 <sup>3</sup> dyne
Discharge	gpm	5.446m <sup>3</sup> /d
Hydraulic conductivity	gpd/ft <sup>2</sup>	0.04070m/d
Length	in	2.540cm
	ft	0.3048m
	mi	1.609km
	lb	0.4536kg
Mass	ton	907.2kg
	lb/ft <sup>2</sup>	47.88N/m <sup>2</sup>
Pressure or stress	psi	6895N/m <sup>2</sup>
	MPa	10 <sup>6</sup> N/m <sup>2</sup>
	Atmos	0.1MPa
	gdp/ft	0.01240m <sup>2</sup> /d
Transmissivity	gdp/ft	0.01240m <sup>2</sup> /d
Velocity	ft/s	0.3048m/s
Volume	yd <sup>3</sup>	0.7646m <sup>3</sup>
	ft <sup>3</sup>	0.02832m <sup>3</sup>

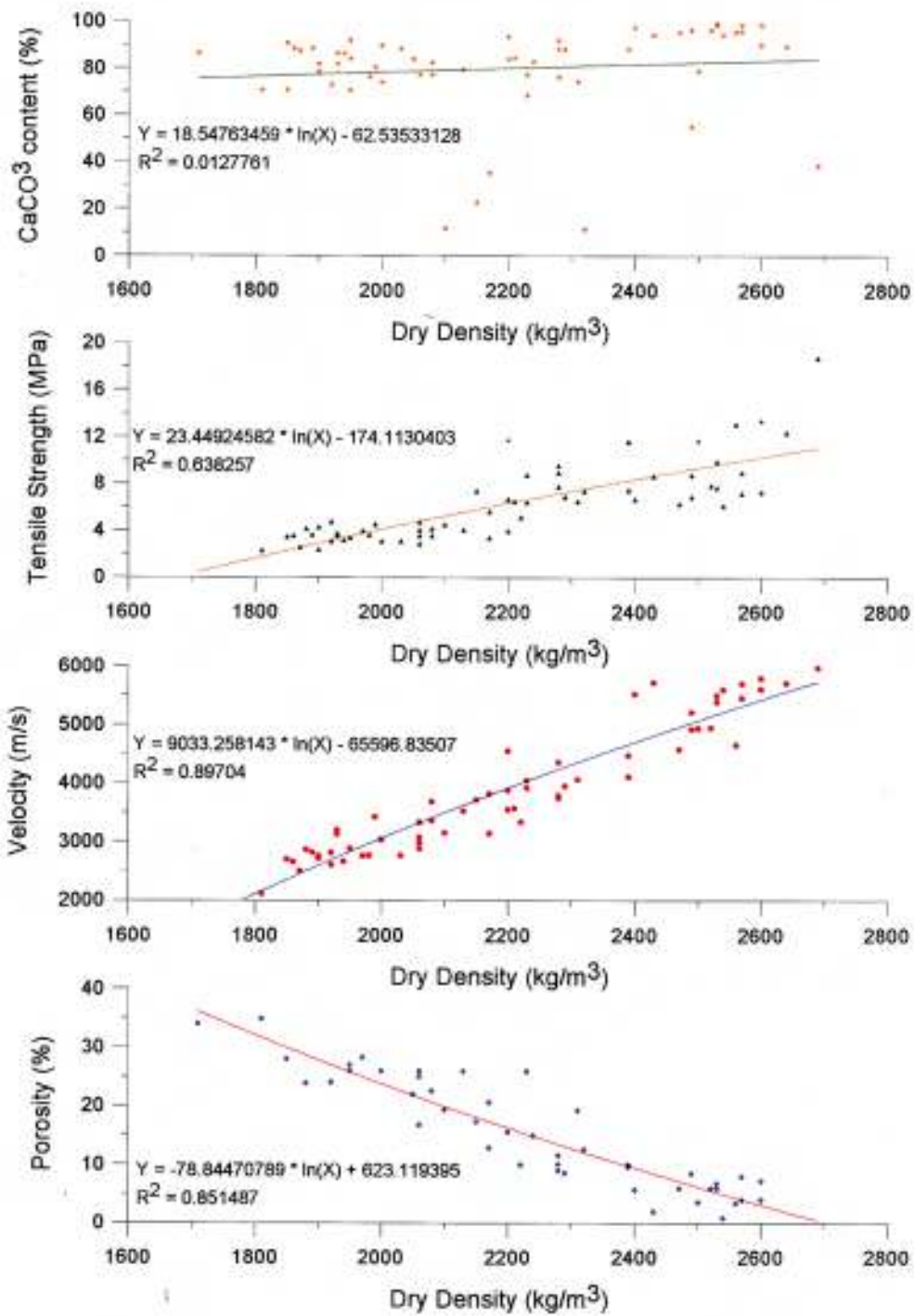
### Appendix III. Measured rock parameters in the Amminadav Formation



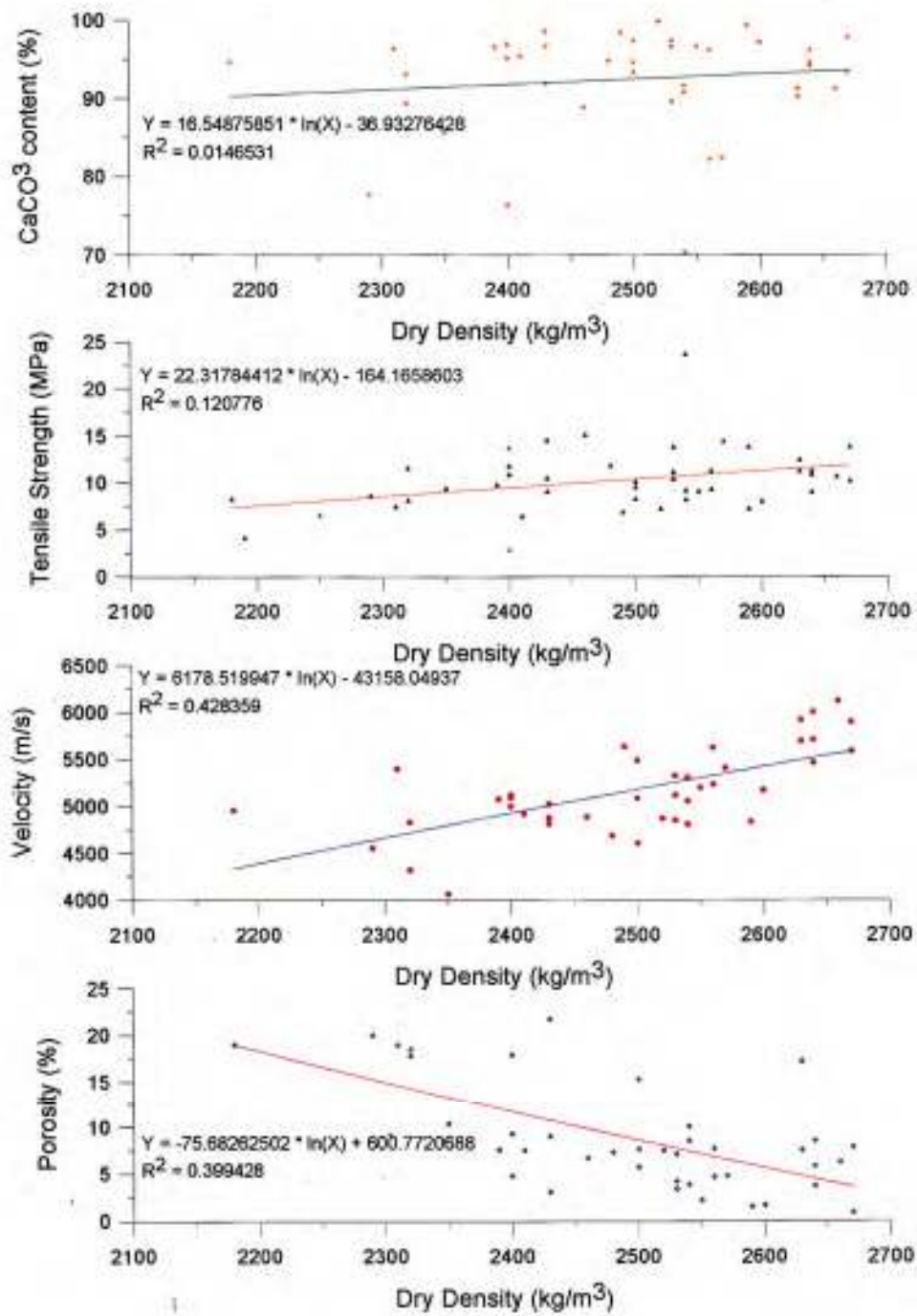




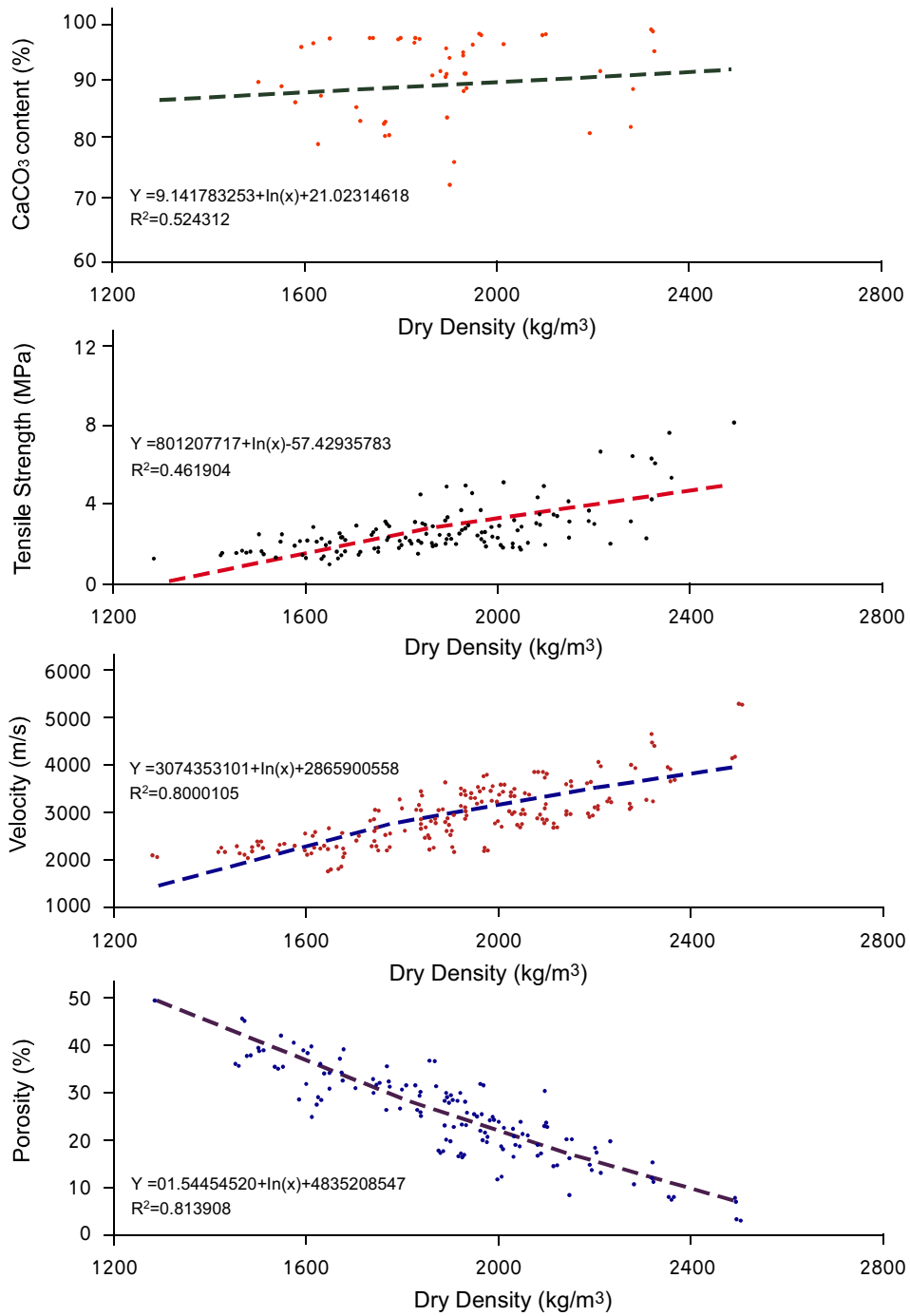
## Appendix III cont. Measured rock parameters in the Kefar Shaul Formation



Appendix III cont. Measured rock parameters in limestone of the Bina and Weradim formations.



Appendix III cont. Measured rock parameters in the Menuha Formation



**Appendix IV. Glossary**

Aqueduct	An artificial channel to convey water from one location to another.
Aquifer	Porous rock formation containing available water.
BCE	Before common Era.
CE	Common Era.
Ku	Geological symbol- Upper Cretaceous (see legend, Figure 8).
kPa	Kilo Pascal.
Lithology	from Greek word <i>Lithos</i> meaning rock.
m <sup>3</sup>	Cubic Meters.
m <sup>3</sup> /day	Cubic Meters/Day.
Mizzi	Rock (in Arabic).
Mg/l	Milligrams/litre.
MPa	Mega Pascal.
Nahal	Wadi, intermittent or ephemeral stream,
Q	Rock Quality.
Rendzina	Gray colored soil developed on chalk or clay.
RMR	Rock Mass Rating.
Roadheader	Tunnel boring machine.
RQD	Rock Quality Designation.
Terra Rosa	Red-brown soil developed on limestone or dolomite.
Viaduct	A bridge that connects points of equal height.

**Appendix V. Author**

**Dr. Yaacov Arkin** was born in Jerusalem in 1935, grew up in Australia and since 1959 lives in Jerusalem, Israel. He graduated with a B.Sc. in Geology in 1957 from the University of Western Australia gained DIC and MSc degrees in Engineering Geology at the Imperial College of Science and Technology, London in 1975 and a Ph.D. in Engineering Geology in 1986 at the University of London, U.K.

His various activities included work in the Bureau of Mineral Resources, Australia; Head of Israeli Geological Technical Assistance team to Ethiopia; Deputy Director of the Geological Survey of Ethiopia; Lecturer, University of Addis Ababa; Head of the Mapping Division of the Geological Survey of Israel; External Lecturer, Ben Gurion University of the Negev, Israel; External Tutor, New York State University, Rockland Center for International Studies; Visiting Research Professor on sabbatical in 1990 at Kent State University, Ohio USA; Elected in 1991 to the Phi Beta Delta, Honor Society for International Scholars at Kent State University; Visiting Research Professor on sabbatical in 1998 at the University of Nevada, Las Vegas, USA.

In 1975 he represented Israel on the International Committee for the Geological Map of the World, Middle East Region; He was awarded a British Council Scholarship in 1975, President of the Geological Society of Israel, 1992-1993, and was awarded the Israel Civil Service Award for Excellency in 1993.

Dr. Arkin has served on several committees of national civil engineering projects such as the Mediterranean-Dead Sea Hydroelectric Scheme.

Recent activities as a senior researcher at the Geological Survey of Israel included both practical work and research on geotechnical problems, practical projects involving the engineering geology of bridges, tunnels and stability problems, particularly around Jerusalem, and research of open fractures and active geological processes, both on the ground and using remote sensing techniques such as radar satellite digital and image data.

At present he is emeritus and is involved in ongoing research projects in geologic ground movements in rift valleys and their tectonic significance.

**Appendix VI.** Author

**Mr. Amos Ecker** was born in 1934 in Israel. He graduated with a M.Sc. degree in Geology in 1962 from the Hebrew University in Jerusalem. Since 1960 he has been on the staff of the Geological Survey of Israel in the field of hydrogeology. Much of his research has been on the coastal aquifers of Israel, which involved the detailed study of the geology and hydrology of the Pleistocene aquifer. His research has included the carbonate aquifer in the Jerusalem and the Yarqon–Beer Sheva basins, dealing with problems of water supply.

Mr. Ecker has been a member of the drilling committees of the Water Commission and the Mekorot Water Company for the past 15 years. In the past few years Mr. Ecker has set up in the Geological Survey a computerized inventory of the water wells in Israel. In 1999 he edited the atlas of selected geological cross-sections and subsurface maps in the coastal aquifer of Israel.

Mr. Ecker worked abroad in several countries in the field of hydrogeology. In Ecuador he was the geologist-team leader for drilling operations. In the Argentine and Chile, he was the hydrogeologist of an agricultural planning team. In the Canary Islands Mr. Ecker joined UNESCO for more than two years in the study of the groundwater behavior in the volcanic aquifer of the island of Tenerife. In Honduras he was the project manager of a hydrogeological project and in Burma, Mr. Ecker was a member of a UNICEF drilling project for clean water supply. He also was a consultant for the UNDP in the Cape Verde Islands, in Che Ju Island (S. Korea) and in Peru.

He is fluent in Hebrew, English and Spanish. Today he is emeritus at the Geological Survey of Israel.

בעבר הרחוק השתרעה ירושלים על שטח מצומצם עם תשתית סלעי גיר שתרמה את רוב אבני הבנין. אספקת המים היתה ממעינות, מבורות אגירה וממערכת של אמות מים, שכללה תעלות, גשרים, מנהרות ובריכות אגירה. עבודות תשתית גדולות אחרות כללו מבנים מפוארים כמו בית המקדש.

התפשטות ירושלים החדשה מערבה נעשתה על תשתית דומה של גיר ודולומיט. שכונות אחדות נבנו כבר על סלעים רכים של קרטון, חוואר וחרסית. ההתפתחות המהירה של העיר בשנים האחרונות המתבטאת במבנים גבוהים, כבישים מהירים, מנהרות רחבות, גשרים, הרכבת הקלה, אספקת מים לכל חלקי העיר, טיפול בשפכים ומניעת זיהום האקוויפר, הציבה אתגרים חדשים למהנדסים.

מגוון טיפוסי הסלע הבונים את התשתית בירושלים וסביבתה, דורשים לכן, כיום, הבנה רחבה יותר בגיאולוגיה ובתכונות הגיאוטכניות של הסלעים. ידע זה הנו הכרחי בכל תכנון וביצוע של עבודת תשתית הנדסית והוא נדרש גם לפני התחלת חפירות מחקר ארכיאולוגיות.

בספר מתוארות התכונות הפיסיקליות והמכניות של היחידות הגיאוטכניות ומוצגים פרמטרים גיאוטכניים שנמדדו בעת בניית מנהרות גילה והגשר שביניהן וחיבת מנהרת הר הצופים, אשר נסתיימו בשנים האחרונות. כמו כן מוצגים פרמטרים גיאוטכניים מפרויקטים אחרים אשר נשמרו במעבדה הגיאוטכנית של המכון הגיאולוגי הישראלי.

בספר מתוארות מגבלות גיאולוגיות בפתוח תשתיות כמו יציבות מדרונות מסוגים שונים, קיים דיון בתופעות קרסט, בורות שקיעה, סיכונים סיסמיים ומחצבות, דברים היכולים להופיע בעת תכנון וביצוע פרויקטים חדשים. מופיע פרק על אספקת המים לירושלים עם דגש על ההידרוגיאולוגיה, האקוויפרים, פרשת המים התת קרקעית וסכנות זיהום האקוויפר שמתחת לעיר.

ניתנים נספחים הכוללים טבלה על ההיסטוריה של ירושלים המתארת סיפור של הריסה ושיקום. פרמטרים גיאוטכניים מדודים של היחידות הגיאולוגיות העיקריות ניתנים בגרפים וברשימות.



משרד התשתיות הלאומיות  
המכון הגיאולוגי

## התייחסויות גיאוטכניות והידרוגיאולוגיות בפיתוח התשתיות סביב ירושלים

יעקב ארקין ועמוס אקר

ירושלים, תמוז תשס"ו, יולי 2007

דוח מס' GSI/12/2007